Miguel João Loureiro Afonso da Rocha Armada

Electrically Stimulated Neural Stem Cells Encapsulated in Gellan Gum Hydrogel for Spinal Cord Injury Repair

UMinho | 2023

Universidade do Minho
Escola de Engenharia

Miguel João Loureiro Afonso da Rocha Armada

Electrically Stimulated Neural Stem Cells Encapsulated in Gellan Gum Hydrogel for Spinal Cord Injury Repair

june 2023

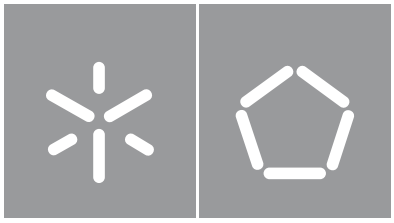

Universidade do Minho
Escola de Engenharia

Miguel João Loureiro Afonso da Rocha Armada

Electrically Stimulated Neural Stem Cells Encapsulated in Gellan Gum Hydrogel for Spinal Cord Injury Repair

Master Thesis
Master in Biomedical Engineering
Biomaterials, Rehabilitation and Biomechanics

Work performed under the supervision of
Dr Nuno Silva
Dr Eurico Seabra

june 2023

Agradecimentos

Ao longo destes incríveis 5 anos, tive a oportunidade de conhecer e partilhar momentos inesquecíveis. A estas pessoas devo um eterno agradecimento, especialmente:

- Aos meus orientadores, Nuno Silva e Eurico Seabra, pelo conhecimento que me transmitiram, paciência, disponibilidade e orientação pela qual permitiram a que conseguisse finalizar este trabalho;
- À minha família pelo eterno apoio mesmo nas alturas mais difíceis. Pela qual sem esse apoio não teria sido possível;
- À minha namorada e melhor amiga, Diana, por ter estado ao meu lado durante este tempo todo e por todas as vezes que insistiu para que me focasse;
- À Tó Team por toda a ajuda e conhecimento que me transmitiram, especialmente à Ana Marote, Diogo Santos, Jonas Campos, Tiffany Pinho e Jorge Cibrão. Obrigado por terem gasto um bocado do vosso tempo para me guiar;
- Aos meus amigos, Jorge e Leonardo, pela companhia e divertimento nas noites de escrita;
- Por último, ao "peste" e descendentes, por terem feito esta viagem muito mais memorável e pela qual agradeço a companhia e todos os momentos que passamos juntos desde o primeiro dia até ao último. Irei levar todas estas as memórias comigo.

Statement of Integrity

I hereby declare having conducted this academic work with integrity. I confirm that I have not used plagiarism or any form of undue use of information or falsification of results along the process leading to its elaboration. I further declare that I have fully acknowledged the Code of Ethical Conduct of the University of Minho.

Copyright And Terms Of Use Of This Work By A Third Party

"All we have to decide is what to do with the time that is given to us."

– J.R.R. Tolkien, The Fellowship of the Ring

Resumo

As lesões da medula espinal podem ter um impacto dramático na vida de um individuo, resultando em incapacidades motoras, sensoriais, psicológicas e sociais. A patofisiologia das lesões da medula espinal é extremamente complexa com vários eventos moleculares e celulares a ocorrerem após a lesão e contribuindo para o desenvolvimento de um microambiente inibitório à regeneração tecidular, o que dificulta o desenvolvimento de terapias eficazes. Neste contexto, terapias que combinam diferentes estratégias têm a vantagem de moderar diferentes eventos críticos após este tipo de lesões. Vários tipos de células têm sido transplantadas de forma a substituir o tecido perdido após lesão. As células mais promissoras são as Células Estaminais Neuronais induzidas (iNSCs), pois permitem transplantes autologos e têm a capacidade de se diferenciarem em neurónios, astrócitos e oligodendrócitos. Para promover a sobrevivência das células transplantadas, biomateriais têm sido utilizados para funcionar como uma matriz extracelular artificial. Adicionalmente, a modulação do ambiente inibitório e por consequente o sucesso do transplante pode ser melhorado através da suplementação com secretoma de células mesenquimais estaminais (MSCs). Por fim, a estimulação eléctrica epidural tem-se revelado como uma terapia muito promissora em pessoas com lesões medulares. Neste projecto propõem-se uma terapia mais holística, que tem em conta vários eventos patofisiológicos da lesão ao invés do foco em apenas um. Desta forma, pretende-se alcançar uma terapia eficaz que combina, simultaneamente, células estaminais, biomaterias, secretoma e estimulação epidural.

Palavras-chave: Medicina Regenerativa; Lesões Medulares; Células Estaminais Neuronais; Células Estaminais Mesenquimais; Secretoma; Biomateriais; Estimulação Eléctrica Epidural

Abstract

Spinal Cord Injuries (SCI) can have a devastating impact on an individual's life, leadind to motor, sensory, psychological and social impairments. The SCI pathophysiology associated is extremely complex, with numerous molecular and cellular events occurring after the initial trauma and that lead to the development of an inhibitory microenvironment in the injury site, which impairs the development of new therapies. Therefore, therapies that combine different strategies have been on the rise for focusing on different critical events. For instance, several types of cells have been implanted in order to replace lost tissue after these types of lesions. Induced Neural Stem Cells (iNSCs) have been the most promising for autologous transplant and differentiation in neurons, astrocytes and oligodendrocytes. To promote the survival of transplanted cells, biomaterials have been implemented to act as an artificial extracelullar matrix. Additionally, some pathological events and, as a consequence, the success of the transplanted cells, can be enhanced using the secretome of mesenchymal stem cells (MSCs). At last, epidural electrical stimulation has revealed to be a promising therapy for SCI, enabling physical rehabilitation and promoting neural plasticity. Therefore, this project aims to combine all this approaches in order to target several pathophysiolgical events of the spinal cord injury, instead of just one. As a result, we perform in vitro studies on the combination of stem cells, biomaterials, secretome and epidural electrical stimulation in order to obtain an effective therapy.

Keywords: Regenerative Medicine; Spinal Cord Injury; Neural Stem Cells; Mesenchymal Stem Cells; Secretome; Biomaterials; Epidural Electrical Stimulation

Contents

List of Figures

List of Tables

Acronyms

Symbols

α**MEM** Minimum Essential Medium α

A

AC Alternating current

ACEFs Alternating Current Electrical Fields

AIS American Spinal Injury Association Impairment Scale

ASCs Adipose Tissue Derived Mesenchymal Stem Cells

B

BDNF Brain-Derived Neurotrophic Factor

BECs Biphasic Electrical Currents

bFGF Basic Fibroblast Growth Factor

BM-MSCs Bone Marrow Derived Mesenchymal Stem Cells

C

cAMP Cyclic adenosine monophosphate

CNTF Ciliary neurotrophic factor

D

DAPI 4-6-diamidino2-phenylindole-dihydrochloride

DBS Deep brain stimulation

DC Direct current

DCEFs Direct Current Electrical Fields

DCX Doublecortin

DMEM Dulbecco's Modified Eagle Medium

DRG Dorsal Root Ganglia

E

ECM Extracellular matrix

EES Epidural electrical stimulation

EES Electrical Epidural Stimulation

EF Electric Fields

EGF Epidermal Growth Factor

EMFs Electromagnetic Fields

ES Exogenous Electrical Stimulation

ESCs Embryonic stem cells

EVs Extracellular Vesicles

F

FBS Fetal Bovine Serum

FCS Fetal Calf Serum

FES Functional electrical stimulation

G

GAP-43 Anti-Growth Associated Protein 43

GDNF Glial-Derived Neurotrophic Factor

GG Gellan Gum

GRGDS Fibronectin-derived peptide

H

HBSS Hanks' Balanced Salt Solution

HGF Hepatocyte Growth Factor

hNSCs Human Neural Stem Cells

I

IBA-1 Ionized calcium-binding adapter molecule1

ICVS Life and Health Sciences Research Institute

IL Interleukin

INL Iberian Nanotechnology Laboratory

iNSCs Induced Neural Stem Cells

iPSCs Induced Pluripotent Stem Cells

ISMS Intraspinal microstimulation

K

Kan Kanamycin

L

LHRH Luteinizing hormone-releasing hormone

LIF Leukemia inhibitory factor

M

MAP-2 Anti-Microtubule-Associated Protein 2

MSCs Mesenchymal Stem Cells

N

NbA Neurobasal-A

NGF Nerve Growth Factor

NSC Neural Stem Cells

NSPCs Neural Progenitor Stem Cells

NT3 Neurotrophin 3 factor

O

O4 Anti-Oligodendrocytes Antibody

OPCs Oligodendrocyte progenitor cells

P

P/S Penicillin-Streptomycin

PBS Phospate-Buffered Saline Solution

PCEFs Pulse Current Electrical Fields

PEMF Pulsed Electromagnetic Field Stimulation

PNS Peripheral nerve stimulation

Pt Platinum

R

RT Room Temperature

S

SC Spinal Cord

SCI Spinal Cord Injury

SEM Standard error of mean

T

tDCS Transcranial direct current stimulation

TE Tissue Engineering

Ti Titanium

TNF Tumor necrosis factor

V

VEGF Vascular Endothelial Growth Factor

1 Introduction

The spinal cord (SC) is part of the central nervous system and provides a means of communication between the brain and peripheral nerves that enter the cord [1, 2]. These spinal nerves of the peripheral nervous system serve as connections between the central nervous system, distal receptors and organs. It is also able to serve as an important relay station for incoming, afferent information from the periphery to central brain regions [3]. The two main cells in the nervous system are the nerve cells, or neurons, and glial cells, or glia.

1.1 Cytoarchitecture of the Spinal Cord

1.1.1 Neurons

Neurons are composed by the cell body, or soma, dendrites, an axon and presynaptic terminals [4, 5]. The cell body is the metabolic center of the cell, as it includes the nucleus and the endoplasmic reticulum, a continuous membrane system where the cell's proteins are synthesised [6]. Neurons are usually composed of a branch of several short dendrites and one long axon [4]. The branch of dendrites has the function of receiving incoming signals from other nerve cells [6]. Before branching, the axon normally extends some distance from the cell body, allowing it to transmit signals to a large number of target neurons [4]. Action potentials are the signals that the brain uses to receive, process, and transmit information [4]. They are triggered by a wide range of environmental events that have an impact on our bodies, ranging from light to mechanical contact, odorants to pressure waves [6].

Large axons are encased in an insulating sheath of a lipid material called myelin to speed up the transmission of action potentials [5]. The Ranvier nodes, uninsulated regions on the axon where the action potential is regenerated, interrupt the sheath at regular intervals [6]. Myelin has two primary proteins in the CNS: myelin basic protein, which is a tiny, positively charged protein found on the cytoplasmic surface of compact myelin, and proteolipid protein, which is a hydrophobic integral membrane protein [6]. Both, it is assumed, offer structural stability for the sheath [4, 5]. Demyelination slows or even prevents action potential conduction in a damaged axons [6]. Demyelinating disorders are thus damaging to neuronal circuits in the central and peripheral nervous systems [6].

Near its terminus, the axon divides into fine branches that communicate with neighbouring neurons via specialized communication zones known as synapses [4]. The nerve cell that sends the signal is known as the presynaptic cell, and the cell that receives the signal is known as the postsynaptic cell [4].

The synaptic cleft is a relatively thin gap that separates presynaptic and postsynaptic cells [6]. Some presynaptic neurons stimulate their postsynaptic target cells, whilst others inhibit them [6].

Thus, neurons are divided into three types: unipolar, bipolar, and multipolar (Figure 1).

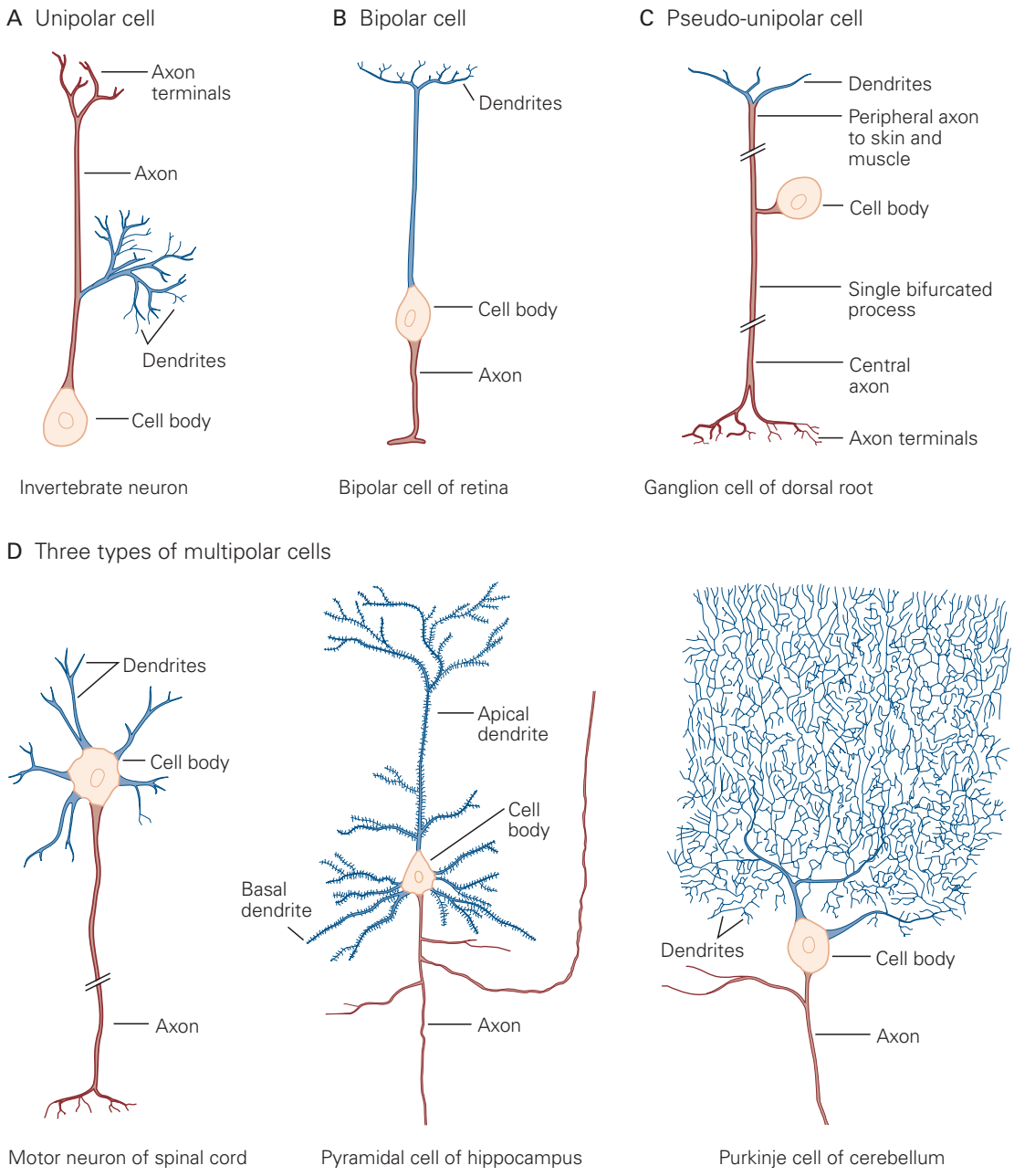

Figure 1. Neurons are characterized as unipolar (**A**), bipolar (**B**), or multipolar (**D**) based on the number of processes that originate from the cell body (Adapted from Kandel et al. [6]).

Unipolar neurons are the most basic since they have a single fundamental mechanism that gives rise to several branches. One branch functions as the axon, while the others serve as receiving structures.

The oval soma of bipolar neurons gives rise to two separate processes: a dendritic structure that receives signals from neighbouring neurons and an axon that transports information to the central nervous system. One axon conveys information from sensory receptors in the skin, joints, and muscle to the cell body, while the other carries same sensory information to the spinal cord. In vertebrate nervous systems, multipolar neurons predominate. A single axon and several dendritic structures protrude from various locations around the cell body. Multipolar cells differ significantly in morphology, particularly in the length of their axons and the amount, size, and complexity of their dendritic branching [6].

Sensory neurons, motor neurons, and interneurons are the three major functional types of nerve cells. Sensory neurons transport data from the body's peripheral sensors into the nervous system for perception and muscular coordination. Some basic sensory neurons are referred to as afferent neurons, and the words are interchangeable. The term afferent (carried toward the central nervous system) refers to all information transported from the periphery to the central nervous system, regardless of whether or not it results in sensation. The term sensory refers to afferent neurons that carry information from the sensory epithelia, joint sensory receptors, or muscle to the central nervous system [6]. The term efferent refers to all information conveyed from the central nervous system to the peripheral organs, regardless of whether or not it results in action [4]. Motor neurons provide instructions from the brain or spinal cord to muscles and glands (efferent information). The classic definition of a motor neuron (or motoneuron) is a neuron that stimulates a muscle, although the term increasingly encompasses additional neurons that do not directly innervate muscle but command movement indirectly [6]. The most prevalent functional category is interneurons [4].

When an action potential reaches a neuron's terminal, it causes the cell to release chemical compounds. Neurotransmitters can be small chemical compounds like l-glutamate and acetylcholine, or peptides like substance P or LHRH (luteinizing hormone–releasing hormone) [5]. Neurotransmitter molecules are stored in subcellular organelles known as synaptic vesicles, which accumulate in axon terminals at specialized release locations known as active zones. Exocytosis occurs when vesicles travel up to and merge with the neuron's plasma membrane, then burst open to release the transmitter into the synaptic cleft. The neurotransmitter molecules that are released are the neuron's output signal [4–6]. The amount of transmitter released is thus graded in the output signal, which is governed by the number and frequency of action potentials that reach the presynaptic terminals. When the transmitter molecules are released, they diffuse across the synaptic cleft and bind to receptors on the postsynaptic neuron. The postsynaptic cell generates a synaptic potential as a result of this binding. The type of receptor in the postsynaptic cell determines whether the synaptic potential is excitatory or inhibitory [6].

Neurons can be excitable both electrically and chemically [4]. The cell membrane of neurons contains specialized proteins called ion channels and receptors that allow certain inorganic ions to flow across the membrane, redistributing charge and causing electrical currents that change the voltage across the membrane [4]. These charge alterations can cause a wave of depolarization in the form of action potentials along the axon, which is how a signal normally travels within a neuron [6].

In the central nervous system, glial cells outnumber neurons by a large margin [7]. They encircle neurons' cell bodies, axons, and dendrites [6]. Glia differ from neurons in that they do not develop dendrites or axons. Glia differ functionally as well. Although they develop from the same embryonic precursor cells as neurons, they lack the same membrane characteristics and so are not electrically excitable [6]. They help electrical signals flow swiftly through the axons of neurons, and they appear to be vital in regulating connectivity during early development and sustaining new or changed connections between neurons that emerge as a result of learning [6].

1.1.2 Glia cells

Glial cells form a tissue network that offers nourishment and operational support to neurons [8]. There are three main types of macroglia: oligodendrocytes, Schwann cells, and astrocytes (Figure 2). Neurons and glia communicate by releasing molecules and receptors-ligands interactions [9].

The insulating myelin sheaths of some axons in the central nervous system are produced by **oligodendrocytes** [4, 5]. Oligodendrocytes are smaller cells with a limited number of processes [6]. They form the myelin sheaths that insulate axons in the white matter [5]. A single oligodendrocyte's can insulate numerous axons [6]. Perineural oligodendrocytes surround and support the cell bodies of neurons in the gray matter [6].

Astrocytes are characterized for their irregular, star-shaped cell bodies and vast number of processes. Astrocytes perform a variety of roles necessary for appropriate neuronal growth, synapse formation, neural circuit function, and action potential propagation [11–13]. Astrocytes are assumed to have a nutritive function since their end-feet make touch with both capillaries and neurons [14]. Astrocytes are also vital in the maintenance of the blood-brain barrier [6]. As physical barriers in healthy tissue, astrocytes prevent the invasion of foreign cells and pollutants from blood arteries or the meninges [15]. This barrier also prevents the transmission of neurotoxic inflammation, which can result from either peripheral infections or injured CNS tissue [16].

Microglia are resident immune cells and phagocytes in the CNS, and are responsible for locating and eliminating invading infections [14]. Microglia make up roughly 5–12% of glia in the CNS [16].

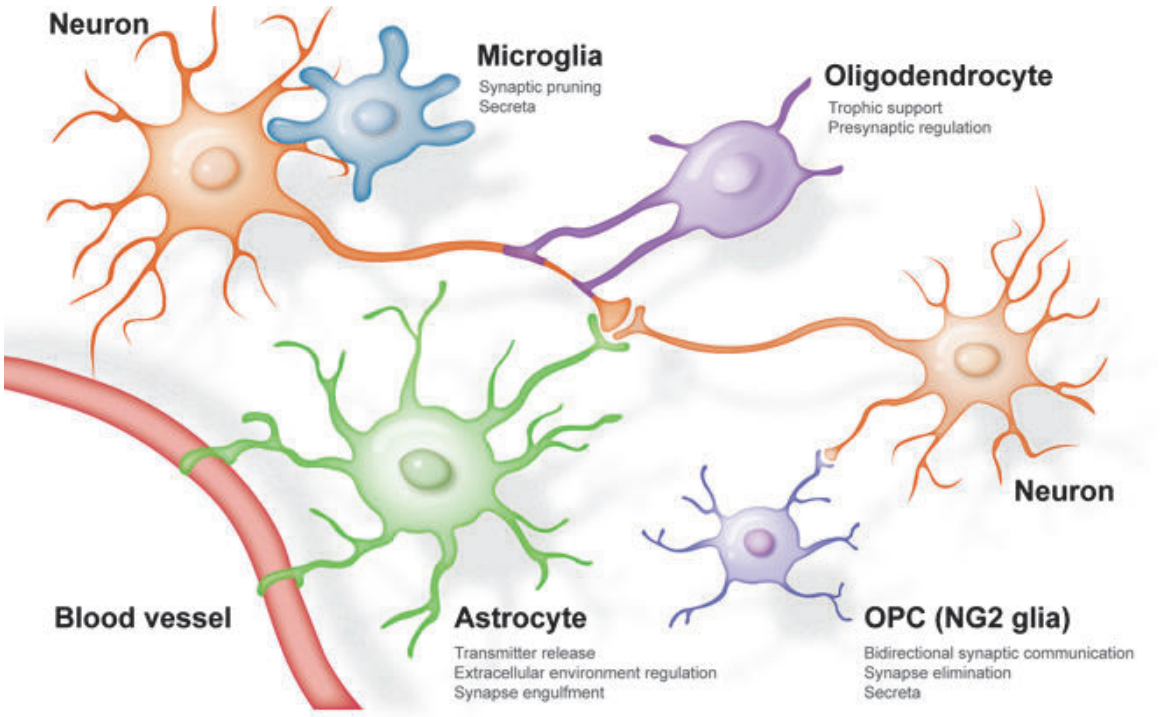

Figure 2. Glial cells in the central nervous system are classified as astrocytes, microglia (active phase), oligodendrocytes, and oligodendrocyte precursor cells (OPCs, also known as NG2 glia) (Adapted from Liu et al. [10]).

Following injury or disease, microglia suffer a major increase in the motility of their processes, as well as changes in shape and gene expression, and can be swiftly drawn to areas of damage where it can play helpful or detrimental roles. Microglia, for example, bring lymphocytes, neutrophils, and monocytes into the CNS and enlarge the lymphocyte population, performing significant immunological activities in infection, stroke, and immunologic demyelinating illness [6]. Microglia also help to lessen the harm brought on by CNS assaults by removing dead and dying tissue following an injury [14] and coordenate the response of astrocytes after trauma [17]. This procedure prepares the area for later healing processes. Microglia constantly survey the environment for signals of either infection by a pathogen or the requirement for the intrinsic components of the CNS to be broken down in order to better fulfil its function [18]. The microglia's scanning state is referred as resting microglia even though it involves CNS-preserving functions [16]. Microglia, while important for the immune response to infection or trauma, also contribute to pathological neuroinflammation by producing cytokines and neurotoxic proteins and causing neurotoxic reactive astrocytes [6]. Microglia play crucial roles in the development of the CNS and are the main agents used to carry out neural remodelling in addition to their functions as macrophages [19]. They can

accomplish this by eliminating immature neurons and dismantling particular neuronal networks according to activity [16].

1.2 Physiology and Anatomy of the Spinal Cord

The SC resides within the spinal canal of the vertebral column and is surrounded by cerebrospinal fluid and meninges [3]. It extends from the base of the brain - in the *medulla oblongata* - through the *foramen magnum* of the skull to the first lumbar vertebra L1 – L2 [3, 20]. The SC is protected by the vertebral column, which is composed of individual vertebrae (Figure 3).

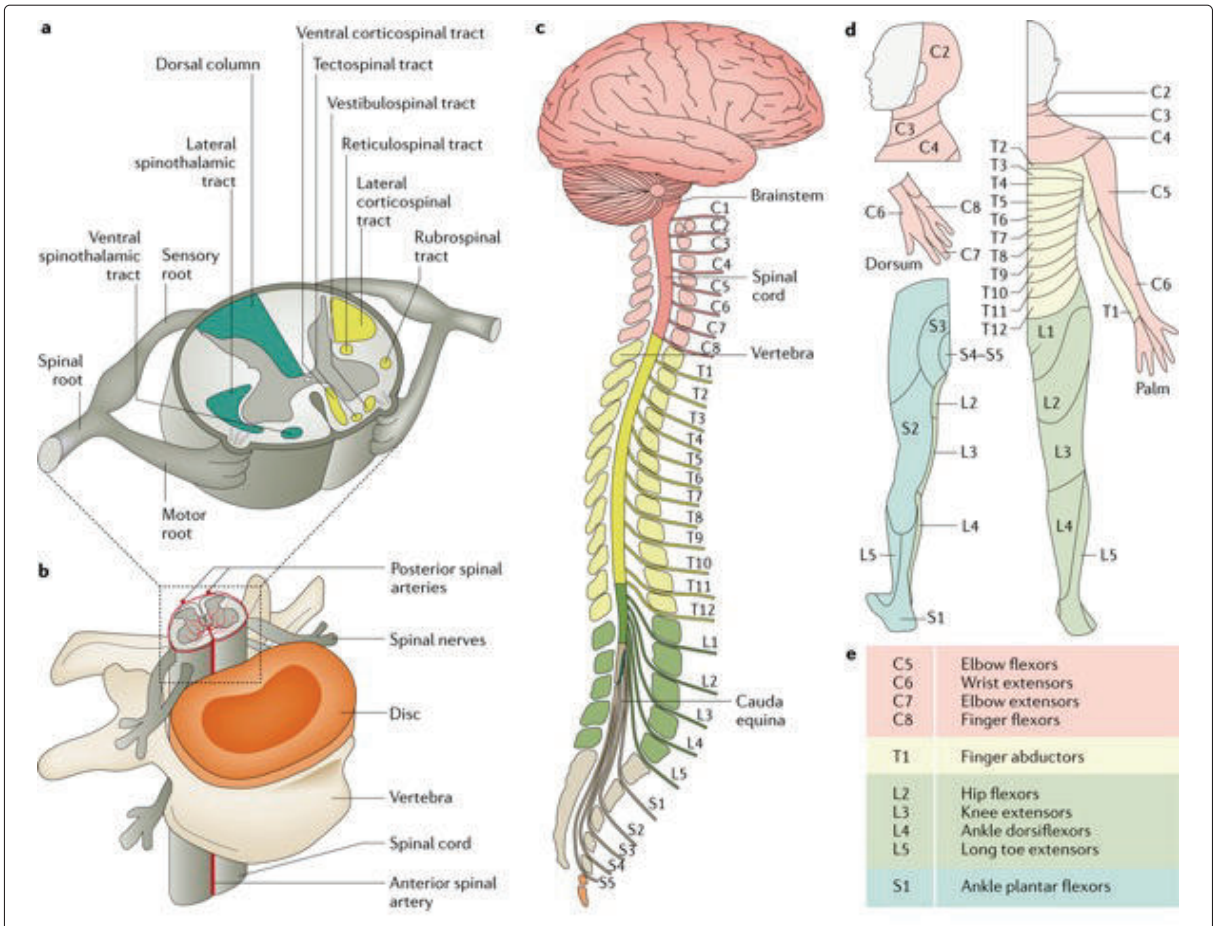

Figure 3. The gross anatomy of the spinal cord, demonstrating its interactions with bony structures and other body parts. The axial spinal slices (**a** and **b**) on the left represent each spinal level and demonstrate the distribution of white and gray matter. The vertebrae on the right (**c**) are color-coded to aid in the identification of the various levels. Each spinal cord segment (**c**) innervates a specific region of the skin (**d**), muscle (**e**), or organ group (Adapted from Ahuja et al. [21]).

It follows the curvature of the vertebral column and has different thicknesses depending on the vertebral levels [22]. The spinal cord is separated into four core areas throughout its length: cervical, thoracic, lumbar, and sacral. The widest segments of the SC are found in the cervical region, followed by the lumbar, thoracic and sacral segments [23].

Cervical spinal nerves control sensory perception and motor function at the back of the head, neck, and arms; thoracic spinal nerves control the upper trunk; and lumbar and sacral spinal nerves control the lower trunk, back, and legs [6]. There are 31 pairs of spinal nerves: 8 cervical, 12 thoracic and dorsal, 5 lumbar, 5 sacral and 1 coccygeal. However, at the cervical level, there are only 7 vertebrae [22]. In the cervical area, spinal nerves leave above their corresponding vertebrae, with the C1 spinal nerves emerging between the C1 vertebra and the skull. C8 exits above T1 as there is no corresponding vertebra [1]. The spinal nerves exit under their respective vertebrae, starting from T1 [1]. Each segment has a pair of dorsal (sensory) and ventral (motor) roots that join to form the spinal nerve, except for C1 which has no sensory dorsal root [1]. The spinal nerves leave the vertebral column through their corresponding intervertebral foramina – or neural foramina – [1, 20].

Because of two organizational properties, the spinal cord changes in size and shape along its rostrocaudal axis. First, only a small number of sensory axons enter the cord at the sacral level. At higher levels, the quantity of sensory axons entering the cord rises (lumbar, thoracic, and cervical). In contrast, the majority of descending axons from the brain terminate at cervical levels, with fewer descending to lower levels of the spinal cord. Thus, the number of fibers in the white matter is greatest at cervical and lumbar levels (where both ascending and descending fibers are greatest) and lowest at sacral levels. As a result, the sacral levels of the spinal cord contain far less white matter than gray matter, whereas the cervical cord contains significantly more white matter than gray matter [6]. The size of the ventral and dorsal horns varies as the second organizational trait. At the levels where motor neurons innervate the arms and legs, the ventral horn is bigger. As a result, a greater number of motor neurons are required to innervate the greater number of muscles and govern the greater complexity of movement in the limbs than in the trunk, resulting in larger ventral regions. Similarly, where sensory nerves from the limbs enter the cord, the dorsal horn is larger. Limbs have a higher density of sensory receptors, which allows for finer tactile discrimination and, as a result, sends more sensory fibers to the cord. These cord enlargements are known as lumbosacral and cervical enlargements [6].

The meninges act as a protective layer, constituting three membranes of connective tissue. It also acts as a support for the structure of the SC and provides stability [3]. From the outside in, the meninges are the *dura mater*, *arachnoid mater* and *pia mater* [20]. These are separated by the subdural and subarachnoid

spaces. The subarachnoid spaces (between arachnoid and pia) are filled with cerebrospinal fluid and a loose network structure of collagen fibers and fibroblasts [3, 20]. The epidural space (between dura and periosteum) is filled with loose fibrous and adipose connective tissue [20].

1.2.1 Gray and White Matter

The SC is composed of gray matter and white matter. The **gray matter** of the SC is located in the center, while the periphery is composed of white matter [24]. The butterfly – or H-shaped – gray matter divides into posterior (dorsal), anterior (ventral) and lateral (intermediate) horns [1]. These horns divide the white matter into dorsal, lateral and ventral columns. Interneurons, efferent neuron cell bodies and dendrites, afferent neuron entering fibers, and glial cells make up the gray matter [1, 24]. Secondary sensory neurons (sensory nuclei) in the **dorsal horn** receive stimulus information from main sensory neurons that innervate the skin, muscles, and joints [6]. The **ventral horn** contains clusters of motor neurons (motor nuclei), the axons of which exit the spinal cord and innervate the skeletal muscles [6].

Groups of myelinated axons make up the majority of the surrounding **white matter**, with the exception of where the dorsal horns touch the spinal cord margins [20, 24]. Bundles of ascending and descending axons are split into dorsal, lateral, and ventral columns in the white matter that surrounds the gray matter [6]. Only ascending axons carry somatosensory information to the brain stem in the **dorsal columns**, which are located between the two dorsal horns of gray matter [6]. Both ascending and descending axons from the brainstem and neocortex innervate spinal interneurons and motor neurons in the **lateral columns** [6]. Ascending and descending axons are also found in the **ventral columns** [6].

These bundle of axons are called fiber tracts or pathways. A tract is a collection of nerve fibers that have a similar function, beginning, course and ending. Fiber tracts run longitudinally through the SC with ascending or descending information from the brain to the periphery, or vice-versa (Figure 4a) [1, 20].

The fiber tracts are critical in the communication between the spinal cord and the brain (Figure 4b) [6]. Afferent (sensory) fiber groups enter the spinal cord from the peripheral nerves via the dorsal roots on the dorsal side of the cord [20]. Efferent (motor) neuron axons exit the spinal cord on the ventral side via the ventral roots [20]. The dorsal root ganglia (DRG) is a small enlargement on the dorsal roots that contain the cell bodies of afferent pseudounipolar neurons, with one process transmitting sensory input from the tissues to the cell body and the other from the cell body to the spinal cord [1, 6]. When the dorsal and ventral roots combine, from the same level, they form a spinal nerve on each side of the spinal cord [20].

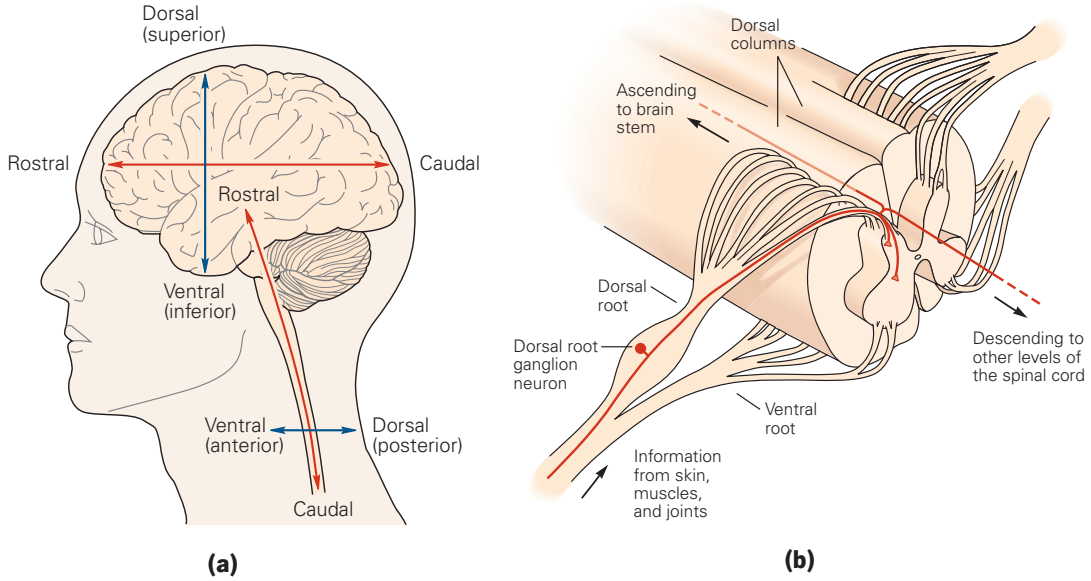

Figure 4. (a) The central nervous system will be described along two major axes; Caudal means near the tail and rostral means toward the nose. In the spinal cord, rostral refers to the direction of the head, caudal refers to the direction of the coccyx (the lower end of the spinal column), ventral (anterior) refers to the direction of the belly, and dorsal (posterior) refers to the direction of the back. Above the spinal cord, rostral refers to the nose, caudal to the back of the head, ventral to the mouth, and dorsal to the top of the skull. Superior is frequently used interchangeably with dorsal, and inferior is synonymous with ventral. **(b)** Dorsal root ganglia and spinal nerve roots. The cell bodies of neurons that carry sensory information from the skin, muscles, and joints are found in the dorsal root ganglia, which are clusters of cells located near the spinal cord. (Adapted from Kandel et al. [6]).

1.3 Spinal Cord Injury

Spinal Cord Injury (SCI) occurs when the spinal cord is damaged and subsequently leads to loss of sensory, autonomic and/or motor function [2, 25, 26]. Spinal cord neurologic damage impacts almost every physiologic system, and patients might present with a wide range of symptoms that have a significant impact on their day-to-day life [24, 25].

In spinal cord injuries, lesions of various sizes can damage motor or sensory pathways located in dorsal, lateral or ventral regions. As a result, there is a disruption in the efferent and afferent pathways from the peripheral nervous system to the spinal cord and brain, particularly descending motor neurons and ascending somatosensory fibers [25]. The symptoms will largely be correlated to the injured tracts

and the level of injury [22, 25]. A SCI has been demonstrated to have a highly heterogeneous lesion and cellular organization, which results in a very unique injuries in each patient [22, 26]. However, SCI can be characterized in a succession of events which go from a primary injury, to a secondary injury (acute and sub-acute) and stabilizing in a chronic phase (Figure 5). Rowland et al. [27] defined the stages of SCI as acute (<48 h), subacute (2 d – 2 w), intermediate (2 w – 6 m), and chronic (> 6 m). The development of successful therapy must be linked to a full understanding of the pathophysiology associated with the aspects of primary and secondary injury of the individuals affected.

SCI is caused by an insult to the spinal cord, which can be classified as non-traumatic or traumatic [28]. Non-traumatic injury occurs when the spinal cord is damaged by an acute or chronic condition, such as a tumor, infection, or degenerative disease [29]. The most common are traumatic SCI, and is caused by a violent impact that fractures or dislocates vertebrae [30]. A **primary injury** is characterized by the neurological damage caused by a sharp penetrating forced, contused or compressed by a blunt force, or tissue death due to a vascular insult [24, 31]. Neurons perish soon after SCI due to initial damage. The number of NeuN-positive cells is reduced by 21% two hours after SCI. At 24 hours, very few neurons are found, and just a few neurons are detected in the dorsal horn's periphery region [32].

Following the initial trauma, a series of biological events begin, designated as **secondary injury**. This injury spans the course of minutes to weeks and leads to more neurological damage in the surrounding tissue, resulting in additional loss [22, 24]. This phase is characterized by ionic imbalances, excitotoxicity, dysfunction vascular and inflammatory events that lead to necrosis and apoptotic cell death [22, 24].

Hemorrhage, vasospasm, thrombosis, disruption of the blood-brain barrier and infiltration of inflammatory cells are all examples of vascular disruptions that lead to a decrease of spinal cord blood flow and result in edema, necrosis and ischemia [24, 31]. These events contribute to free radical production and lipid peroxidation that cause further damage [20]. Depolarization of cell membranes, ATPase failure, and a rise in intracellular Ca^{2+} occur when the ionic balance of K^{+}, Na^{+}, and Ca^{2+} is disrupted [20, 29]. Moreover, after SCI, there is an increase in the release of extracellular amino acids, specifically glutamate, which causes excessive activation of glutamate receptors, resulting in excitotoxicity and additional neuronal cell death [33]. Apoptosis – a form of programmed cell death – also occurs after SCI in neural and glial cell population, which may be caused by microglia activation [20]. Microglia cells retract their processes and adopt an amoeboid shape, preparing for phagocytosis and debris clearance [28].

Inflammation has been found to be beneficial after SCI for neural tissue repair, as it may lead to cellular debris removal, extracellular matrix remodelling and axonal regeneration [20]. However, the timing and

scale of immune response may be a significant factor in whether it is damaging or therapeutic [20].

Weeks to years after the injury, the patient is in a **chronic phase**, characterized by neurological impairments in SC, as well as possible reorganization of brain regions [20]. This phase includes processes such as white matter demyelination, gray matter disintegration, connective tissue deposition, which results in the formation of glial scars [24, 28, 31]. The glial scar is a physical barrier formed mainly by reactive astrocytes, microglia, macrophages and extracelullar matrix molecules, that prevent axons to grow through [24]. Furthermore, in around 25% of SCI patients, the glial scar surrounds a cystic cavity that gradually grows, resulting in a disease known as syringomyelia [20]. The lesion ceases to progress further and deficits are stabilized within 1 to 2 years after the injury [22].

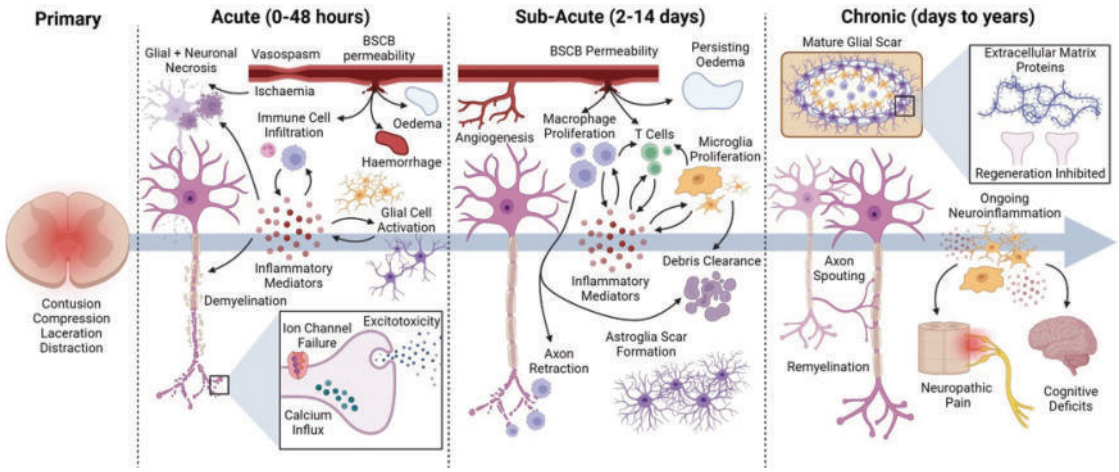

Figure 5. A summary of secondary injury events that occur after traumatic SCI, highlighting significant pathophysiological processes that occur throughout the acute, subacute, and chronic stages of injury (Adapted from Dorrian et al. [34]).

Because many neurons have long axons and small cell bodies, most injuries to the central or peripheral nervous system ultimately mean axon damage. Axotomy is the removal of an axon by cutting or crushing, and the implications are varied [6]. Axotomy separates the axon into two segments: a proximal segment that remains linked to the cell body and a distal segment that has lost this critical attachment [6]. When axons are transected, the distal segment degenerates, a process called Wallerian degeneration [35]. The proximal segment and cell body alter, as do the synaptic inputs and targets of the damaged neuron. Synaptic transmission is disrupted at damaged nerve terminals, and calcium levels within the axon rise. Calcium activates proteases, resulting in cytoskeletal disintegration and degradation, as well as physical axon degeneration [6]. Even though the proximal end of the axon is still linked to the cell body, it suffers as well. In rare situations, the neuron itself dies of apoptosis [6].

The distal segment of an axona in the central nervous system disintegrates and myelin fragments after it is sectioned. Furthermore, reactive astrocytes and macrophages are drawn to the lesion site. A glial scar is a complicated biological environment that limits axonal regrowth. Neuronal degeneration can spread through a circuit in both anterograde and retrograde directions as a result of these transsynaptic processes [6]. The scar, on the other hand, inhibits regeneration in two ways: works as a mechanical barrier to axon regrowth and has growth-inhibiting proteins produced by cells within the scar [6].

The regeneration of cut axons is robust in the peripheral nervous system and in lower vertebrates' central nervous systems, but very weak in mammals' central nervous systems [6], usually resulting in permanent functional deficits [25, 26, 31, 36].

Central neuronal tissue is a poor source of growth-promoting molecules, containing low levels of trophic molecules. One explanation is because the environment experienced by severed core axons is both deficient in growth-promoting chemicals and abundant in growth-inhibiting substances, some of which are generated from myelin (e.g. NOGO) [6]. Therefore, supplementing the central environment with growth-promoting molecules might improve regeneration.

Environmental factors cannot fully explain the inadequate regeneration of central axons. Central neurons' growth capacity declines with age, whereas mature peripheral neurons grow axons robustly in a suitable environment. Variation in the expression of proteins known to be important for proper axon elongation is one possible explanation for this disparity. The 43 kDa growth-associated protein, or GAP-43, is one example. The amount remains high in mature peripheral neurons and grows even more after axotomy, whereas it declines in central neurons as development progresses [6].

1.3.1 Incidence, prevalence and causes

Every year, around 1 million new SCI cases are reported worldwide [37], with a prevalence of 27.04 million cases worldwide [14, 24, 31]. Although the global prevalence is equivalent between genders, men have a higher incidence than women between the ages of 20 and 40 [24].

There is no national database for SCI injuries in Portugal, therefore it is difficult to predict the true nature of the prevalence of SCI. In 1988, Martins et al. [38] claims the annual incidence rate was estimated at 57.8 per million inhabitants, with an annual survival rate of 25,4 per million inhabitants. However, this study was done in Portugal's central region and not representative of the country's overall SCI population. Furthermore, the major causes of injury were traffic accidents and falls, representing 57.3% and 37.4%, respectively [24, 38].

1.3.2 Classification of Neurological Injury

The current international standard method of classification is the American Spinal Injury Association Impairment Scale (AIS). SCI can be complete or incomplete according to the extent of the damage to the spinal cord [2, 25]. Complete SCI are characterized by a cease of all neural communications across the transection site [26]. Meanwhile, incomplete SCI are formed by smaller or discontinuous lesions that maintain sufficient neural tissue to guarantee neural communication [26].

Grade A patients have complete spinal cord injuries and hence no motor or sensory function (including sacral roots) below the site of lesion. Grade B patients have sensory function but no motor function. If a patient has a motor strength of less than 3/5 in more than half of the major muscle groups below lesion, it is classified as Grade C. On the other hand, patients that have motor strength of 3/5 or more have a Grade D. Grade E patients have complete motor and sensory function after SCI [25, 39, 40]. The most common injury is currently incomplete tetraplegia (45%), followed by incomplete paraplegia (21.3%), total paraplegia (20%), and complete tetraplegia (13.3%) [41].

1.3.3 Consequences of Spinal Cord Injury

The level of SCI is significant because sensory and/or motor dysfunction occurs below the level of injury, with higher lesions affecting a broader portion of the body [2]. In addition to the loss of control in the upper and lower limbs, SCI can lead to various problems, such as infections of the bladder and kidneys, as well as bowel, heart, sexual and respiratory system disorders [42].

Lower cervical (C5 – C8) SCI can result in varying degrees of upper extremity function loss. SCI from C1 to C4 frequently results in *tetraplegia* (paralysis of the four limbs). The C5 nerve root primarily innervates the deltoid muscle, which is in charge of shoulder abduction as well as elbow flexion. As a result, C5 complete SCI (ASIA A) is the most dependant on assistance with everyday life. The C6 nerve root controls wrist extension and biceps flexion, the C7 nerve root controls elbow extension and wrist flexion, and the C8 nerve root controls finger flexion. Individuals with incomplete SCI below C6 have significantly greater independence, with patients able to move autonomously with (C6) or without (C7 or C8) the use of a transfer board [2, 24].

Patients with *paraplegia* or *tetraplegia* do not pressure their spines or limbs due to movement restrictions, resulting in mechanical unloading that disrupts bone homeostasis. In some patients, losing weight causes increased bone resorption and inhibits bone formation. The resulting osteoporosis is largely limited to the long bones that have been damaged, increasing the risk of fragility fractures.

[2, 25]. On the other end, ulceration develops as a result of continuous pressure over a bony prominence caused by immobility, poor nutrition, and changes in skin physiology [25]. The annual incidence of pressure ulcers in SCI patients ranges from 20% to 31%, resulting in quadrupling annual costs when compared with SCI patients without ulcers [25].

SCI in the cervical or upper thoracic regions can impair respiratory muscle function, resulting in exercise intolerance or even severe respiratory failure necessitating mechanical ventilation [25]. Moreover, because of the higher prevalence of coronary artery disease and hypertension following SCI, patients are at an elevated risk of ischemic heart disease [25]. The sedentary nature of SCI patients aggravates this condition.

SCI also interferes with both bladder storage and emptying. As a result of these disorders, many patients require intermittent catheterisation or indwelling catheters, which raises the risk of urinary tract infection [25].

Sexual dysfunction frequently results after SCI, in addition to urological difficulties [1]. Impotence affects around 75% of males following SCI, with the severity of the damage dictating the kind of sexual dysfunction [25]. If there is a lesion at the sacral roots level, the parasympathetic innervation will be ceased and erections from tactile stimulation are impacted (reflexogenic erections) [25]. Psychogenic erections are also affected when lesions affect sympathetic pathways originating from T10 – T12 [25]. Moreover, women with SCI have been reported to have a reduced capacity to experience orgasm following SCI [25].

Finally, in many cases, SCI results in the development of pain syndromes, anxiety and depression [20, 24].

1.4 Spinal Cord Injury Therapies

Neurons are the most important components of the spinal cord, and neuron loss is the primary cause of poor functional recovery following SCI. The fundamental goal of SCI therapy is to reduce secondary neuronal loss or regenerate neurons. To restore the lost function due to the injury, scientific innovations have been put in place. Therapies can target a variety of issues, such as improving strength and range of motion [2].

The discovery that the spinal cord possessed plastic characteristics led to the development of novel rehabilitation treatments for SCI in humans [20]. Patients with incomplete SCI benefited significantly from regular training on a moving treadmill [20]. Physical training is standard practice for incomplete SCI

patients all around the world [24]. Current treatment techniques are restricted and mainly focused on the use of anti-inflammatory drugs such as methylprednisolone, although recent trials have failed to show compelling beneficial results [42].

Significant evidence from animal models show that spinal cord decompression promotes functional recovery and reduces secondary injury following SCI [20]. However, there are currently no effective and reliable clinical treatments available for SCI patients. The most common surgical procedures performed by physicians are spinal cord stabilisation and decompression combined with a high dosage of methylprednisolone therapy [20].

Animal research has made advances in recent decades toward preventing subsequent damage after injury, repairing the axons of injured neurons in the spinal cord, and promoting the regeneration of severed axons through and beyond the site of injury. In many cases, axon regeneration has been linked to recovery of locomotor function. However, none of the regeneration procedures have progressed to the point where they may be employed safely in patients with spinal cord injuries [6].

In recent years, the function of rehabilitation in SCI treatment has grown in importance. Appropriate rehabilitation training aids in the amelioration of cardiorespiratory dysfunction and the prevention of muscle atrophy following SCI, implying its value in improving residual functions and regaining lost functions [14]. Repetitive, weight-supported stepping on a treadmill is a particularly effective strategy for improving walking in patients with partial spinal cord injury [6].

1.4.1 Cell Therapies

Cell transplantation into the spinal cord, such as olfatory ensheating glia cells, neural stem/progenitor cells (NSPCs), mesenchymal stem cells (MSCs), and more recently, induced pluripotent stem cells (iPSCs), is one method currently under development for regeneration of lost tissue following SCI [24, 31, 42, 43].

Controlling the differentiation of stem cells into neural cells with precision and efficacy is a precondition for using stem cells in nerve tissue creation [43].

a) Mesenchymal Stem Cells

MSCs are immunogenic and immunomodulator multipotent cells, that do not form malignancies, and have a pathotropic – moves towards site of lesion – function [20]. These cells are also simple to isolate and expand from easily accessible sources of adult or post-natal tissues, such as bone marrow (BM-MSCs), adipose tissue (ASCs), umbilical cord, and others [44]. Furthermore, they can be readily applied in

autologous transplants and secrete neurotrophic factors, anti-inflammatory cytokines, extracelullar matrix proteins, neuroprotective and neurodifferentiation agents that aids tissue repair [44].

Although the mechanism of action is not fully understood. Various studies point to secreted proteins and vesicles – their secretome – as agents for cellular differentiation rather than differentiation into new neural tissue [44]. The concept of secretome is subject to change, however it is recognized that, in addition to soluble components, the secretome contains lipids and extracellular vesicles (EVs) containing essential molecules [16, 44]. Growth factors that have been reported in BM-MSCs and ASC secretome include: glial-derived neurotrophic factor (GDNF); vascular endothelial growth factor (VEGF); nerve growth factor (NGF); brain-derived neurotrophic factor (BDNF); basic fibroblast growth factor (bFGF); hepatocyte growth factor (HGF); insulin-like growth factors 1 and 2 (IGF-1 and IGF-2); transforming growth factor beta 1 (TGF-β1) [16, 44]. The effects of these cytokies are presented in table 1.

Table 1. Main effects of MSC secretome composition [14, 16, 44–46].

Growth Factor	**Effect**
VEGF	Neurogenesis, Neuromaturation, Neuroprotection, Neuroregeneration, Angiogenesis, Cell Survival and Immunomodulation
GDNF	Neuroprotection
bFGF	Cell survival, Cell growth, Immunomodulation, Cell Migration, Development, and REgulating Apoptosis
NGF	Axonal Growth, Vascularogenesis and Cell survival and Cell growth
HGF	Axonal Growth, Vascularogenesis, Angiogenesis, Differentiation, Cell growth and survival
BDNF	Axonal Growth, Vascularogenesis, Synaptogenesis
IGF	Cell survival, Cell growth and Angiogenic

Moreover, MSCs can release a number of soluble molecules with anti-inflammatory properties, such as tumor necrosis factor (TNF)-β1, interleukin (IL)-13, IL-18 binding protein, ciliary neurotrophic factor (CNTF), neurotrophin 3 factor (NT3), IL-10-, IL-12p70, IL-17E, and IL-27 [47]. Furthermore, MSCs can suppress the release of pro-inflammatory cytokines such as interferon, TNF, and IL-10, resulting in a regulated host cytokine output [46].

Extracellular vesicles play a crucial role in transporting materials from donor cells to recipient cells and acting as intercellular communication mediators [16]. The EVs contain nucleic acids, bioactive lipips and

proteins that are released to the extracellular space via membranal fusion [16, 44]. However, the genetic and epigenetic memory of the cells, their pathogenic state, etc., as well as the source of the MSCs, donor-related characteristics like age and health status, etc., determine the composition of the EVs [16]. EVs can influence the activity of target cells by interacting directly with the cell membrane via antibody receptors or releasing their biologic content on cell cytoplasm, ultimately promoting angiogenesis, neurite outgrowth and regulation of inflammatory responses [44]. ASC secretome, for example, has previously been shown to be a potent modulator of neuronal and glial cell survival and differentiation, as well as a promoter of neurite formation and inducer of new vascularization [48]. Therefore, it is of interest to investigate the effects of these secretome components on CNS cells survivability and differentiation. Additionally, it has been shown that the secretome of MSCs affects axonal function by stimulating their growth via the action of trophic factors such BDNF, HGF, and VEGF and by strengthening neuronal connections [16]. Studies have demonstrated that injecting secretome into injured animals increases neuroprotection, attenuates cavity development, and preserves the spinal tracts [16].

MSC-based therapies are not regarded as the norm at the clinic due to a number of barriers to their use. First, the lack of regular practices for cell culture, ex vivo growth, cryopreservation, and differentiation alters the characteristics of MSCs and, as a result, causes stemness attenuation and replicative senescence [16]. To make a noticeable difference in transplanting, a large number of cells are needed [16]. In addition to having a low survival rate after this surgery, MSCs also seldom integrate into the damaged location, as previously discovered by cell tracking research [16]. When choosing these cells for transplantation, it is also important to take into account challenges in developing a proper therapeutic rationale, such as choosing the best dosage type, frequency of administration, mode of infusion, and efficient delivery route [16].

Given the aforementioned drawbacks, the use of MSCs as a whole has recently been put on hold, and in their place, a direct application of their secreted trophic factors is being investigated as part of a rapidly developing cell-free therapy approach. These factors may be the fundamental building blocks needed to develop effective cellular strategies [16].

b) Neural Stem Cells

Neural Stem Cells (NSC) have self-renewing capabilities and are able to differentiate in to neurons and glial cells in the nervous system (Figure 6) [31, 36, 42, 49]. Therefore they have the capacity to renew the lost tissue at neuronal injury sites. NSCs can influence the inflammatory and immunological microenvironments, polarizing macrophages to the anti-inflammatory M2 subtype [31]. They can also

produce growth factors to promote axonal development in motor and sensory neurons [6, 31].

Neural stem cell therapy appears to be a promising option for regenerating damaged neurons, assisting functional restoration via stem cell differentiation into neurons and glial cells, secreting cytokines and growth factors, activating endogenous repair via immunomodulation, and inhibiting cell apoptosis and fibrosis [50].

Figure 6. Neural Stem Cell Differentiation (Adapted from Kandel et al. [6]).

NSCs can be sourced from differentiation of pluripotent stem cells – such as iPSCs – and transdifferentiation from somatic cells [24, 31, 36].

NSCs can be isolated and grown into single-cell suspensions, which eventually form normal

neurospheres [24]. These non-adherent neurospheres are particularly intriguing due to their potential to self-renew and to produce a favorable extracellular-matrix that aids in stemness maintenance [24]. Furthermore, neuspheres can be subcultured and grown to increase the available cell pool [24]. Adult NSCs, on the other hand, have the disadvantage of not being able to be used as an autologous cell source [24].

The spinal cord contains a niche of NSCs which do not demonstrate multipotency or undergo neural differentiation *in vivo* [20, 51]. Spinal cord derived-NSCs, on the other hand, are capable of generating neurons when extracted and injected into the brain. This led to the theory that the spinal cord microenvironment inhibits the stemness capability of these cells [51].

c) Induced Pluripotent Stem Cells

One of the most significant breakthroughs in regenerative medicine and biological research was the finding of iPSCs [24]. The idea of converting adult somatic cells, such as blood cells or skin fibroblasts, into NSCs via iPSCs sparked a flurry of research in the subject [24]. iPSCs-derived-cells have an advantage in being adult-derived and can be transplanted autologously, avoiding both ethical problems and immunological rejection [31, 36]. Skin fibroblasts are the most common source of human iPSCs. A skin biopsy, however, may not be the best source due to the risk of infection and scarring. As a result, different less invasive somatic cell sources, such as peripheral blood, have been investigated because of the minimal procedures necessary to collect it [24]. iPSCs are regarded as substitute embryonic stem cells (ESCs) with infinite proliferation in culture since they have the same potential for differentiation as ESCs (both spontaneously and in response to particular signals). From the three layers of embryonic germ cells, they can develop into all known cell types (ectoderm, mesoderm, and endoderm) [16].

After transplanting iPSC-derived NSCs into SCI animal models, promising results were seen in terms of cell survival, tissue preservation, and neural development of cells [24]. Furthermore, functional recovery was found in the spinal cord via axon remyelination and activation of supporting neurotrophic factors [24]. Preliminary animal investigations, however, indicate that tumor growth is a severe issue caused by undifferentiated iPSCs [31]. Furthermore, these are very expensive, and more research is needed to understand their truly therapeutic potential and safety after SCI [31].

NSCs can also be created from somatic cells using iPSC-derived NSCs and iNSCs. Somatic cell candidates include astrocytes, fibroblasts, and human umbilical cord blood cells. Somatic reprogramming can be triggered by specific transcription factors and/or pharmacological compounds. Finally, iNSCs are obtained by direct reprogramming, bypassing the iPSC stage. When compared to iPSC-derived NSCs,

iNSCs have the distinct advantages of less expensive preparation techniques and lower tumorigenic risk, making them attractive candidates for NSC-based therapy [31].

1.4.2 Pharmacological and Molecular Therapies

The purpose of molecular therapeutic intervention is to promote axonal regeneration and sprouting, protect neurons from cell death, and improve nerve fiber transmission [52]. There are numerous chemicals that can be employed to either mitigate the harm caused by secondary injury or to encourage regeneration and restore lost connections and functions in the spinal cord following injury [52]. Some molecular compounds that have been used after SCI will be discussed in this chapter.

a) Anti-inflammatory Molecules

Methylprednisolone is a synthetic glucocorticoid agonist that is useful in the early stages of acute SCI due to its anti-inflammatory and neuroprotective properties, primarily in the prevention of lipid peroxidation [14, 53]. However, these clinical trials demonstrated only minimal functional improvement, which was linked with significant immunodepression and recurring infections, discouraging its usage [53].

Minocycline is a clinically accessible anti-inflammatory drug that works by inhibiting neuroinflammation and neurodegeneration via retinoic acid signaling [52]. It has been found in preclinical studies to limit subsequent growth of the lesioned region, hence lowering autonomic dysreflexia [52]. Minocycline can improve the local inhibitory microenvironment after SCI, mostly by slowing cell death and lowering levels of free radicals, inflammatory cytokines, and MMPs [28, 54, 55]. SCI is frequently associated with the activation of numerous cell death signals, which results in the death of neurons and oligodendrocytes. Minocycline therapy not only opposes the inflammatory environment by raising interleukin-10 expression and decreasing tumor necrosis factor-alpha expression, but it also prevents further apoptosis development following injury by drastically decreasing caspase-3 activity [14].

b) Voltage-Gated Cation Channels Antagonists

Riluzole is an FDA-approved sodium channel blocker used to slow the course of amyotrophic lateral sclerosis. The negative consequences following SCI eventually lead to an increase in cell mortality due to the progression of cell edema, glutamine excitotoxicity, and acidosis [14]. In animal models, riluzole-induced voltage-gated sodium channel blockage lowers both glutamate release and excitotoxicity following SCI [28, 52, 56]. Nonetheless, in the high-dose administration experiment, some unanticipated adverse

effects, including as locomotor ataxia and lethargy, occurred [57].

Diazoxide is a potassium channel activator that is often used to treat hyperinsulinemic hypoglycemia [58]. Yamanaka et al. [59] demonstrated that Diazoxide injection resulted in considerable activation of STAT3, which resulted in retained neuronal viability, motor function, and protection against the intrinsic apoptotic pathway, hence attenuating spinal cord ischemia-reperfusion injury.

c) Growth and Neurotrophic Factors

Growth factors and neurotrophic factors are neuronal cell secreted biomolecules that promote neuronal cell development, differentiation, and survival, neurite outgrowth, synaptic plasticity, and neurotransmission by influencing the topography of axonal projections during development and regeneration. Most neurotrophic factors belong to one of the three families: (A) neurotrophins (NGF, BDNF, NT3, and NT4), (B) glial cell-line derived neurotrophic factor family ligands (GDNF, Neurturin, Artemin, Persephin), and (C) neuropoietic cytokines (CNTF, leukemia inhibitory factor (LIF), IL6, and others) [14, 52].

1.4.3 Electrical Stimulation

Endogenous electrical stimulation occurs *in vivo*. Impermeable membranes separate ions and other charged biomolecules from the extracellular and intracellular regions. Ions can move within the cell and be selectively transported by ion channels located in the membrane. The asymmetric distribution of ion channels at the apical and basal membranes results in a unique pattern of ions and biomolecules, as well as separate charge domains. This causes an electrical potential differential between the cell membrane and the extracellular space, known as a membrane potential (V_{mem}) [51]. This endogenous electrical stimulation has been found to induce tissue regeneration, recruit NSC to the injury site and improve healing [49]. It is also possible to apply an exogenous electrical stimulation (ES) that allows for artificial stimulation of action potentials by inducing electrical charge to the cell and manipulate ion channels [49, 51].

While glial cells are not classically excitable by electrical stimulation (they do not generate action potentials), they are extremely sensitive to both the direct effects of electrical stimulation on nervous tissue and the indirect effects on nearby neurons affected by stimulation [60]. Although microglia do not conduct action potentials like neurons, their activities are influenced by membrane potentials and ion channels [61, 62]. Similarly, astrocytes have ion channels that control the flow of ions (e.g., K^+, Na^+, Ca^{2+}) between the cytosolic and extracellular areas [63, 64]. Transient elevations in calcium ion concentrations in astrocytes, for example, have been shown to influence processes such as plasticity and neurotransmitter

and gliotransmitter release at the synapse [65, 65]. Ishibashi et al. [66] found that astrocytes promoted myelination in response to biphasic electrical impulses.

There are three types of ES delivery methods *in vitro*: direct coupling, capacitive coupling, and employing an electromagnetic field (Figure 7) [67].

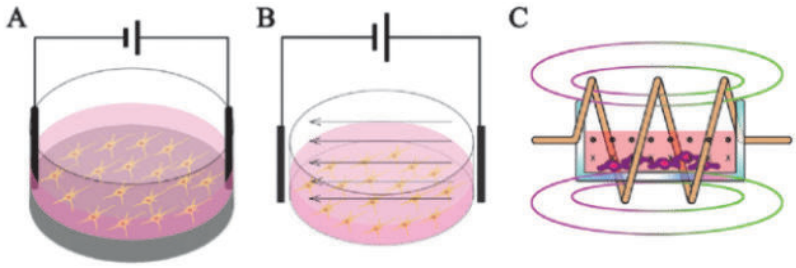

Figure 7. (a) Direct Coupling; (b) Capacitive Coupling; (c) Inductive (Adapted from Chen et al. [67]).

To provide ES, electrodes are inserted directly into the growth media and linked to the scaffold by direct connection [67]. This approach is the most common for its simple application. Some drawbacks must be addressed such as: insufficient biocompatibility of the electrodes, temperature increase of the medium when in contact with the electrodes; pH changes; creation of hazardous byproducts [67].

On the other hand, capacitive coupling is considered more safe as it the device does not come in contact with the cells. Two electrodes are placed on opposite ends to apply a uniform electric field to cells seeded on the scaffold. Additionally, this system does not need a conductive scaffold to provide the uniform ES [67].

Finally the inductive coupling allows for the use of a controllable electromagnetic field generated by a conductive coil placed around the cell culture [67]. This device is called pulsed electromagnetic field stimulation (PEMF).

a) Generating ES Signals

An electrical stimulation signal can be varied depending on the waveform and intensity by altering its parameters, according to the application [51]. The intensity of the electrical impulses is controlled by three parameters: the duration, amplitude and frequency of the pulse (Figure 8) [2, 25]. The pulse duration or pulse width is the amount of time the stimulation is present. The pulse amplitude is the magnitude of the stimulation and determines which type of nerve fibers respond to the stimulation [2, 25]. The rate at which stimulation pulses are given is defined as pulse frequency (1/Frequency).

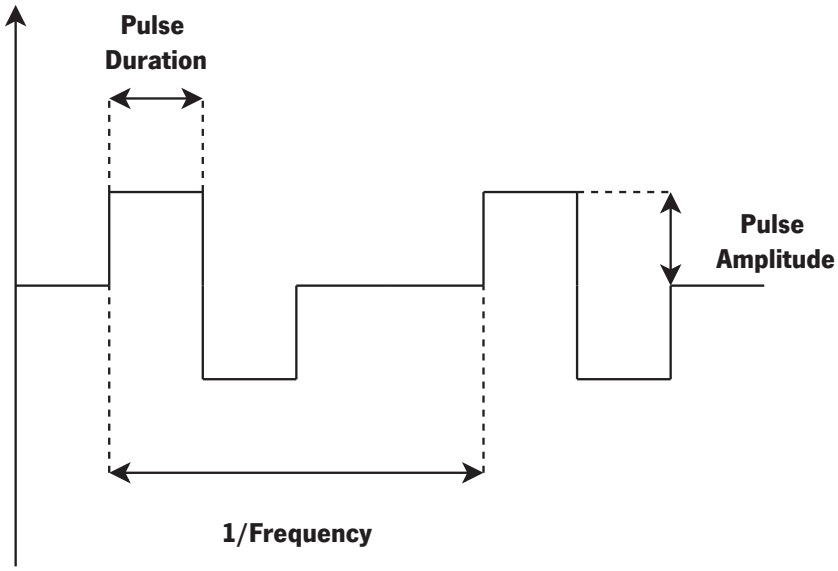

Figure 8. Electrical stimulation parameters: pulse duration, pulse amplitude, and pulse frequency.

Electrostimulation pulses can be monophasic, also known as direct current, or biphasic, also known as alternating current. Monophasic pulses are unidirectional, whereas biphasic pulses are bidirectional having a positive and negative phase [25]. ES can produce monophasic and biphasic waveforms with pulse, sinusoidal, square, triangle, and sawtooth patterns (Figure 9) [67]. EFs can be further divided according to the direction of current with time, these can be categorized as direct current electrical fields (DCEFs) where magnitude and direction do not change with time, alternating current electrical fields (ACEFs) where magnitude and direction change periodically with time, pulse current electrical fields (PCEFs) where the current is unidirectional or bidirectional for a short duration, and biphasic electrical currents (BECs) where the current is bidirectional.

This process is non chemical and allows for change of parameters to vary according to stem cell and has been used *in vivo* and *in vitro* [49].

The ES affects the physiology of the cell surface such as enzyme activity, membrane protein functions, membrane receptor complex and ion-transporting channels by changing charge distribution [49]. ES can be divided in two categories: Electrical Fiels (EF) and Electromagnetic Fields (EMFs).

Neuromodulation methods have since changed their focus to attaining functional recovery following SCI. Post-SCI, epidural electrical stimulation (EES), peripheral nerve stimulation (PNS), and functional electrical stimulation (FES), among other forms of stimulation, have been used with encouraging outcomes [34].

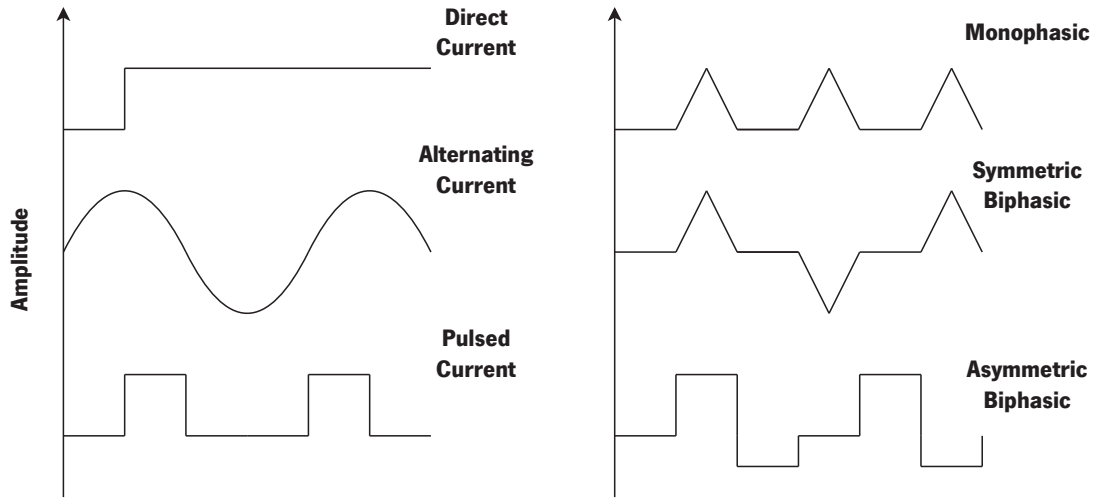

Figure 9. Examples of electrical stimulation waveforms.

b) Epidural Electrical Stimulation

The use of epidural electrical stimulation (EES) on SCI has been present for over half a century [25]. In the 1960s, one of the earliest applications of electrical stimulation was to stimulate the peroneal nerve to activate muscle action and correct foot drop in patients of stroke-related hemiplegia [25].

Due to damaged pathways, complete SCI prevents any signal from descending below the level of the lesion [25]. Some pathways are intact even in complete SCI injuries, albeit these circuits are frequently insufficient to produce an adequate level of excitability to excite motor neurons caudal to the lesion [25]. Electrical stimulation is thought to act by causing neuroplastic changes at synapses in the spinal cord [25].

Several trials utilizing epidural electrical stimulation (EES) have recently demonstrated promising outcomes in facilitating mobility and carrying weight following severe SCI [68–72]. Nonetheless, the neurophysiological processes behind EES are mainly unclear [34, 72]. The neuromodulatory potential of ES to drive motor output originates from its ability to bring spinal neural networks closer to excitation threshold levels, allowing residual descending supraspinal input and afferent feedback to enable intentional movements [73]. Even in patients who have "clinically complete" injuries, evidence of remaining supraspinal connections below the injury site is detected post-SCI [34].

EES is administrated over the spinal cord through an implanted paddle electrode array. To stimulate mobility, stimulation is typically given across the lumbosacral spinal cord. However, cervical EES may also be employed depending on the intended goal [74]. A paddle electrode array is surgically placed across

the spinal cord by a laminectomy to deliver EES, with electrode location validated using x-ray, fluoroscopy, and electrophysiology [75].

Harkema et al. [70] found that EES and intense rehabilitation allowed full weight-bearing locomotion on a patient with chronic, motor-complete and sensory incomplete SCI (AIS B). There is evidence that electrical stimulation of the cord can increase expression of BDNF/ TrkB in spinal motor neurons [74]. Electrical stimulation of the nervous system can cause intracellular calcium influx, resulting in an increase in BDNF expression in the spinal cord that is ERK-dependent. As a result, EES might possibly promote neuroplasticity via comparable biological mechanisms [76].

Baba et al. [77] discovered that epidural electrical stimulation of the rat brain has neuroprotective effects after ischemic stroke. Neurotrophic factors (glial cell line-derived neurotrophic factor, brain-derived neurotrophic factor, vascular endothelial growth factor) were shown to be upregulated. Electrical stimulation also increased angiogenesis while suppressing the growth of microglia and astrocytes.

EES has certain limitations, despite the anticipated improvements in motor and autonomic functioning. Notably, electrode implementation necessitates an intrusive surgical procedure that, while normally absent of consequences, can harm spinal stability and increase the risk of infection [78]. EES requires a surgical implant to be placed on the dorsal surface of the spinal cord, making it more invasive than transcranial direct current stimulation (tDCS), but it lacks the target specificity provided by penetrating electrodes used in procedures such as deep brain stimulation (DBS) and intraspinal microstimulation (ISMS) [60].

An invasive implant triggers a foreign body reaction mediated by microglia and astrocytes. This might potentially worsen any tissue reaction to the device where gliosis will ensue and a scar will form that encapsulates the implant.[60]. The magnitude of this reaction is partially determined by the stiffness of the material with stiffer materials such as metals, mechanical mismatch between the implants and tissue is exacerbated by micromotion-induced stresses [79]. The materials are typically inert, meaning they do not leak harmful particles into the surrounding tissue on their own [60]. The material used to manufacture the implant, as well as the characteristics of the paradigm itself, determine whether electrical stimulation results in electrochemical reactions at the interface that produce hazardous chemicals [79, 80].

Stimulation settings are frequently patient-specific, and adjusting activation patterns takes time and may cause rehabilitation to be delayed [74]. According to studies in animal models and people, the most efficient EES stimulation frequencies for permitting standing are 5-20 Hz, whereas frequencies in the range of 25-60 Hz are better for locomotion [34, 74]. Finally, participants in EES research frequently undergo intensive physical rehabilitation that far beyond what is routinely offered post-SCI [78]. Rowald et al. [81]

did a study with EES and participants received 1 to 3 hours of personalized rehabilitation for 4 to 5 days each week over 5 months, accumulating 80 to 300 hours. In contrast, the average rehabilitation received by individuals is an average of 55.3 hours during inpatient programs [34].

1.4.4 Tissue Engineering

Tissue Engineering (TE) is a field that aims to combine cells and molecules into functional structures that have the potential to repair, replicate or replace an injured or diseased tissue [14, 67]. It involves the knowledge from material science, engineering, physics, chemistry, biology and medicine. As a result, TE usually combines cells, bioactive molecules and biomaterials [20]. The primary function of biomaterials in TE is to encapsulate and support living cells. For this very reason, many of the biomaterials used are sourced or resemble the extracellular matrix [82].

Cell–cell and cell–extracellular matrix interactions within a native tissue generate a communication network via biochemical and biophysical cues, which is critical in maintaining tissue specificity and homeostasis. These interactions allow for proliferation, migration and apoptosis [83]. TE seeks to replicate the shape and function of tissues or organs by using designed scaffolds that improve cell–biomaterial interaction and mimic the original environment [67].

In order to ensure the success of the therapy, scaffolds need to possess a number of properties. The biomaterials chosen should: be **biocompatible**, as not to elicit an immune response post implantation; have **mechanical properties** that resemble the tissue to be replaces, which includes a large surface area, high porosity, interconnected geometry and mechanical strength; be **biodegradable**, as to degrade over time after implantation as new tissue is regenerated; **surface properties** that improve the chemical and topographical signals that modulate cell organization and behaviours [20, 67, 82, 83].

The mechanical properties of the native spinal cord must be considered when designing and fabricating scaffolds for SCI: favorable surface chemistry, sufficient pore size, porosity, and surface area for cell loading and cell surface interaction, as well as axon regrowth, nutrient transport, and a biodegradation profile that produces adequate residence time [84]. Hydrogels, due to their physical qualities, may be the best biomaterial for repairing soft tissues such as nerve tissue [85].

In neural tissue engineering, natural polymers can be modified to have different roles, such as matrix formers, gelling agents and drug release modifiers [86]. Furthermore, the use of these biomaterials of natural origin are beneficial for their biocompatibility, biodegradation and modifiable chemically properties [86]. A successful scaffold structure has shown to improve neurite growth, inhibition of formation of scar tissue, provide guidance for axonal growth, promote regeneration and stimulate the integration of existing

healthy tissue [86].

Lu et al. [87] treated SCI with NSCs and discovered that NSCs alone did not fill the transection site. As a result, they employed fibrin matrices containing a mixture of growth factors and NSCs. The graft's axons extended into the host tissue, and the host's axons likewise extended into the graft. Based on these findings, fibrin matrices loaded with NSCs and a combination of growth factors may be able to change the unbalanced microenvironment to promote regeneration.

Polysaccharides are a group of biomaterials with a significant potential to be utilized in TE for being processable and biocompatible [82].

a) Gellan-Gum

Gellan gum (GG) is a polysaccharide produced as a fermentation product of *Pseudomonas elodea* as a major constituent of their extracelullar matrix [82, 88]. GG is a linear, anionic and high molecular weight polysaccharide composed of repeating tetrasaccharide unit consisting of two glucose residues, one glucuronic acid and one rahmnose residue (Figure 10) [42, 89]. Due to its chemical composition multiple hydroxyl groups are available for chemical modification [42]. GG exists in the acetylated (native) form and in the deacetylated form. Both these forms are capable of forming a gel after transition from a coiled form to a double helix structure when cooled [88]. The mechanical properties and gelation of the GG can be modulated according to the degree of deacetylation [88, 89]. The junction zones of GG networks are strongly stabilised by divalent cations, such as Ca^{+2} and Mg^{+2} in a process known as ionic crosslinking [82, 88].

Characteristics such as noncytotoxicity, heat and acid resistance, biodegradability make for a desirable material in the use of neural tissue engineering. However some limitations have been shown on these hydrogels, such as insufficient mechanical proprieties, high gelling temperature and the absence of specific anchorage sites for cells [88]. To overcome these issues, chemical modifications allow for a tuning of physicochemical and biological properties.

To better mimic the extracellular matrix, Silva et al. [42] modified GG with a fibronectin-derived peptide sequence GRGDS via Diels-Alder click chemistry. GRGDS has been found to improve cell–biomaterial interactions, promote cell survival, and impact cell morphology [42]. The GG–GRGDS demonstrated a profound positive effect on NSPCs morphology and proliferation, however the differentiation profile was unchanged. Silva et al. [91] reported GG-GRGDS to be biocompatible and nontoxic after injection in a hemisection SCI rat model. Subsquent works demonstrated that GG-GRGDS implantation in lumbar or cervical injuries of the spinal cord lead to locomotor and respiratory recovery [92, 93].

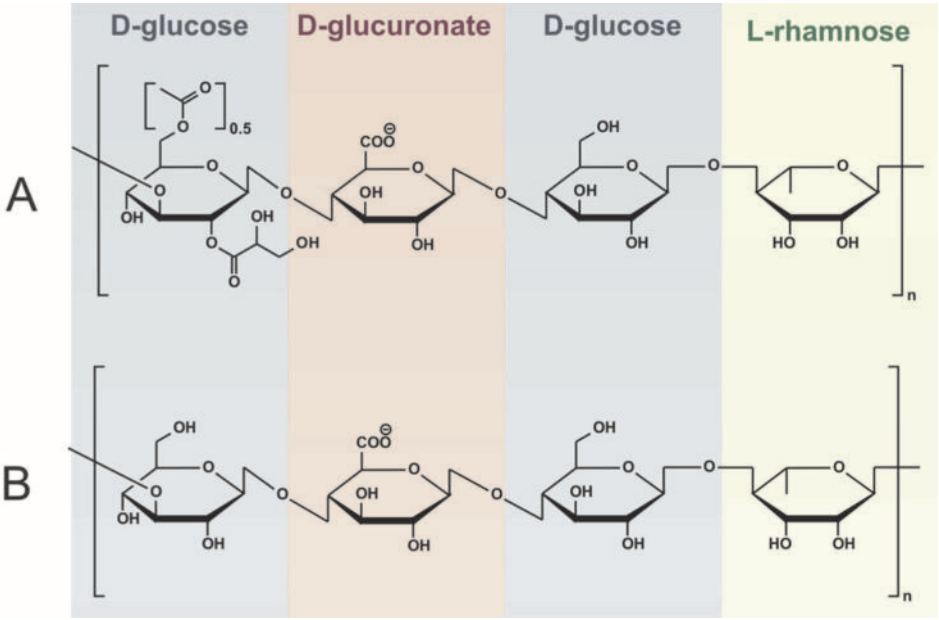

Figure 10. Structure of native (A) and deacetylated form (B) (Adapted from Osmałek et al. [90]).

The gellan gum hydrogel is also appealing because it may be injected to form a gel *in situ* in a minimally invasive process by filling the lesion cavity [28, 42].

Having into account the complexity of the pathophysiology and the different therapeutic approaches mentioned above, the main aim of this thesis is to test different therapeutic combinations for SCI repair.

2 Objectives

The main objective is to develop a multidisciplinary approach that targets the major aspects of the pathology around the SCI. Not only promoting neuroregeneration and foster neuroplasticity of the injured tissue but also the development of an artificial extracellular matrix to support cell growth and survival. A diagram with the proposed therapies can be seen on Figure 11. To achieve this therapy, the specific aims of this thesis are:

Objective 1: Study how Electric Stimulation can modulate the 2D hNSCs differentiation *in vitro*;

Objective 2: Study how Electric Stimulation can modulate the secretome of ASCs *in vitro*;

Objective 3: Study the effect of Electrically Stimulated ASCs secretome on glial cells.

Objective 4: Study the effect of Electrical Stimulation in the growth and morphology of ASCs encapsulated in the Gellan Gum hydrogel;

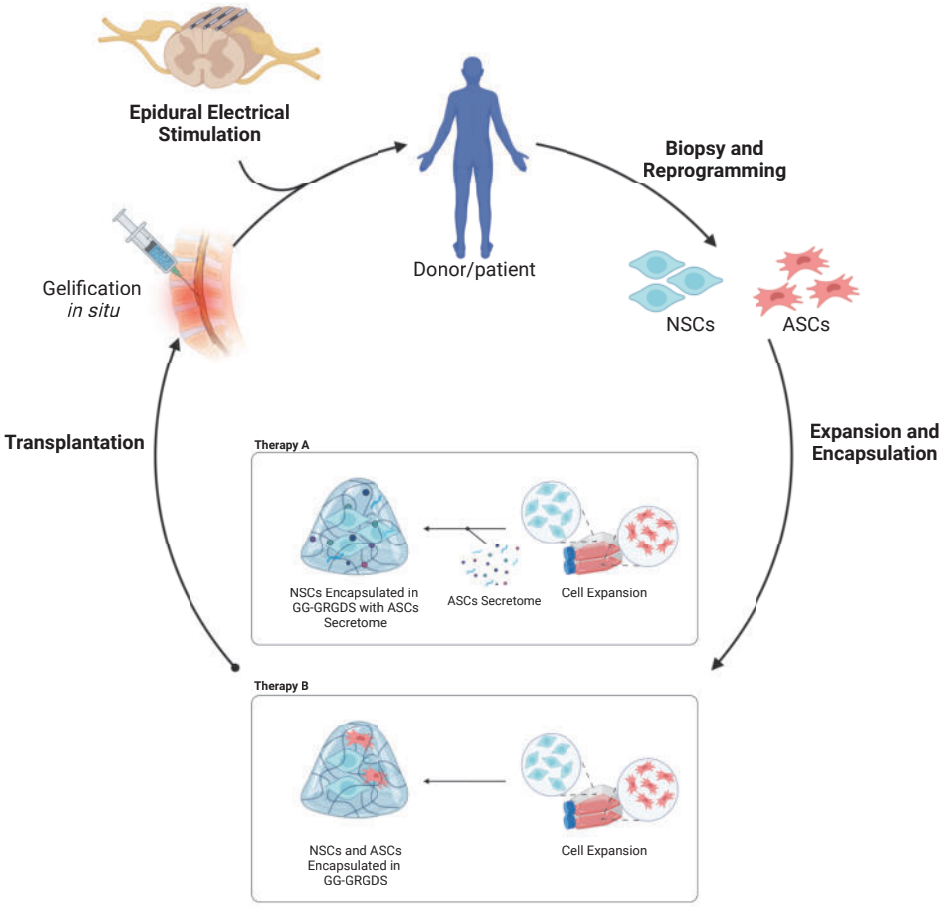

Figure 11. Diagram of proposed therapy. Autologous NSCs and ASCs are expanded. Two therapies are proposed: Therapy A) Encapsulating NSCs with secretome from ASCS in GG-GRGDS; Therapy B) Encapsulate NSCs and ASCs in GG-GRGDS. Then, the biomaterial is transplanted *in situ* in the glial scar. Finally, EES is applied to allow for a greater cell survival and differentiation. (Made with Biorender)

3 Materials and Methods

In this chapter, all the procedures and materials used are described. From the isolation and culture of the cells to differentiation, electrical stimulation, immunocytochemistry and finishing with imaging and statistical analysis.

3.1 Cell Isolation and Expansion

3.1.1 Human Neural Progenitor Stem Cells

hNPCs were kindle provided by Dr Leo A. Behie. Human Neural Stem Cells (hNSCs) were isolated from the telencephalon region of a 10-week postconception (gestational age) fetus (Dalhousie University, Halifax, Nova Scotia, Canada [94]) using the protocols developed at the Queen Elizabeth II Health Sciences Centre under strict ethical guidelines; Ethical consent was approved by the Conjoint Health Research Ethics Board (CHREB), University of Calgary (ID: E-18786). These cells were thawed at 37° and transferred into a T-25 cm^2 cell culture flask. Two days later, the cell sample was mechanically dissociated, in a consistent rhythm approximately 40 – 50 times, until single–cell suspension was achieved. This suspension was centrifuged at 200 x g for 10 minutes. The supernatant was discarded. Trypan Blue and a Neubauer chamber were used to count the cells. Then, the cells were seeded at a density of 1 x 10^4 viable cells/cm^2. The culture was incubated at 37°C and 5% of CO_2 in a humidified incubator.

Complete NeuroCult™ Proliferation Media was prepared according to the STEMCELL Technologies™ protocol [95]. The prepared medium was then supplemented with the following cytokines: Human Recombinant EGF (Sigma Aldrich) 1:1000 (V/V%), Human Recombinant bFGF (Sigma Aldrich) 1:2000 (V/V%) and Heparin Solution (Sigma Aldrich) 1:1000 (V/V%).

The morphology of neurospheres and medium color changes were monitored daily. The medium was replenished every 2 days, with 1 mL of fresh Complete NeuroCult™ Proliferation Media with supplements, until the cells were ready for subculture.

3.1.2 Adipose Stem Cells

ASCs were purchase from Obatala Sciences (New Orleans, LA, USA), thawed at fifth passage (P5). Each condition was seeded in cell culture flasks with a density of 4.0 x 10^3 cells per cm^2 and expanded in αMEM medium (Minimum Essential Medium α) (α αMEM, GIBCO, USA) supplemented with 10% of Fetal Bovine Serum–FBS (FBS,Invitrogen, USA), 1% Penicillin-Streptomycin (P/S, Invitrogen USA). Every 3

days the medium was changed and cells were passed by dissociation with 0.05% trypsin-EDTA (Invitrogen, USA) once 80 – 90% of cells were confluent. The cells were maintained in a 37° humid atmosphere with 5% CO_2.

a) hASCs Secretome Collection

hASCs were plated at a density of 12 x 10^3 cells per cm^2. After 72h, the medium was removed, cells were washed 4 times with phosphate-buffered saline (PBS) without Ca^{2+} and Mg^{2+}. For the electrically stimulated group, hASCs were electrically stimulated for 30 minutes in Neurobasal-A (NbA, Thermo Fisher Scientific, USA). After stimulation, the medium was replaced and the cells conditioned with 0.74 mL of new Neurobasal-A with 1% Kanamycin (Invitrogen USA), for 24h. Following this conditioning period, medium containing the factors secreted by hASCs – conditioned medium or secretome – was collected and stored at – 80°C to preserve its biological features.

3.1.3 Isolation of Cortex Cells

A mixed population of glial cell (Microglia and Astrocyte) was obtained from newborn Wistar pups (P5 – P7). The pup's brains were dissected in Hanks' Balanced Salt Solution (HBSS). The meninges were removed and the cortex collected. After mechanical dissociation with the use of scapels, DNAse (30 U/mL) and trypsin-EDTA (Invitrogen, USA) were added and incubated for 15 min at 37°C. This allows for improved cell separation from surrounding tissue. The enzymatic digestion was stopped by adding 40% of FCS into the cell suspension that is further centrifuged at 800rpm for 2min to obtain the glial cells. In case of tissue debris being present, a second centrifugation is done to remove it. The cells were then suspended in Dulbecco's Modified Eagle Medium (DMEM) supplemented with 10% FBS and 1% P/S. Cell counting was performed in a dilution of 1:1 of cells and Trypan Blue (Sigma, USA) in a light microscope (Olympus IX51, USA) using a Neubauer chamber (Marienfeld, Germany). Isolated cells were then platted on poly-D-lysine-coated coverslips at a density of 4 x 10_4 cells/cm_2 and allowed to grow for 7 days in a humidified incubator with 5% CO_2 at 37°C. The medium was replaced every 2 days.

3.2 Electrical Stimulator

The stimulation of the cells was done using an *in vitro* stimulator, developed by INL (Iberian Nanotechnology Laboratory, Portugal) and ICVS (Life and Health Sciences Research Institute, Portugal). A visual schematic of the stimulation can be seen on Figure 12. An electrical field is generated at the bottom of the well plate with field strengths of 10 to 150 V/m with pulse length of 0.5 to 10 ms and frequencies of 2 to 600 Hz. Several defined parameters can be used for stimulation, however the one selected was 25 V/m, 125 ms pulse, 4 Hz.

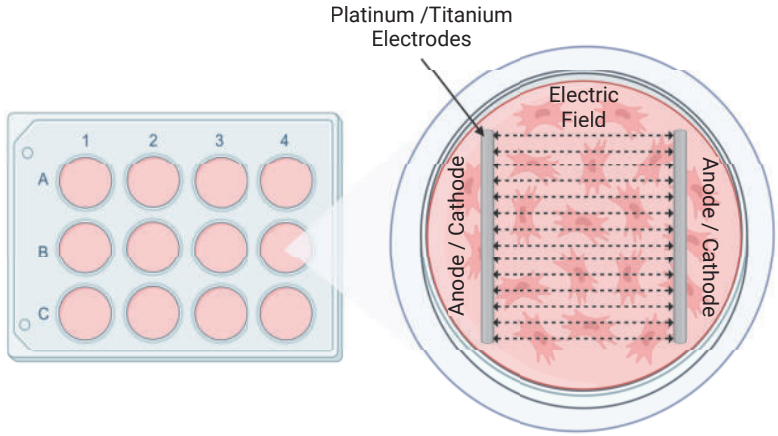

Figure 12. Setup for delivering electrical stimulation to the cells. (Made with Biorender)

The electrodes are composed of Titanium (Ti) stripes coated with Platinum (Pt) for electrochemically stability and biocompatible electrode surface. Noble metals (platinum, gold, iridium, and corresponding oxides/alloys) have emerged as preferred electrode materials due to their corrosion resistance [96, 97]. Prior to usage of this stimulator in a flux chamber the device is left on UV lights for 1 hour to reduce the likelihood of contamination.

3.2.1 Electrical Field Strength Measurements

In order to ensure the exact electrical field being applied at the bottom of the well where the cells are located (Figures 13a and 13b). A Multicomp Pro™ MP720776 Oscilloscope was used for the measurement of the electrical field with the use of a wire, as shown on Figure 13c.

Volumes of 1mL and 2mL were used to find potential differences in the field being applied to the cells. NeuroBasal-A was used for the electrical stimulation.

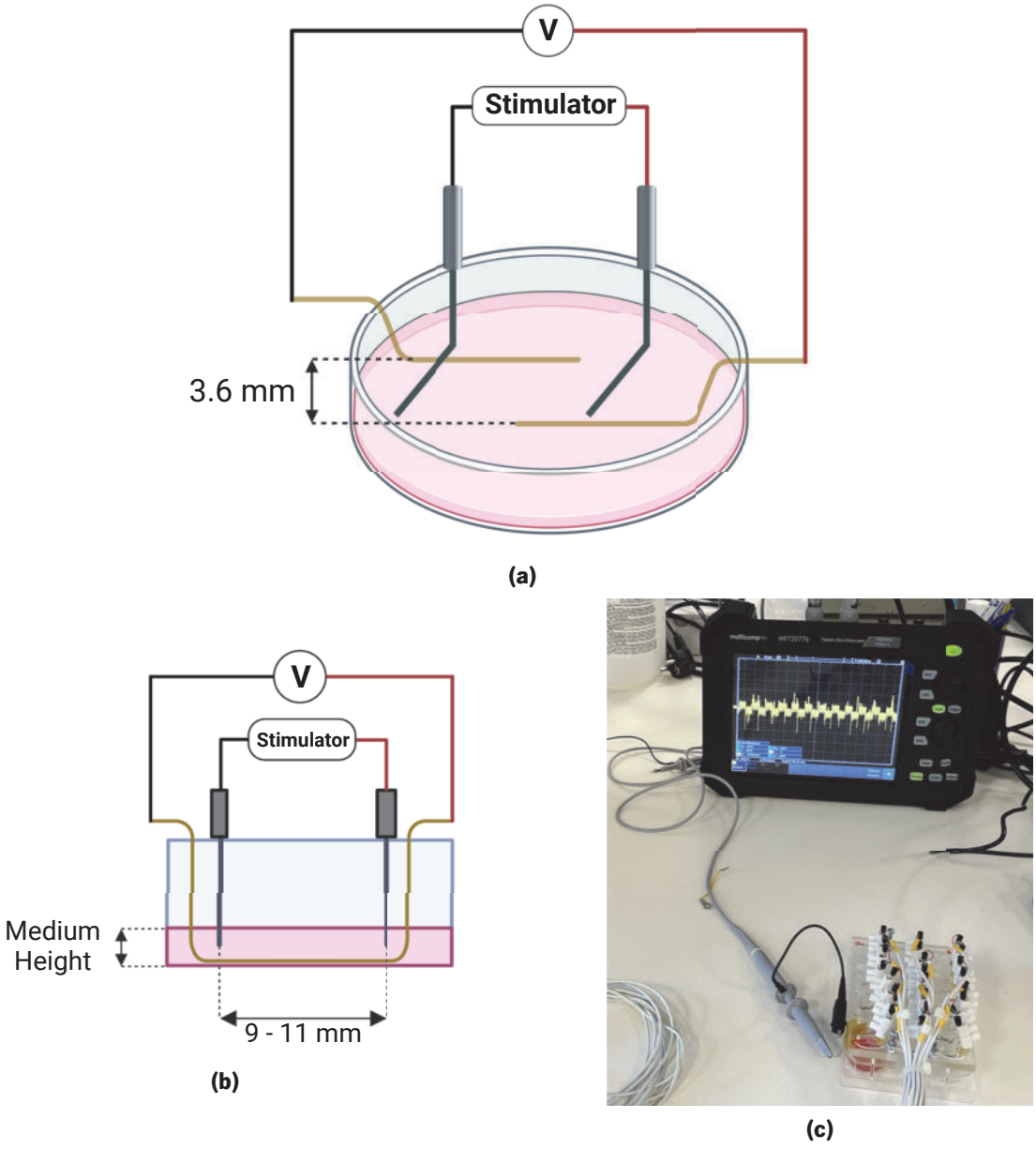

Figure 13. a) Orthogonal view of the diagram of the electrical circuit used; b) Front view of the diagram of the electrical circuit used; c) Setup used to measure the strength of the electrical field; (Schematic figures were created with Biorender).

3.3 Temperature Measurements

Due to the potential of increased temperature caused by the electrical stimulation, temperature was measured for the time points used in the assays (10 and 30 minutes), before and after each stimulation. This was done using two different media, PBS and Neurobasal-A. The measurements were done using IKA™ Hot Plate Stirrer, 310°C, Aluminum Alloy with the aid of an included PT 1000 temperature sensor

(PT 1000.60).

3.4 hNSC Differentiation with ES Exposure

Neurospheres were mechanically dissociated and transferred to differentiation medium consisting of Neurobasal A (Thermo Fisher), 2% B-27 (Thermo Fisher), 1% Glutamax (Thermo Fisher), 1% Kanamycin (Kan, Thermo Fisher Scientific) and 0,05% bFGF (Sigma Aldrich). Then, these were seeded in a 12 well culture plate treated with poli-D-lysin (Sigma Aldrich) and laminin (Sigma Aldrich), with a cell density of 60.000 cells per well. The cells were maintained in a 37° humid atmosphere with 5% CO_2 in this condition for 24 hours.

In order to have a correlation between the electrical stimulation and differentiation of hNSCs, an experiment containing 4 groups was done. Two groups were maintained in the differentiation media, which only one of these groups was electrically stimulated. The remaining two groups were cultivated in a negative control media (without differentiation factors), which only one group was stimulated. The negative control contains 98% Neurobasal-A (Thermo Fisher), 1% Glutamax (Thermo Fisher) and 1% Kanamycin (Kan, Thermo Fisher Scientific). The setting 1 was used for the electrical stimulation of NSCs for 10 minutes, every 24 hours, for two days. After 24 hours passed since the last stimulation, the cells were fixed for immunocytochemistry.

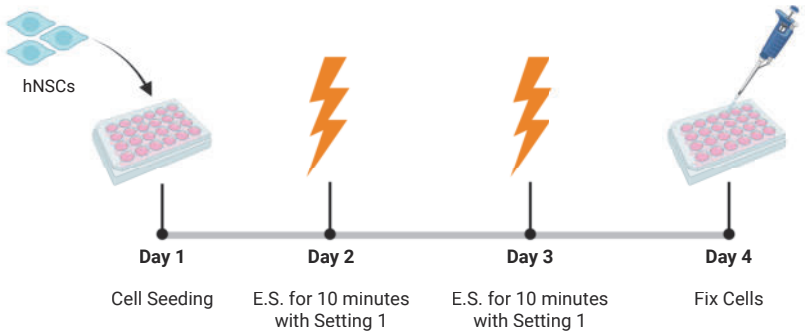

Figure 14. Diagram of E.S. assay on NPCs. (Made with Biorender)

3.5 hNSC Differentiation with MSC Secretome

To assess the impact of electrical stimulation on ASC secretome, hNSCs were incubated with secretome from hASCs during 24h. hASCs secretome was obtained following the protocol mentioned at

"hASCs Secretome Collection". Afterwards three groups were defined: NSCs cultured in stimulated secretome; NSCs cultured in control secretome (no electrical stimulation); and NSCs cultured in negative control containing 98% Neurobasal-A (Thermo Fisher), 1% Glutamax (Thermo Fisher) and 1% Penicillin-Streptomycin (Invitrogen USA).

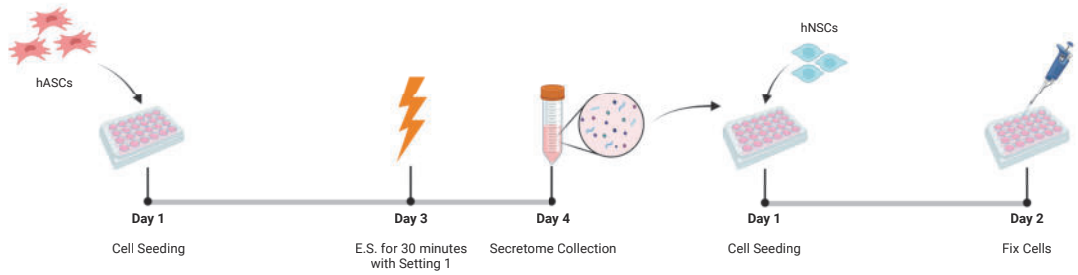

Figure 15. Diagram of E.S. assay on MSCs. (Made with Biorender)

3.6 Secretome from Electrically Stimulated ASCs on Mixed Glial Cell Population

Mixed glial cell cultures were incubated with hASCs secretome for 24h. hASCs secretome was obtained following the protocol mentioned on section a). Three experimental groups were defined: Glial cells cultured in control secretome (no electrical stimulation); Glial cells cultured in stimulated secretome (from electrically stimulated hASCs); and cultured in control medium Neurobasal-A and 1% Kanamycin.

3.7 Gellan Gum Formulation

Gellan gum (GG, Sigma, USA) was modified with the fibronectin-derived peptide (GRGDS) as described by Silva et al. [42]. The following protocol was used to prepared GG-GRGDS hydrogel for *in vitro* 3D cultures:

1. Gellan Gum-GRGDS lyophilized powder was weighed in order to prepare a solution at 1.25 % w/v in MiliQ Ultrapure Water.
2. Before adding the appropriate volume of water, the gel was sterilized by exposure to UV lights for 20 – 30 min.
3. After the addition of water, the gel preparation was heated in a water bath at 38 °C with constant agitation until an homogenous solution was obtained.

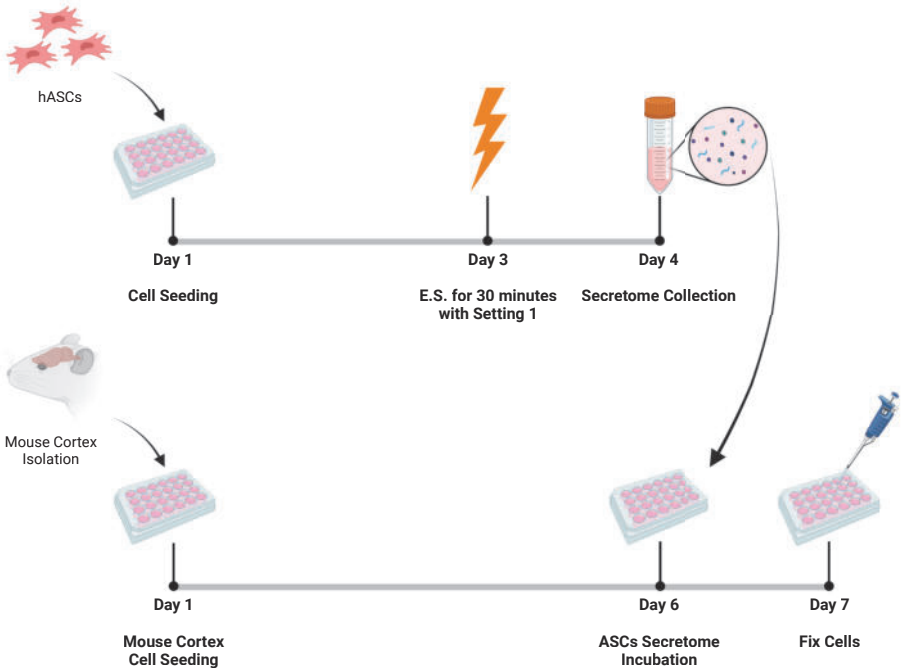

Figure 16. Diagram of secretome from electrically stimulated ASCs on Mixed Glial Cell Population assay. (Made with Biorender)

3.8 Encapsulation and Electrical Stimulation of hASCs in GG-GRGDS

Cultures of hASCs were done in GG-GRGDS hydrogel to find potential morphological changes in the cells while in a 3D environment. hASCs were obtained with the protocol used in section 3.1.2 and the hydrogel with the protocol in section 3.7. A total of 60 x 10^3 of ASCs per 100 µL of GG-GRGDS was placed on each well of a 12 well cell plate. After 72h ASCs were electrically stimulated for 30 minutes in Neurobasal-A and afterwards conditioned in Neurobasal-A with 1% Kanamycin. After 24h secretome was collected. Afterwards, phalloidin and DAPI protocol on section 3.10 was performed and sampled were analysed by an Olympus FV1200 confocal microscopy.

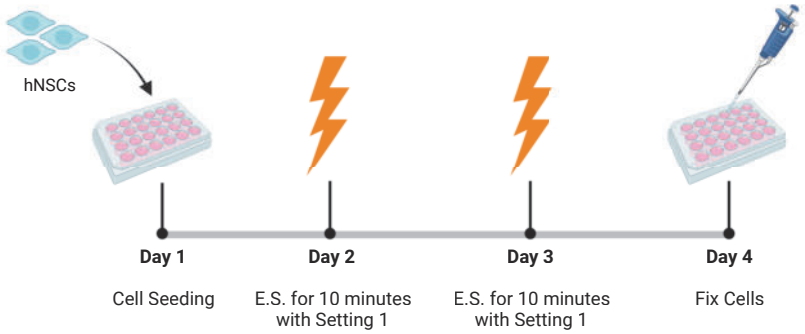

Figure 17. Diagram of hASCs encapsulated in GG-GRGDS assay. (Made with Biorender)

3.9 Immunocytochemistry

The cells were fixed with a solution of 4% PFA for 30 minutes, at room temperature (RT). After washing with PBS, the cell membranes were permeabilized with 0,5% Triton-X (Sigma) for 5 minutes at RT. Non-specific binding sites were blocked with 10% Fetal Calf Serum (FCS) in PBS for 1 hour at RT. Primary antibodies were diluted with 10% FCS in PBS and incubated for 1 hour at room temperature. Washes with 0,5% FCS in PBS were done to remove excess antibodies. Afterwards, the secondary antibodies, diluted in 10% FCS in PBS, were added for 1 hour at RT. Another wash with 0,5% FCS in PBS was done. Cell nucluei were counterstained with 4-6-diamidino2-phenylindole-dihydrochloride (DAPI) for 5 minutes at RT. Utilizing an Olympus BX61 fluorescence microscope 5 images were obtained per sample.

3.9.1 hNSC Differentiation with MSC Secretome

The immunocytochemistry was done to assess the differentiation of NPSC into Neurons in assay described on section 3.5. For this purpose MAP-2 (Mature Neuronal Marker, Sigmam Aldrich, mouse, 1:500) and DCX (Immature Neuronal Marker, Abcam, rabbit, 1:300) antibodies were used to identify neurons, respectively.

Corresponding secondary antibodies Alexa Fluor 488 anti-mouse or Alexa Fluor 594 anti-rabbit (1:1000, Invitrogen) were utilized.

3.9.2 hNSC Differentiation with ES Exposure

Likewise, for assay described on section 3.4, MAP-2 (Sigma Aldrich, mouse, 1:500) and GAP-43 (Axonal Regeneration Marker, Abcam, rabbit, 1:500) antibodies were used to identify neurons and axonal

regeneration, respectively.

Corresponding secondary antibodies Alexa Fluor 488 anti-mouse or Alexa Fluor 594 anti-rabbit (1:1000, Invitrogen) were utilized.

3.9.3 Secretome from Electrically Stimulated ASCs on Mixed Glial Cell Population

On section "Secretome from Electrically Stimulated ASCs on Mixed Glial Cell Population", IBA-1 (FUJIFILM Wako Pure Chemical Corporation, rabbit, 1:1000) and O4 (Sigma-Aldrich, mouse, 1:1000) antibodies were used to mark microglia and oligodendrocytes, respectively.

Corresponding secondary antibodies Alexa Fluor 488 anti-mouse or Alexa Fluor 594 anti-rabbit (1:1000, Invitrogen) were utilized.

3.10 Phalloidin/DAPI staining

ASCs were fixed in 4% PFA for 20 minutes at room temperature. The cells' membranes were then permeabilized with 0.3% Triton X-100 before being rinsed three times with PBS (1x). Following the washes, the cells were treated with a 10% FCS in PBS (1x) solution containing Phalloidin (1:500, Sigma) and DAPI (1:1000, Invitrogen) for 30 minutes at RT. Phalloidin and DAPI staining was done for 45 minutes.

3.11 Imaging Analysis with ImageJ Software

Imaging analysis was performed with Image J (NIH). A Cell Counter (Kurt De Vos,University of Sheffield, Academic Neurology) plugin was used to count the number of cells marked with the used antibodies, as well as to perform morphological analysis such as circularity, cell area and neurite length.

3.12 Statistical Analysis

The statistical analysis was carried out using GraphPad Prism version 9 (GraphPad Software, USA).

Before applying any test, normal distribution was evaluated with D'Agostino & Pearson test, Anderson-Darling test, Shapiro-Wilk test and Kolmogorov-Smirnov test for normality distribution. If all samples followed a normal distribution, a One-way ANOVA was used followed by the Tukey post-hoc test. If the samples did not follow a normal distribuition, a Kruskal-Wallis was used followed by a Dunns'

post-hoc test. A Mann-Whitney test was done between two samples if one failed a normality test. A T-test was done between two samples if both followed a normal distribution.

Values were accepted as significant if the p-value was higher than 0.05 (95% confidence level). All data is presented as mean ± standard error of mean (SEM).

4 Results and Discussion

4.1 Electrical Field Measurements

A measurement of the electrical signal at the bottom of the well was done to confirm the electrical field being applied to the cells. Two different volumes of medium were used being 1mL and 2mL. The voltage, frequency and pulse duration were analysed for each medium volume (Table 2).

Table 2. Results of the E.S. Readings

Medium Volume [mL]	Voltage [mV]	Frequency [Hz]	Pulse Duration [ms]	Electric Field [V/m]
2	10	4	125	**2.78**
1	15	4	125	**4.19**

The geometry of the well and the electrodes is generally ignored in this approach, and the field is assumed to be spatially uniform, which is only a reasonable approximation for parallel plate capacitor designs with accurately big electrodes. The estimate of the field strength is: $E = \frac{U}{d}$ .The electrical field was measured as a relation between the voltage (U) and the known distance between the wires (d), 3.6 mm (Figure 13).

As such, the electric field was measured at 2.78 V/m and 4.19 V/m for 2 mL and 1 mL, respectively. The electrical field seems to decrease as there is a volume increase. As the medium volume increased, the voltage measured decreased, whereas the frequency and pulse duration remained constant. Zimmermann et al. [96] and Pavesi et al. [98] found a decrease in the field strength with increasing volume during electrical stimulation. Based on Pouillet's law, the electrical resistance (R) of the culture medium decreases with the increase of the height/thickness of the medium on the well [99, 100]. It is also important to note that the conductivity of the culture medium used can influence the resistivity, being inversely proportional (Appendix A). The conductivity of Neurobasal-A was measured to be 1.069 – 1.38 $S{\cdot}m^{-1}$ at 37°C [96, 101]. DMEM medium was also found to have a greater electrical conductivity at 1.593 $S{\cdot}m^{-1}$ [101]. Furthermore, it was found that supplemented antimicrobial drugs (penicillin/ streptomycin 1%; amphotericin 0.2%) on culture medium does not affect conductivity [101]. Therefore, it is important to use the same culture medium throughout the different assays to maintain consistency in the electrical stimulation parameters. Basing on Ohm's law, the electrical potential difference measured across the culture medium is $U = R \cdot I$, where R is the electrical resistance of

the culture medium. Being that the electrical resistance is inversely proportional to the height of the medium volume (Appendix A), the potential difference decreases as the medium volume increases.

An electric field of 2.78 V/m was used for the stimulation, therefore a volume of 2mL was the one selected for the stimulation of both hNSCs and MSCs. This wave used can be characterized as symmetric and biphasic (Figure 18).

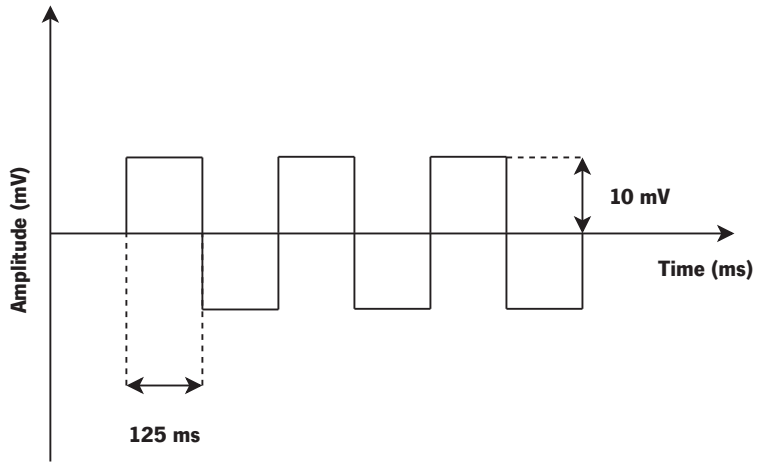

Figure 18. Waveform with 10 V, 125 ms pulse and 4 Hz.

4.2 Effect of Electrical Stimulation on Medium Temperature

Analyzing the effect of AC stimulation on the culture medium is a critical step in excluding changes in liquid characteristics, such as pH value, as a cause of the subsequent cellular adaption/behavior.

Even though human cells can sustain a 1 – 3 °C rise in temperature, accumulation of Joule heating energy remains a key barrier for therapeutic use of electrical stimulation [102]. Staehlke et al. [103] analysed the temperature, $\%H_2O_2$ and the pH of medium after 10 minutes of stimulation and found differences in temperature after stimulation with 5V but not with 1V with DMEM medium. This may be due to the electric energy deposited into each well, which increases with electric field strength. A temperature reading was done at 0, 10 and 30 minutes of electrical stimulation with an electric field of 2.78 V/m with NB-A and PBS medium (Figure 19).

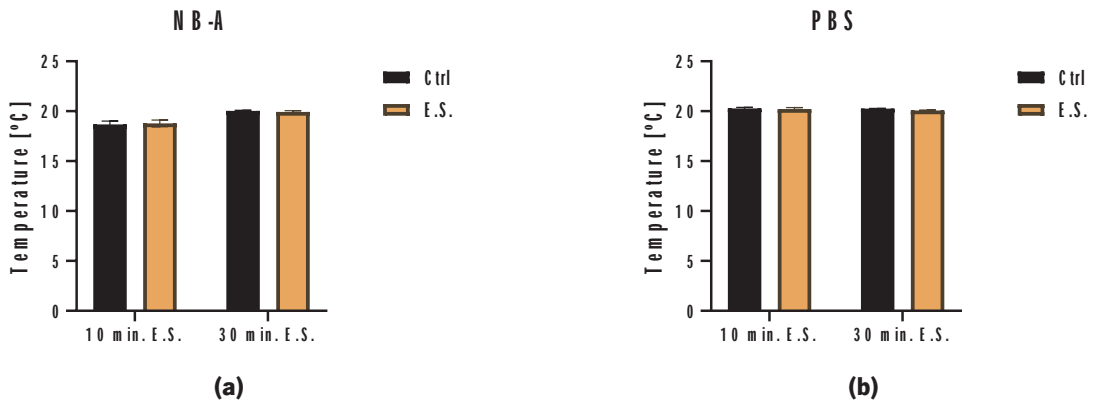

Figure 19. Temperature readings after E.S. (a) Temperatures after 10 and 30 minutes of E.S. on NB-A medium. (b) Temperatures after 10 and 30 minutes of E.S. on PBS medium. n = 4.

It is important to note that constant direct current stimulation can produce electrothermal and electrochemical damage in cells and tissue [25, 49]. Prolonged contact with DC EFs causes charge buildup at the electrode-tissue interface. Such charge accumulation causes electrochemical processes that can lead to electrode degradation, the creation of hazardous chemical species, and tissue injury [79, 104]. In addition, excessive charge buildup at the electrodes may obstruct current passage from the stimulating electrodes [105]. Likewise, a monophasic stimulation may create reactive oxygen species via the oxidation-reduction process at the surface of a metal electrode [67]. Biphasic stimulation may be more beneficial because it prevents charge accumulation, by alternating anode and cathode electrodes, generates lower levels of electrolysis products at the electrodes and can be used for longer periods of time and at greater voltages [2, 25, 67, 106].

The Joule heating effect may cause cell injury when large current pulses are applied at prolonged durations and/or high frequency [67]. Joule's first law states that the amount of heat (Joule heating) generated by and electric current through a bulk material is $Q = I^2 \cdot R$ [99]. Assuming a constant electrical current (I), we can assume that the electrical energy deposited will increase as the resistance (R) increases, which is the case as the volume of the culture medium decreases (Appendix A). However, no statistical differences (Table 3) were found between the groups, which concludes that the electric energy deposited during the electrical stimulation is efficiently thermally lost to the environment.

Table 3. Statistical analysis of the temperature readings done after 10 and 30 minutes of electrical stimulation on PBS and NB-A medium.

Group			n	Mean ± SEM	P value
Medium Temperature after 10 min. of E.S.	NB-A	Control	4	18.68 ± 0.3425	>0.9999[a]
		E.S.	4	18.78 ± 0.3301	
	PBS	Control	4	20.28 ± 0.1109	0.7921[b]
		E.S.	4	20.23 ± 0.1436	
Medium Temperature after 30 min. of E.S.	NB-A	Control	4	20.03 ± 0.06292	0.5183[b]
		E.S.	4	19.93 ± 0.1315	
	PBS	Control	4	20.25 ± 0.02887	0.0857[a]
		E.S.	4	20.08 ± 0.04787	

n, Number of temperature readings.

[a] *P* values were determined by a Mann-Whitney test.

[b] *P* values were determined by an unpaired t-test.

The layer at the electrode surface where the concentrations of the charged species deviate from their bulk value is typically in the order of μm and has a pH value differing from the bulk solution [96]. A change in pH value caused by electrical stimulation would be detected by a color change in the cell culture media, due to the presence of phenolphthalein. During and after the stimulation, no color change was detected in the medium which indicates that no drastic pH alteration was happening.

Srirussamee et al. [107] electrically stimulated MSCs (DC, 2.2 V) for 1 hour and found no changes pH, whereas electrically generated H_2O_2 was detectable. Extracellular H_2O_2 concentrations greater than 10 μM have been linked to oxidative stress and cellular damage [108].

However, the potential for faradic byproducts such as H_2O_2 to be generated is not of concern since the medium is changed after stimulation, removing any potential for cell death caused by H_2O_2.

4.3 Effect of Electrical Stimulation on NSC differentiation

The effect of ES on neuronal differentiation of hNPCs was first assessed by immunostaining for neural regeneration (GAP-43) and mature neurons (MAP-2) (Figure 20). The number of cells was obtained by quantification of DAPI+ marked neurons (Figure 21). The population obtained for %GAP-43+ and %MAP-2+ refers to the number of GAP-43+ and MAP-2+ relative to the total number of DAPI+ cells (Figure 22). The mean neurite length per Neuron refers to the length of each neurite, from the soma to the end of a bifurcation, marked morphologically by MAP-2 (Figure 21).

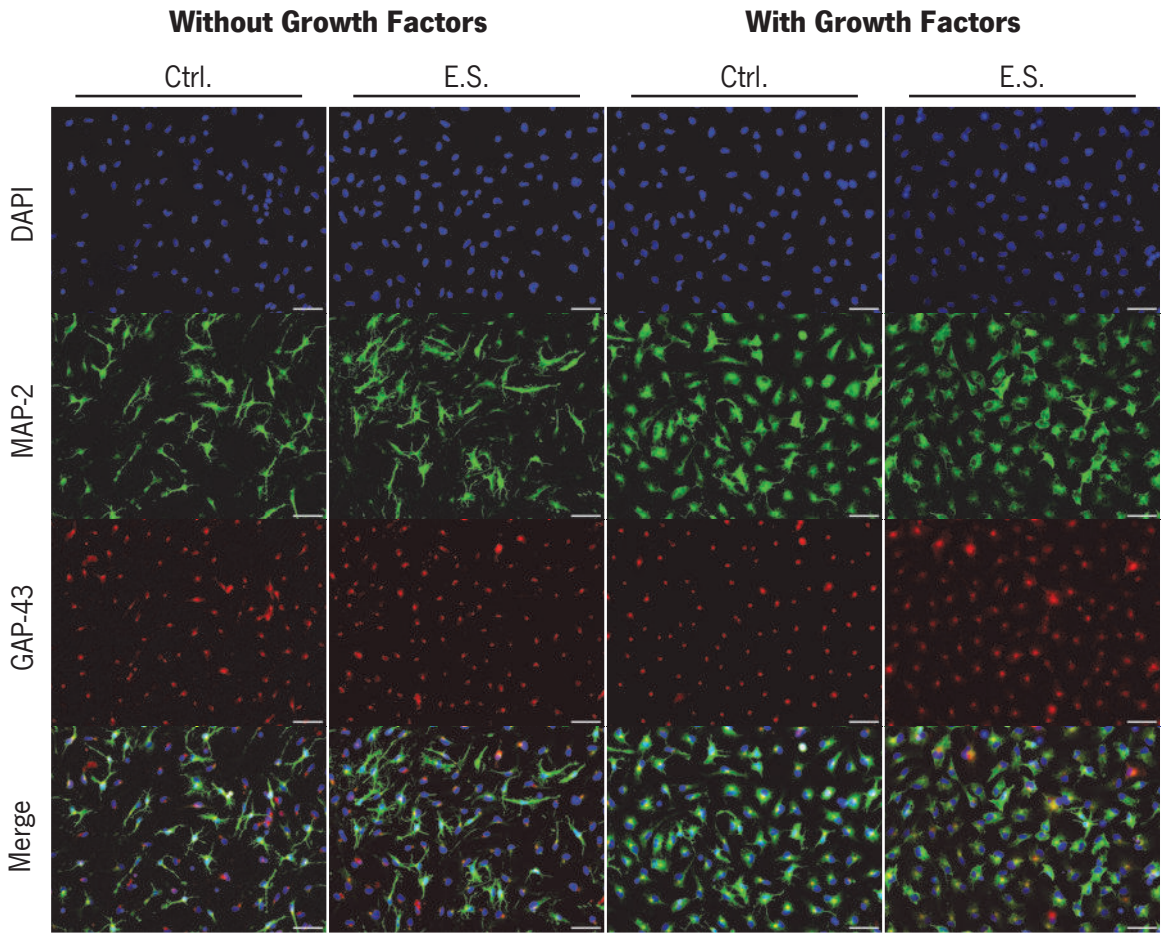

Figure 20. Representative fluorescence microscopy images of NPCs when electrically stimulated and cultured with and without growth factors. Scale bar: 50 μm

No significance difference was found for the number of DAPI+ cells in each group ($p = 0.1714$ and $p = 0.1123$, Table 4), suggesting that neither the electrical stimulation or medium supplemented with growth factors influenced the proliferation of the cells.

The mean neurite length per neuron was statistically different between the groups without growth

factors ($p < 0.0001$, Table 4), which seems to suggest that the electrical stimulation induced greater neurite growth. When growth factors and present there is no statistical difference between the groups ($p = 0.6049$, Table 4), which could possibly suggest that the presence of growth factors eliminates the neurite length growth promoted by the electrical stimulation.

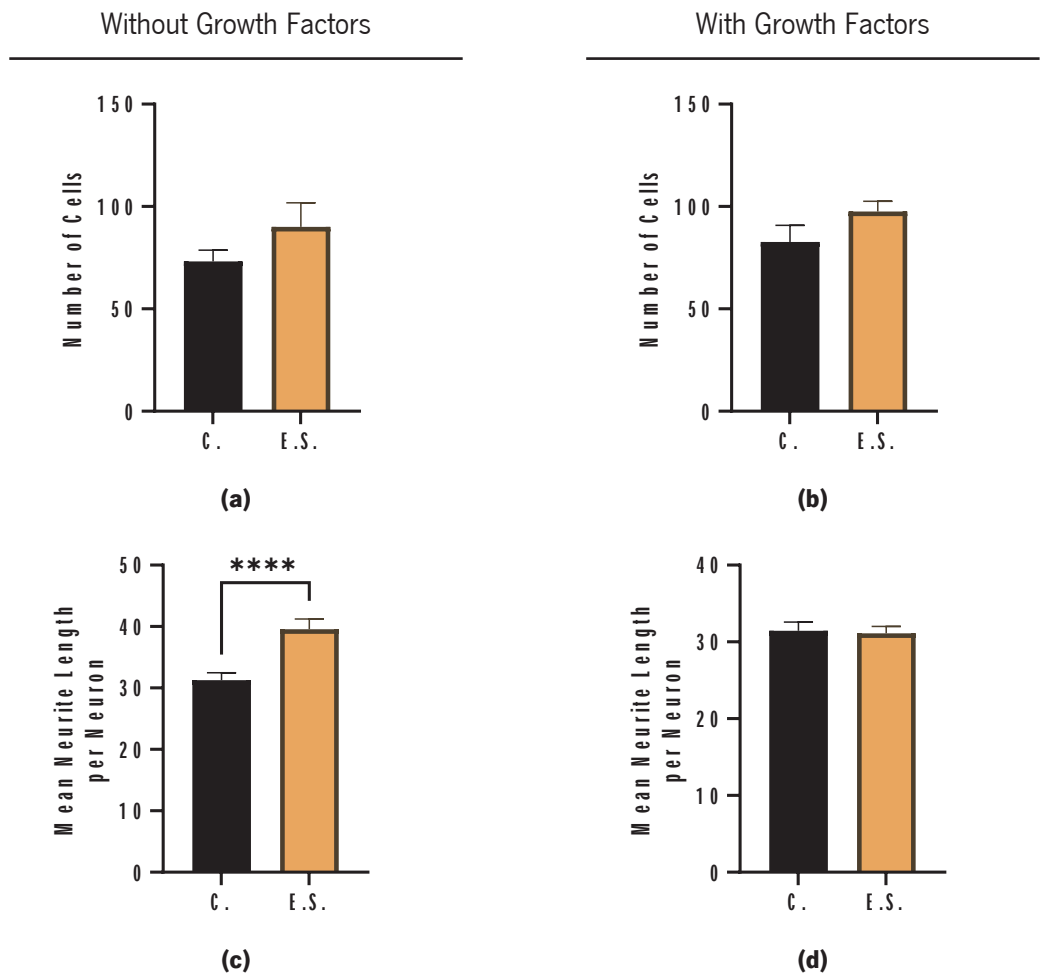

Figure 21. hNSCs were exposed to intermittent (10 minutes) ES for 2 days. (a) Represents the population of DAPI+ cells without growth factors. (b) Represents the population of DAPI+ cells with growth factors. (c) Represents the mean neurite length per neuron without growth factors. (d) Represents the mean neurite length per neuron with growth factors. 'C.' denotes the control group. 'E.S' denotes the group that was electrically stimulated. ****p value < 0,0001.

However, for the %MAP-2+, statistical difference was found between the control and E.S. groups ($p = 0.0009$, Table 4) without growth factors. No statistical difference was found between the control and E.S. ($p = 0.7668$, Table 4) with growth factors. This suggests that the presence of growth factors seems to be enough to cause a maturation of neurons, where there isn't a change caused by the presence of electrical

stimulation. When no growth factors are present, the electrical stimulation seems to allow for a greater number of mature neurons, as compared with the control.

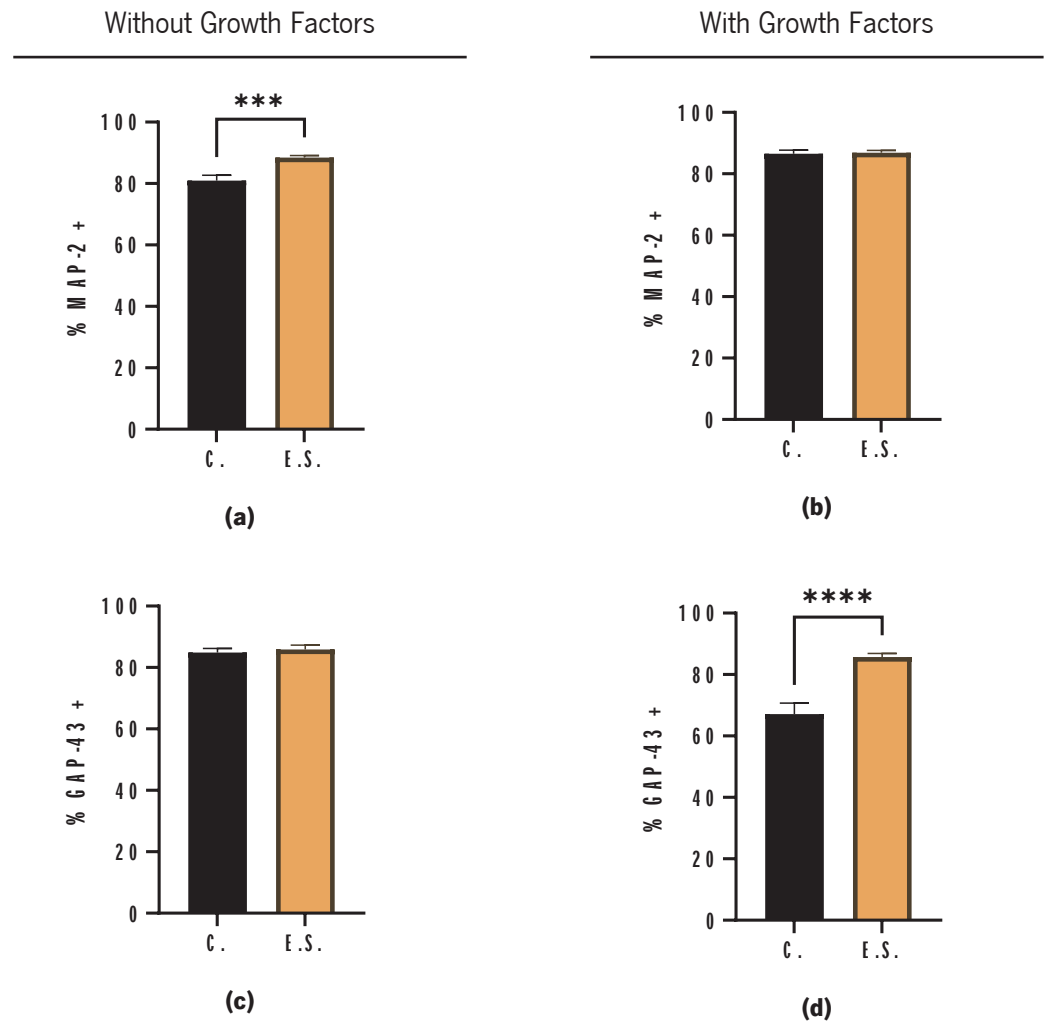

Figure 22. hNSCs were exposed to intermittent (10 minutes) ES for 2 days. (a) Represents the population of MAP-2+ cells relative to the population of DAPI+ cells without growth factors. (b) Represents the population of MAP-2+ cells relative to the population of DAPI+ cells with growth factors. (c) Represents the population of GAP-43+ cells relative to the population of DAPI+ cells without growth factors. (d) Represents the population of GAP-43+ cells relative to the population of DAPI+ cells with growth factors. 'C.' denotes the control group. 'E.S' denotes the group that was electrically stimulated. ***p value < 0,001; ****p value < 0,0001.

Statistical difference was found between the control vs. E.S. groups (p = 0,0201, Table 4) groups with growth factors for %GAP-43+. The expression of GAP-43 is high in both groups without growth factors (≈ 80%). However, only the electrically stimulated group had significant increase in mean neurite length per

neuron. Whereas with the presence of growth factors, the expression of GAP-43 was significantly greater in the electrical stimulated group when compared to the control ($p < 0.0001$, Table 4). In comparison with the mean neurite length per neuron on the groups with growth factors, no difference was found. A possible explanation could be that the timepoint used for this assay (3 days) is not enough to find the neurite outgrowth when growth factors are present, whereas without growth factors this is not the case.

Table 4. Statistical analysis of the number of cells, mean neurite length per neuron and percentage of neuronal markers on NPCs culture.

Group			n	Mean ± SEM	P value
Number of Cells	Without Growth Factors	Control	20	73.15 ± 5.548	0.1714[a]
		E.S.	15	90.00 ± 11.83	
	With Growth Factors	Control	15	82.67 ± 8.088	0.1123[a]
		E.S.	20	97.50 ± 5.037	
Mean Neurite Length per Neuron (μm)	Without Growth Factors	Control	100	31.27 ± 1.206	< 0.0001[b]
		E.S.	75	39.54 ± 1.677	
	With Growth Factors	Control	65	31.46 ± 1.122	0.6049[a]
		E.S.	105	31.12 ± 0.908	
% MAP-2 +	Without Growth Factors	Control	20	86.50 ± 1.230	0.0009[a]
		E.S.	15	86.90 ± 0.718	
	With Growth Factors	Control	15	85.28 ± 5.352	0.7668[a]
		E.S.	20	90.96 ± 1.069	
% GAP-43 +	Without Growth Factors	Control	20	84.85 ± 1.400	0.6199[a]
		E.S.	15	85.87 ± 1.417	
	With Growth Factors	Control	15	67.14 ± 3.590	<0.0001[a]
		E.S.	20	85.68 ± 1.190	

n, Number of photos analysed per group.

[a] *P* values were determined by an unpaired t-test.

[b] *P* values were determined by a Mann-Whitney test.

Throughout embryonic development, NSCs develop and progress to proliferation and differentiation in the presence of a physiological electric field of 75-450 V/m formed by the trans-epithelial potential and trans-neural tube potential across the developing neural tube [109, 110]. Many biophysical techniques have been developed to improve the efficiency of stem cell neuronal development, particularly electrical

stimulation. ES has been shown to improve stem cell proliferation and differentiation, induce directed cell migration, and promote neurite development and elongation [43]. Furthermore, low-frequency ES has been shown clinically to be beneficial in regenerating nerves, resulting in regeneration and functional recovery [43].

The influence of an EF can be seen on the differentiation, survival and maturation of NCS, including migration direction and speed of NSC, proliferation, alignment and differentiation [49, 51, 67]. Stewart et al. [111] obtained an increase in cells expressing neuron marker MAP-2 with exogenous electrical stimulation, indicating neuron differentiation.

The migration rate increased in EFs with a range between 0 and 250 V/m [49]. This effect can be particularly useful for the recruitment of NSC to the injury site. Du et al. [112] improved the viability of NSC cultured on PCEFs with a field strength of 200 V/m, frequency of 20 Hz and 100 µs pulse. In comparison to alternating and pulse currents, continuous current can promote NSC alignment and become perpendicular to the EF vector. Constant current can generate a rather uniform ionic distribution of the cell membrane [49, 67].

Long stimulation times or high field strengths might have harmful impacts, such as decreased neurite length or unorganized morphology [49]. Biphasic pulses have a net charge of zero as the initial phase elicits an action potential in nearby nerves and the second phase balances the charge injection to protect surrounding tissue [25].

Cell death appears to be related to the duration and quantity of electrical stimulation pulses when cells are stimulated *in vitro*. Furthermore, electrical stimulation at higher voltages promotes the formation of pores in cell membranes (electroporation), which can result in the triggering of apoptosis or necrosis [51, 67].

The potential mechanism of the effect of ES on NSCs differentiation or proliferation may lie on the influence of the electric field on microfilament recombination, surface receptor redistribution and intracellular Ca^{2+} changes [49]. Some studies have pointed to the Ca^{2+} fluctuations to activate several important downstream cellular mechanisms including neuron extension, differentiation and plasticity [113, 114].

Calcium ions produce varied intracellular signals that can elicit reactions such as altered gene expression and neurotransmitter release from synaptic vesicles, hence influencing essential neuronal activities [45]. Ca^{2+} is an important element in NSC functional activities as migration, proliferation, and differentiation. ES may enhance intracellular Ca^{2+}, including Ca^{2+} inflow and intracellular Ca^{2+} release [49, 67]. Ca^{2+} influx has been proven in studies to be critical for stem cell fate determination. By

elevating cytoplasmic Ca^{2+} and cyclic adenosine monophosphate (cAMP), ES can promote neuronal development toward neurotrophic growth factors [43]. Additionally, an applied external EF may induce an actin cytoskeleton reorganization by causing a cell membrane redistribution. This allows for growth factors, such as EGF, GFG and TGF-b1, to bind to specific receptors and activate signaling pathways, causing localized alterations in actin dynamics [49].

The processes underlying cell alignment and migration are assumed to involve voltage-gated ion channels, G-protein coupling receptors, integrins, cell polarization, and endogenous electric fields [67]. Ca^{2+} is normally an ion that only penetrates the plasma and ER membranes via channel proteins. When pulsed electric fields are applied to cells in a medium containing Ca^{2+} (among other substances), Ca^{2+} enters the cell from the outside and, if the electric field amplitude and pulse length are large enough, Ca^{2+} is released from the cell's inner reserves [115]. Exogenous ES can offer artificial stimulation that directly conveys electrical charge to neurons because they are electrically active cells [43].

Electric stimulation directly impacts the cytoskeleton by converting electrical stimulation into mechanical activity, producing cytoskeletal filament reconfiguration and actin redistribution and regulating a variety of cellular functions, particularly migration [49].

Kobelt et al. [116] found that applying DC EFs of 0.53 and 1.83 V/m for 10 minutes a day, for 2 days, produced morphologically mature neurons with longer neurite lengths compared to no stimulation and a change in the intracellular Ca^{2+} levels upon stimulation. This is consistent to the results obtained in this experiment with the groups which were electrically stimulated without growth facts that had a greater MAP-2 value than the corresponding control group. Tomaskovic-Crook et al. [117] and Stewart et al. [111] both obtained a larger population of cells expressing neuron marker MAP-2 and increased neurite outgrowth after applying an exogenous electrical stimulation. However, this was not the case when growth factors were present. This finding seems to suggest that the presence of growth factors alters or attenuates the influence of electrical stimulation on the MAP-2 expression. Furthermore, Kobelt et al. [116] observed an initial retraction after applying an electric field, followed by neurite extension after stimulation. Xiong et al. [118] found elevated intracellular calcium levels in neuroblast cell line SH-SY5Y during stimulation with 5 V square waves and, stimulation with 150 mV/mm DC field.

Wang et al. [119] studied the effect of biphasic pulsed 25 V/m and 50 V/m on NPCs and found a decrease of apoptosis and necrosis when cultured in serum-free conditions. An upregulation of BDNF was also registered despite the absence of growth factors in culture conditions. BDNF is known to contribute to neural cell survival, growth, differentiation and maturation [51].

Wood and Willits [120] applied a 25 V/m DC EF for 10 minutes, during 3 days and found an increase

and sustained DRG neurite outgrowth and growth rates for up to 2 days following stimulation. The neurite outgrowth registered in several studies points seems to suggest that an analysis of the neurites may provide additional information of the effect of the ES on hNSCs.

Liu et al. [121] found that NPCs show a cathodal migration upon electrical stimulation (DC, 400 mV/mm, 2 to 6 h) and that reversing the ES direction resulted in a reversed direction of NPCs migration. Additionally, Babona-Pilipos et al. [106] found a cathodal migration with NPCs electrically stimulated with DC EF (≈288 V/m) for 2.5 to 6 hours and found no migration when applying a balanced biphasic bipolar 250 V/m pulse. Ariza et al. [122] found that the majority of NPCs in the 437 V/m DC EF aligned perpendicular to the EF vector when compared with alternating EF. Therefore, symmetrical biphasic pulses would presumably elicit identical cellular responses during each phase but in opposing directions, yielding no net bias in migratory behavior [123]. This is consistent with the findings in the present work, where no directional bias was identified.

Overall, ES promoted NSC differentiation into neurons of high maturity and electrophysiological activity in the absence of the chemical mediators ordinarily required for neurogenesis, as shown previously on literature [45]. In conclusion, ES is a promising technique to promote NSC differentiation and maturation in order for it to be a viable clinical option to use in addition to NSC transplantation therapies. Furthermore, electrical stimulation has the ability to control neuroinflammation, a significant cause of neuronal death after spinal cord injury [51]. ES can also be used in combination with other techniques to form a broader therapy and solve problems that exist in tissue engineering [67]. However there is still more need of research in optimizing electric field parameters for ideal NSC stimulation.

4.4 Effect of Electrical Stimulation on ASCs Morphology

After the electrical stimulation of ASCs and collection of secretome, the cells were marked with phalloidin and DAPI for further analysis (Figure 23 and Figure 24).

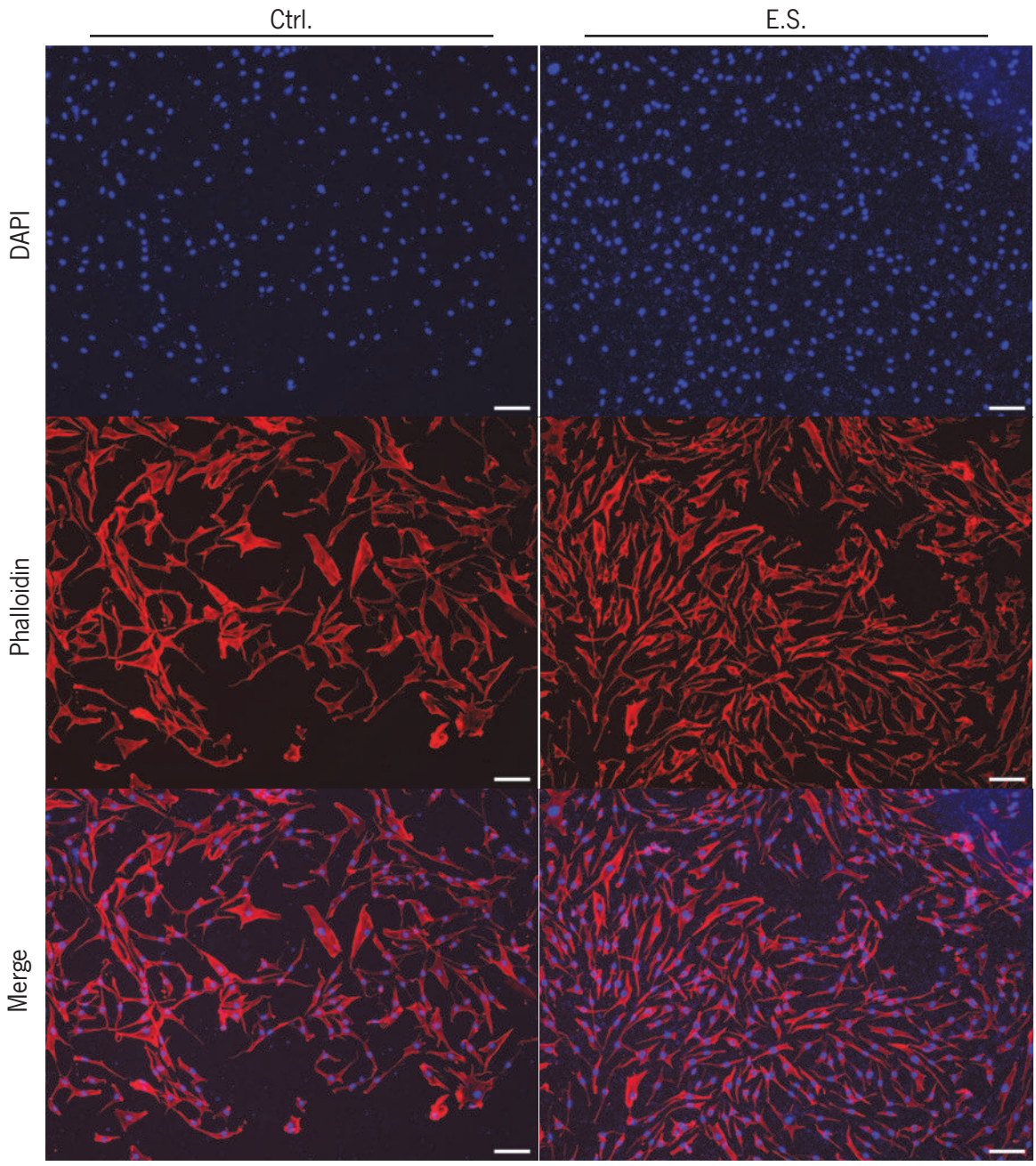

Figure 23. Representative fluorescence microscopy images of ASCs when electrically stimulated and control group. Scale bar: 100 μm.

No statistical difference was found in the number of cells, which are DAPI+ (p = 0.8064, Table 24a).

This seems to suggest that the electrical stimulation does not influence the ASCs proliferation.

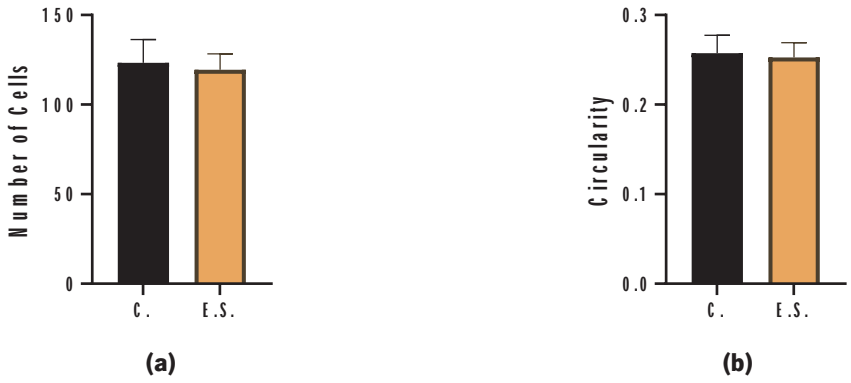

Figure 24. ASCs 2D after 30 minutes of electrical stimulation. (a) Represents the population of DAPI+ cells. (b) Represents the circularity of the cells based on the morphology of phalloidin staining. 'C.' denotes the control group. 'E.S' denotes the group that was electrically stimulated.

Pavesi et al. [98] electrically stimulated six chambers with monophasic (8 V for 2 ms, 1 Hz), and six chambers with biphasic square-wave pulses (+4 V for 1 ms, –4 V for 1 ms, 1 Hz) for 72 h and found no change in cell number.

In order to know the effect of electrical stimulation on the ASCs morphology, the circularity was calculated for each ASC marked with phalloidin. The circularity is a relation between the area and perimeter, where the closer the circularity is to 1.0, the more circular is the shape (Appendix B). The normal morphology of ASCs is spindle-shaped [124], where a circularity value is very low.

Table 5. Statistical analysis of the number of ASCs and corresponding circularity.

Group		n	Mean ± SEM	P value
Number of Cells	Control	11	123.3 ± 13.02	0.8064[a]
	E.S.	12	119.4 ± 8.895	
Circularity	Control	11	0.2573 ± 0.02018	0.8918[b]
	E.S.	12	0.2528 ± 0.01642	

n, Number of photos analysed per group.

[a] *P* values were measured by an unpaired T-test.

[b] *P* values were measured by a Mann–Whitney test.

In both the control and electrically stimulated group, the average value of circularity is around 0.25, which suggests that the stimulation does not affect greatly the morphology of the ASCs. Furthermore, no

statistical difference was found between both groups ($p = 0.8918$, Table 5). Tandon et al. [125] found that hASCs demonstrated alignment in a direction perpendicular to the applied electric field within 2 hours of the onset of stimulation (DC, 2 hours, 6 V/cm). However, no preferential alignment was found in the current experiment. This could possibly be explained by the fact that AC is used as opposed to DC, as well as a shorter electrical stimulation timeframe (30 minutes).

4.5 Effect of Electrically Stimulated ASCs secretome on NSCs culture

The effect of ES on the secretory profile of ASCs was assessed by incubating the secretome of these cells with hNSCs (Figure 25). Neuronal differentiation of hNSCs was assessed by immunostaining for early and mature neurons, with DCX and MAP-2, respectively (Figure 26). The number of cells was obtained by quantification of total DAPI+ cells (Figure 26a). The population obtained for %MAP-2+ (Figure 26c) and %DCX+ (Figure 26d) refers to the number of DCX+ and MAP-2+ relative to the total number of DAPI+ cells. The average neurite length per neuron (Figure 26b) was obtained by measuring the neurites from the soma to a bifurcation on MAP-2 marked morphology.

No significance difference was found between the groups in number of DAPI+ ceells ($p = 0.1021$), suggesting that the stimulated secretome did not influence the total hNSCs population. However, a significant difference ($p = 0.0015$) was obtained between the electrically stimulated secretome group (E.S) and control for the population of MAP-2+ cells.

Moreover, the number of DCX+ cells was very low in all groups and significant difference was identified ($p = 0.0534$), which indicates a very small population of immature neurons and that most of neurons successfully matured.

Hlavac et al. [126] found that secretome from ASCs stimulated for 24 h at 1 Hz (20 mV/mm) has a significance increase in BDNF concentration. Furthermore, this secretome when applied on SH–SY5Y neuroblastomas cells two days after seeding, achieved an increase in neurite extension when compared to non-stimulated group. However, it was found that ASCs are sensitve to ES parameters such as pulse frequency and stimulation duration. The stimulation used in this project consists of 10 minutes of stimulation at 4Hz for 2 days and the NSCs used in this assay were incubated in secretome for 1 day after seeding. This indicates that an increase in the application of ES on ASCs may produce a secretome that could possibly induce an increase in neurite outgrowth on NSCs. However, the timeframe used in this project may not be sufficient to find a greater average neurite length per neuron when compared to secretome from ASCs that were not electrically stimulated.

Although E.S. has been proven to mostly increase the rate of cell proliferation, there are contradictory data that demonstrate E.S. can also decrease or have no effect on cell proliferation [50, 127]. Several studies have shown that when cultivated in 2D or 3D (with scaffolds), daily administration of 50-150 mV/mm DC E.S. has no effect on rat BM-MSC and ASC growth [128–130]. The effect of E.S. on cell proliferation and death appears to be strongly dependent on cell type and origin, stimulation regimen, and

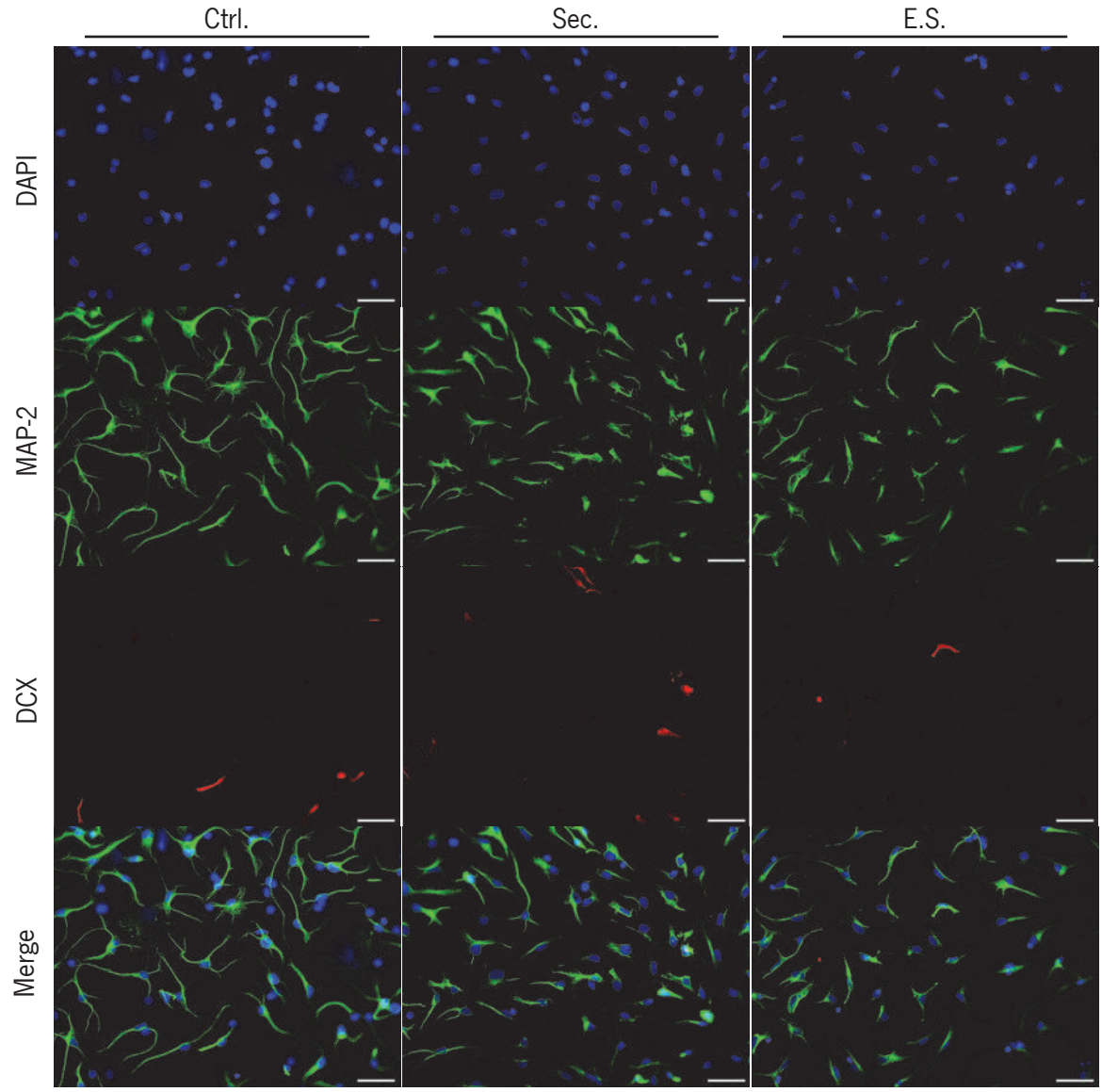

Figure 25. Representative fluorescence microscopy images of NPCs when incubated with secretome from electrically stimulated ASCs. Scale bar: 50 μm.

culture conditions [131, 132].

Cell alignment has been demonstrated to be considerably affected by DCES. Several in vitro 2D-culture experiments show that DCES causes MSC to retract and elongate, resulting in the realignment of the long cellular axis perpendicular to the electric field [125, 133, 134].

Two proposed cell mechanisms involve the asymmetric redistribution/diffusion of electrically charged cell membrane receptors in response to electric fields, which activates a variety of downstream signaling cascades and/or cell membrane depolarization caused by direct activation of voltage-gated Ca^{2+} channels, which results in an increase in intracellular calcium ion concentration, a cellular response that has been

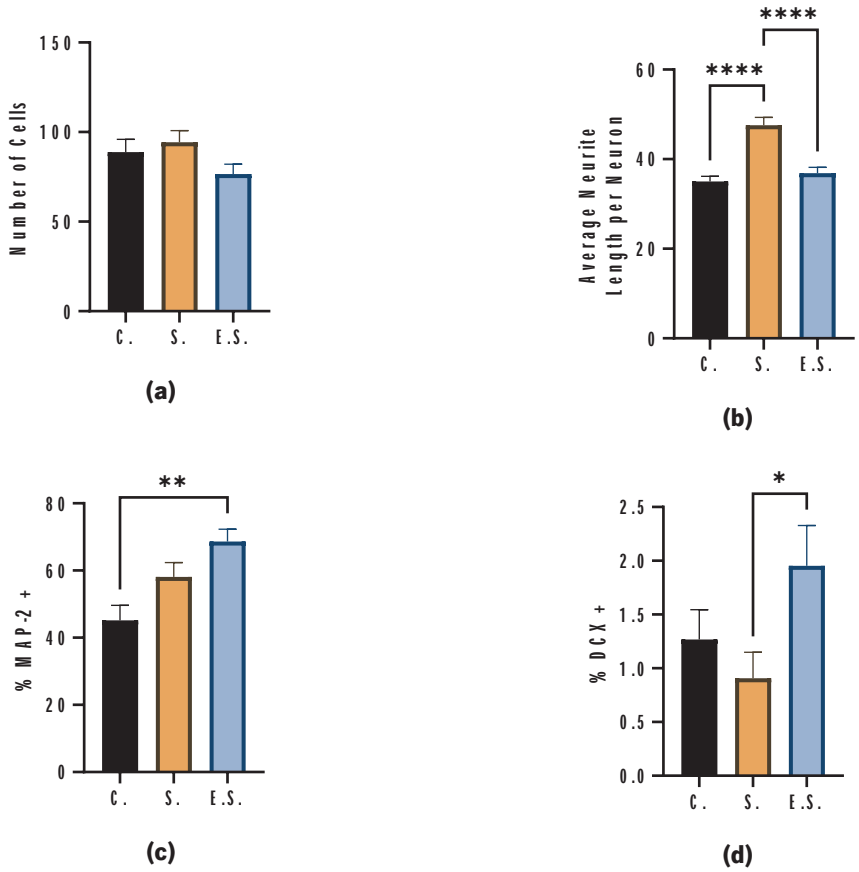

Figure 26. Secretome from ASCs exposed to intermittent (30 minutes) ES for 1 day was incubated on hNSCs. (a) Represents the population of DAPI+ cells. (b) Represents the population of MAP-2+ cells relative to the population of DAPI+ cells. (c) Represents the population of DCX+ cells relative to the population of DAPI+ cells. 'C-' denotes the control group. 'S' denotes the group with non-stimulated secretome. 'E.S.' denotes the group with electrically stimulated secretome. *p value < 0,05; **p value < 0,01; ****p value < 0,0001.

frequently described in response to electric stimulation [50]. Hanna et al. [135] was able to induce Ca^{2+} spikes caused by the penetration of Ca^{2+} from the extracellular medium, through the transiently electropermeabilized plasma membrane when applying electrical stimulation in hASCs.

DCES has been found to activate major angiogenic responses in vascular endothelial cells and to selectively regulate the production of angiogenesis-related growth factors and cytokines via a feedback loop mediated by VEGF receptors [136, 137].

Beugels et al. [138] found significantly augmented concentrations of the pro-angiogenic proteins VEGF-A on ASCs secreted proteins following E.S. (biphasic electrical current of 4 V/cm, 6ms pulse duration with

Table 6. Results of the number of cells on electrically stimulated ASCs.

Group		n	Mean ± SEM	P value
Number of Cells	Control	20	88.75 ± 7.152	0.1021[a]
	Sec.	34	94.29 ± 6.473	
	E.S.	34	76.59 ± 5.445	
% MAP-2 +	Control	20	45.13 ± 4.513	0.0015[a]
	Sec.	34	58.13 ± 4.222	
	E.S.	34	68.64 ± 3.650	
% DCX +	Control	20	1.268 ± 0.2767	0.0534[a]
	Sec.	20	0.9066 ± 0.2416	
	E.S.	20	1.953 ± 0.3742	

n, Number of photos analysed per group.

[a] *P* values were measured by an ordinary one-way ANOVA test.

[b] *P* values were determined by a Kruskal-Wallis test.

a frequency of 2 Hz, after 72h). Tandon et al. [125] found an upregulation of vascular endothelial growth factor (VEGF) and fibroblast growth factor (FGF) genes after 2 hours of E.S. (DC, 2 hours, 6 V/cm).

These findings corroborated with those obtained in this study. The possible greater concentration of VEGF and FGF on secreted proteins by ASCs could explain the greater %MAP-2+ found after incubating secretome from E.S. ASCs on hNSCs.

4.6 Effect of Secretome from Electrically Stimulated ASCs on Mixed Glial Cell Population

Following a SCI not only NSCs are affected, but also glial cells. A potential therapy involving secretome must not only allow for a regenerative effect on NSCs but also glial cells.

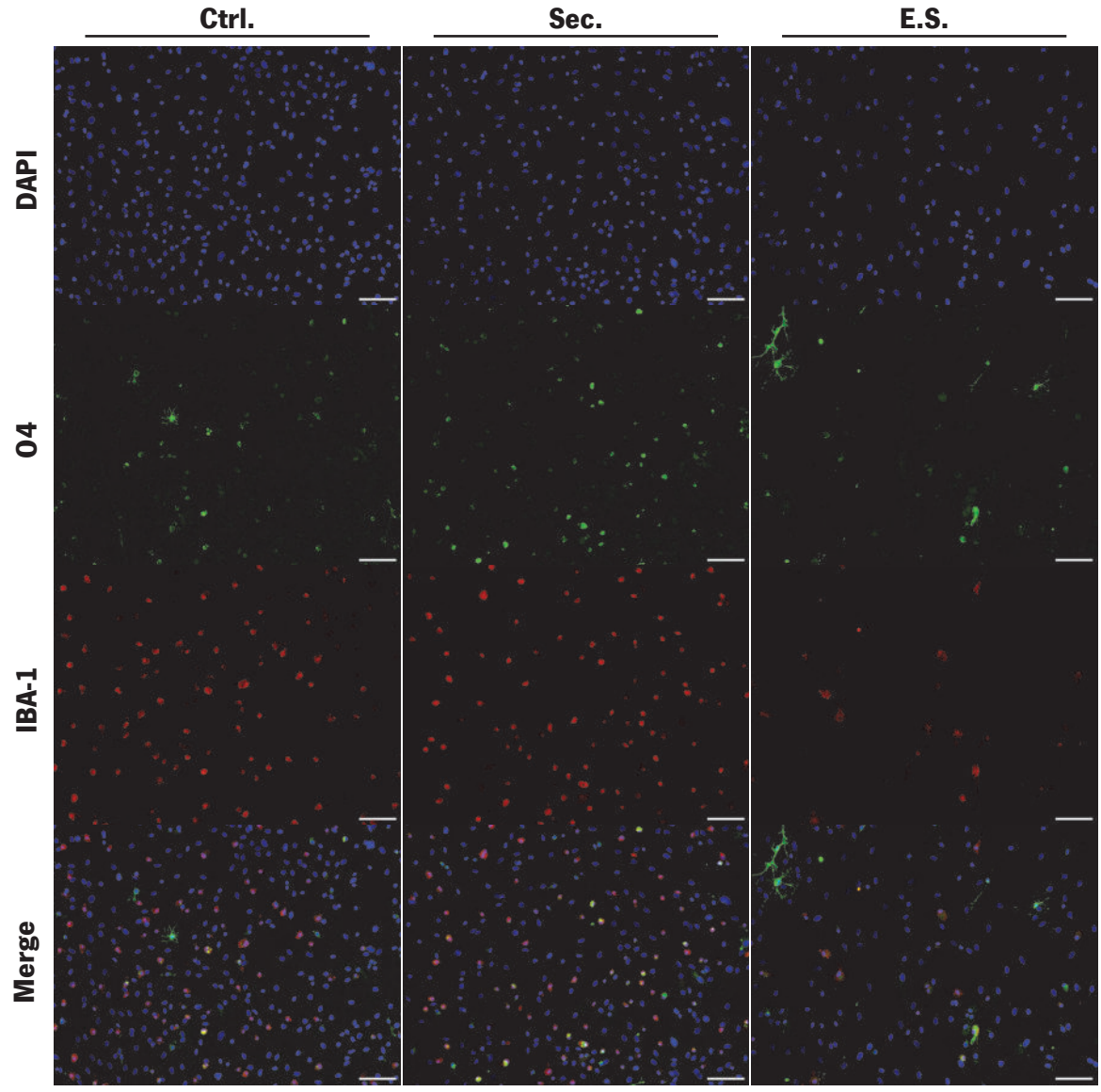

Figure 27. Representative fluorescence microscopy images of glial cells when incubated with secretome from electrically stimulated ASCs. Scale bar: 100 μm.

To better understand the effect of secretome from E.S. and non-E.S. ASCs, glial cells obtained from cortex were incubated with the secretome for 24h. The glial cells were identified by immunostaining for

microglia (IBA-1) and Oligodendrocytes (O4) (Figure 28). The number of cells on each group was not statistically significant (p = 0.1398, Table 7). This seems to indicate that the secretome overall did not influence the total number of cells marked by DAPI and does not have a proliferate effect.

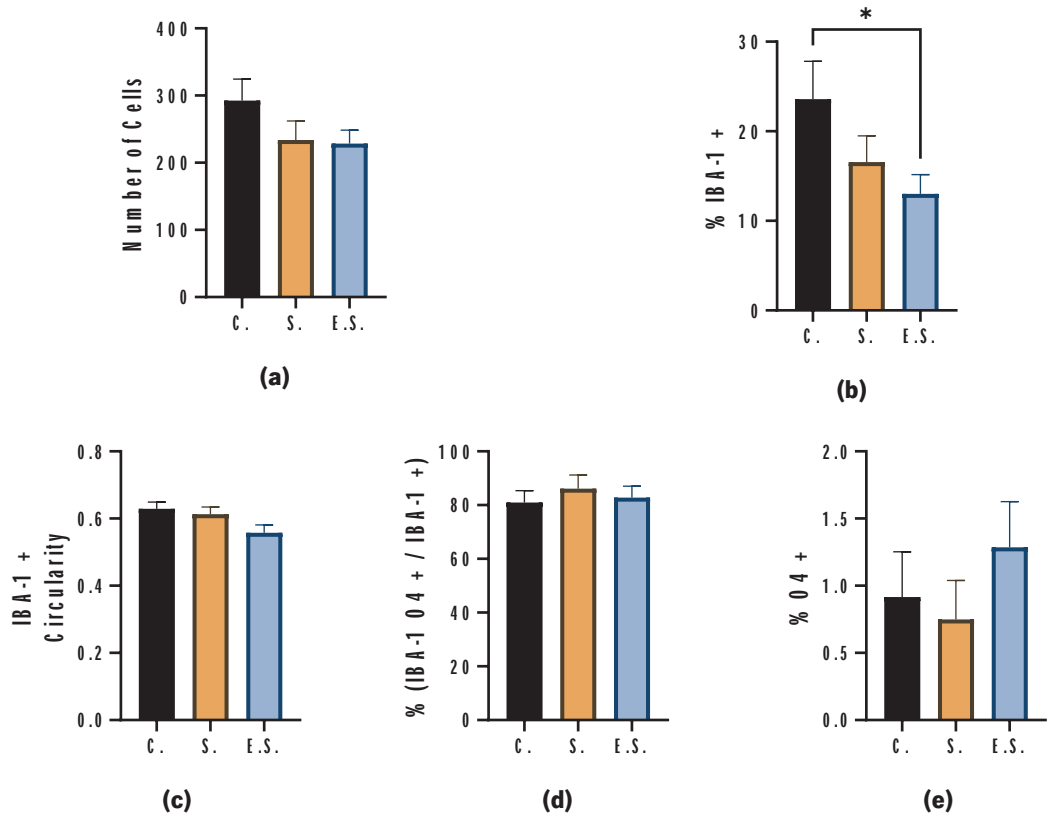

Figure 28. Secretome from ASCs exposed to intermittent (30 minutes) ES for 1 day was incubated on glial cells isolated from cortex. (a) Represents the population of DAPI+ cells. (b) Represents the population of IBA-1 + cells relative to the population of DAPI+ cells. (c) Represents the circularity of IBA-1 + cells based on the morphology of IBA-1 staining. (d) Represents the population of IBA-1 and O4 + cells relative to the total population of IBA-1 + cells. (d) Represents the population of O4 + cells relative to the population of DAPI+ cells. 'C.' denotes the control group. 'S.' denotes the group with non-stimulated secretome. 'E.S..' denotes the group with electrically stimulated secretome. *p value < 0,05.

On the contrary, the number of cells marked with IBA-1 was significantly lower in the group with secretome from ASCs that had been E.S. when compared to the control (p = 0.0458, Table 7). No further significant differences were observed between the remaining groups.

MSC-produced cytokines that influence neuroinflammation by suppressing microglial activation as well

Table 7. Statistical analysis of the number of cells, percentage of microglia and oligodendrocytes, shape and behavior of microglial cells present on mixed glial cultures from cortex.

Group		n	Mean ± SEM	P value
Number of Cells	Control	12	292.5 ± 32.11	0.1398[a]
	Sec.	20	233.9 ± 28.32	
	E.S.	28	228.5 ± 20.16	
% IBA-1	Control	12	23.58 ± 4.236	–
	Sec.	20	16.55 ± 2.949	0.4901[b]
	E.S.	28	13.00 ± 2.158	0.0458[b]
IBA-1 Circularity	Control	12	0.6288 ± 0.02058	0.2773[c]
	Sec.	20	0.6128 ± 0.02153	
	E.S.	28	0.5575 ± 0.02332	
% IBA-1 O4 + / IBA-1+	Control	12	80.92 ± 4.427	0.5141[c]
	Sec.	20	86.15 ± 5.029	
	E.S.	28	82.75 ± 4.333	
% O4 +	Control	12	0.9167 ± 0.3362	0.0167[c]
	Sec.	20	0.7500 ± 0.2891	
	E.S.	28	1.286 ± 0.3406	

n, Number of photos analysed per group.

[a] *P* values were determined by an ordinary one-way ANOVA test.

[b] *P* values were measured by an unpaired T-test with respect to the control group.

[c] *P* values were determined by a Kruskal-Wallis test.

as modulating microglial activation [46]. Which seems to indicate that a smaller number of microglia are activated, due to a possible greater anti-inflammatory cytokine presence in the secretome from E.S. ASCs.

The cell body to cell size ratio correlates strongly with microglial activity as evaluated by the visual characterisation approach [139]. Microglia have a ramified shape and monitor the CNS in order to respond properly to danger signals under steady-state environments [46]. Immunologically active microglia have an amoeboid shape, with larger somas and fewer ramified processes. Surface proteins linked with traditional immunological activities (e.g., antigen presentation, phagocytosis) are related with microglia activation and vary greatly depending on the kind and intensity of insult [28, 140]. A mechanism to analyse the active microglia involves analysing the shape of the microglia, where a circularity above 0.5 is considered

a more spherical shape, rather than elongated. Herein, no statistical differences were found between the circularity of the microglia between the groups ($p = 0.2773$, Table 7). This seems to suggest that the secretome did not alter the activation of the microglia.

Furthermore, phagocytosis behavior can be seen on the immunostaining assay by the marking of O4 inside the microglia. No differences of %(IBA-1 O4 + / IBA-1 +) were found between the groups in this assay ($p = 0.5141$, Table 7), showing that the percentage of microglia phagocytizing myelin debris was similar in all groups.

Likewise, the % O4+ is rather constant between the groups and not significantly different. It is important to note that the percentage of oligodendrocytes in all groups is rather small. This could possibly be due to the isolation process of the cells from the cortex which could result in a lower yield of oligodendrocytes.

4.7 Effect of Electrical Stimulation on ASCs in GG-GRGDS

To study if electrical stimulation influence the 3D cultures of ASCs, an assay was done using GG-GRGDS hydrogels and the analysis were focused on proliferation and morphology of the cells (Figure 29 and Figure 30).

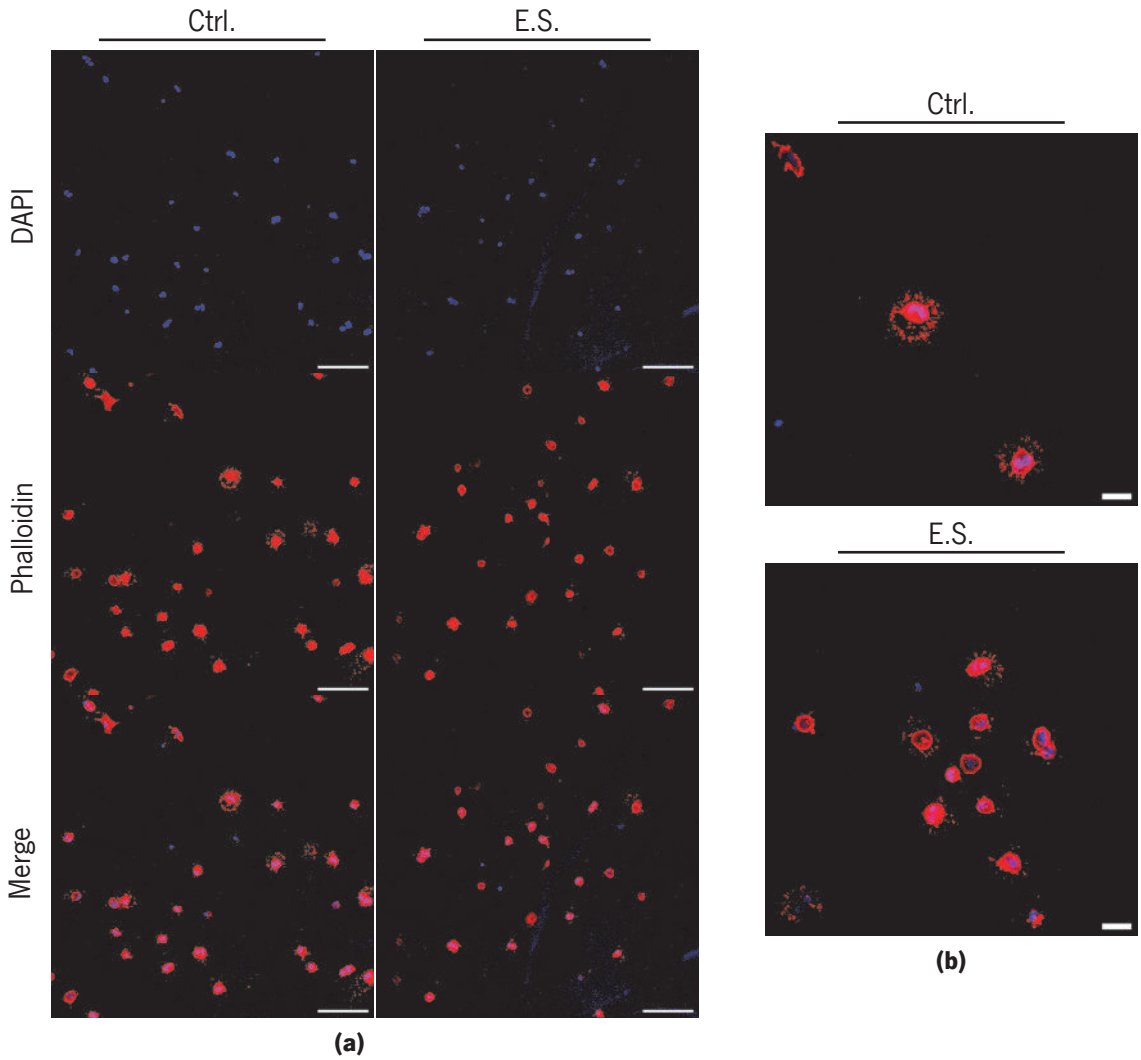

Figure 29. Representative fluorescence microscopy images of ASCs encapsulated in GG–GRGDS when electrically stimulated and control group. a) Scale bar: 100 μm; b) Scale bar: 50 μm.

A total number of cells was calculate on each group and results shown that there were no difference in total number ($p = 0.8804$, Table 8). This suggests that electrical stimulation does not influence the proliferation of the ASCs when culture in 3D conditions.

As for the shape of the ASCs, a more oval morphology was identified with a circularity close to 0.6

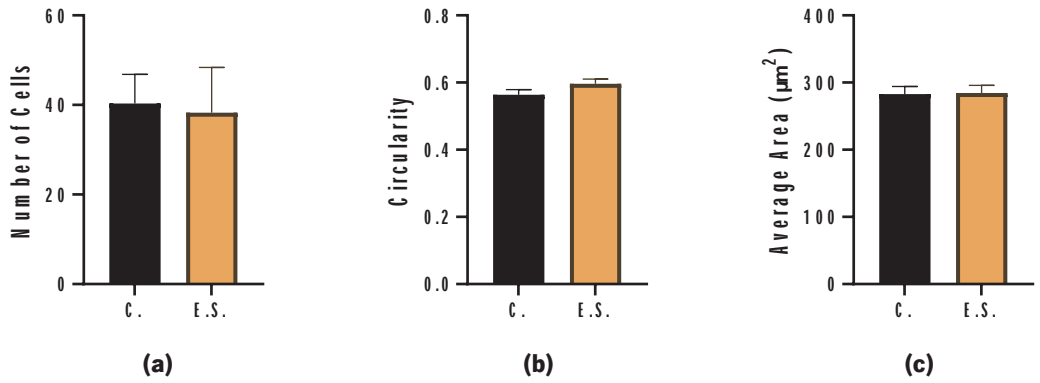

Figure 30. ASCs in 3D culture after 30 mintes of electrical stimulation. (a) Represents the population of DAPI+ cells. (b) Represents the circularity of the cells based on the morphology of phalloidin staining. (c) Represents the average area of the cells based on the morphology of phalloidin staining. 'C.' denotes the control group. 'E.S' denotes the group that was electrically stimulated.

(Appendix B). No significant differences were found between the groups (p = 0.1192, Table 8). A more oval morphology, as opposed to spindle, seems to suggest a lower adhesion of the cells to the biomaterial. However, a star shape around the cells is observed as possible anchorage points to the GRGDS peptide (Figure 29b). These results indicate that the hydrogel modification on this batch may not has been as successful as previous modifications.

Silva et al. [141] found that BM-MSCs encapsulated in GG-GRGDS were able to migrate and successfully expand throughout the hydrogel and with a typical spindle like cell morphology. Oliveira et al. [85] encapsulated ASCs in GG-GRGDS and found spindle-like shaped morphologies after cultured for 7 days. However, the attempt for the ASCs to bind to the hydrogel may also suggest that 72h of encapsulation used in this assay may not be enough to allow ASCs to proper adhere and spread in the hydrogel.

As for the overall size of each cell, no statistical differences were found between the groups (p = 0.8274, Table 8). Which seems to indicate that the size of each cell is not affected by the electrical stimulation.

Yang et al. [134] found cell galvanotaxis responses were subject to the synergistic effect of applied EF (6 V/cm EF for 6 h) and scaffold materials. Fast cell movement and intracellular calcium activities were observed in ASCs encapsulated in a collagen hydrogel. Moreover, Silva et al. [141] found that the secretome obtained from BM-MSCs encapsulated in GG-GRGDS hydrogels, is able to protect CNS neurons

Table 8. Statistical analysis of the number, circularity and average area of ASCs encapsualted in GG-GRGDS when electrically stimulated.

Group		n	Mean ± SEM	P value
Number of Cells	Control	3*	40.33 ± 6.489	0.8804[a]
	E.S.	4*	38.25 ± 10.13	
Circularity	Control	121**	0.5636 ± 0.01548	0.1192[a]
	E.S.	153**	0.5963 ± 0.01401	
Average Area (μm^2)	Control	121**	282.8 ± 11.45	0.8274[b]
	E.S.	153**	284.4 ± 11.32	

* *n*, Number of photos analysed per group.

** *n*, Number of cells analysed per photo.

[a] *P* values were measured by an unpaired T-test.

[b] *P* values were measured by a Mann–Whitney test.

significantly higher than the secretome obtain from cells in unmodified gels. This trend was also observed with cell metabolic viability.

Ideal 3D *in vitro* models include not just the right cell types and biomimetic ECM, but also biochemical (e.g. growth factors) and biophysical cues, like mechanical or electrical stimuli [83]. These findings may indicate that secretome from ASCs encapsulated in GG-GRGDS could produce a better secretome than in a 2D culture, however, more experiments are needed using proper modified GG-GRGDS hydrogels to draw such conclusions.

5 Conclusions and Future Work

Patients with spinal cord injuries still have a poor prognosis. Despite all of the efforts made in this field, single therapies frequently fail when they are tested in clinical trials. In this sense, it is important to test combinatorial treatments like the one presented herein in order to understand if synergetic effect can be obtain.. The present work aims at studying the effect of electrical stimulation on the differentiation and proliferation of hNSCs and on the secretome of ASCs. The first step involved the study of the impact of the electrical stimulation on the culture medium, with parameters of 2.78 V/m, 125 ms pulse and 4Hz. No statistical difference was found between the temperature, as the deposition of electrical energy could give rise to the temperature of the medium. Having established that the parameters used are safe for the cells, the effect of direct electrical stimulation was assessed on hNSCs. Results indicated a greater MAP-2 expression and greater neurite outgrowth when no growth factors were present. However, when growth factors are added, the expression of GAP-43 is significantly increased, indicating a possible delay on the differentiation and outgrowth which was not apparent with the time frame used of 3 days of total differentiation. As for the direct stimulation of ASCs, no difference was found between the number of cells or the circularity, indicating that the parameters used for electrical stimulation did not affect the proliferation nor the morphology of the ASCs. However, the secretome of ASCs was clearly affected by the electrical stimulation. This was assessed by incubating the secretome of electrically stimulated ASCs on hNSCs. Results demonstrated a greater expression of MAP-2 on the hNSCs incubated with secretome from electrically stimulated ASCs, when compared to the control. This indicates the a change in secretory profile of the ASCs. However, no neurite outgrowth was found with the group with secretome from electrically stimulated ASCs. In fact, the group with the greatest neurite outgrowth was in the secretome from ASCs that had not been electrically stimulated. This finding further indicates a change in the constituents of the secretome when electrical stimulation is applied. Furthermore, the secretome from electrically stimulated ASCs were incubated with glial cells isolated from cortex. This assay revealed that the secretome did not influence the population of oligodendrocytes (O4), but did reveal a lower presence of microglia (IBA-1) when compared to the control. The morphology and phagocytic behavior of the microglia was not statistically different between the groups. As a potential therapeutic approach for transplantation of ASCs, gellan gum functionalized with a GRGDS peptide was used to encapsulate ASCs. Furthermore, electrical stimulation was applied to assess the effect on the morphology of the cells. The results demonstrated that neither the proliferation or morphology of the cells were altered when electrical stimulation was applied. However, it is important to note that the ASCs did present a more rounded morphology rather than spindle-like. This indicates a poor adhesion to the biomaterial on the time frame

used of 3 days. Nonetheless, some problems arise from the use of electrical stimulation. The applied electric current and field are likely to fluctuate, resulting in poor stability and reliability, as well as presenting barriers to scaling up for cell treatment. Furthermore, the use of metal electrodes produced a risk of electrolysis of the cell culture medium. There is great debate over the effectiveness of ES as a regenerative strategy, largely due to a lack of agreed upon stimulation type (DC/AC) and parameters. Therefore, significant work remains to be done to better understand these findings and to find optimal protocols. Our results shown that electrical stimulation is able to influence NSCs differentiation and ASCs secretome. However, more studies are needed in order to understand if an approaches that combines NSCs, ASCs secretome, functional hydrogels and electrical stimulation is able to repair the injured spinal cord and promote functional recovery. Future studies will be focused on analysing the secretome of ASCs using proteomics as well as on using complex in vitro models of SCI, then the neurological benefits of our therapeutic approach may be tested in animals models.

Bibliography

[1] Tracey A. Cho. Spinal cord functional anatomy. *Continuum (Minneapolis, Minn.)*, 21(1 Spinal Cord Disorders):13–35, February 2015. ISSN 1538-6899. doi: 10.1212/01.CON.0000461082.25876.4a.

[2] Cesar Marquez-Chin and Milos R. Popovic. Functional electrical stimulation therapy for restoration of motor function after spinal cord injury and stroke: A review. *BioMedical Engineering OnLine*, 19 (1):34, May 2020. ISSN 1475-925X. doi: 10.1186/s12938-020-00773-4.

[3] Norbert Weidner, Rüdiger Rupp, and K.E. Tansey. *Neurological Aspects of Spinal Cord Injury*. Springer International, June 2017. doi: 10.1007/978-3-319-46293-6.

[4] Dale Purves, editor. *Neuroscience*. Oxford University Press, New York, sixth edition edition, 2018. ISBN 978-1-60535-380-7.

[5] Estomih Mtui and Mtui. *Fitzgerald's Clinical Neuroanatomy and Neuroscience*. Elsevier, 2023.

[6] Eric R. Kandel, John Koester, Sarah Mack, and Steven Siegelbaum, editors. *Principles of Neural Science*. McGraw Hill, New York, sixth edition edition, 2021. ISBN 978-1-259-64223-4.

[7] Nicola J. Allen and David A. Lyons. Glia as Architects of Central Nervous System Formation and Function. *Science (New York, N.Y.)*, 362(6411):181–185, October 2018. ISSN 0036-8075. doi: 10.1126/science.aat0473.

[8] Marvi A. Matos and Marcus T. Cicerone. Alternating current electric field effects on neural stem cell viability and differentiation. *Biotechnology Progress*, 26(3):664–670, 2010. ISSN 1520-6033. doi: 10.1002/btpr.389.

[9] Zsuzsanna Szepesi, Oscar Manouchehrian, Sara Bachiller, and Tomas Deierborg. Bidirectional Microglia–Neuron Communication in Health and Disease. *Frontiers in Cellular Neuroscience*, 12, 2018. ISSN 1662-5102.

[10] Yao Liu, Xi Shen, Yuhan Zhang, Xiaoli Zheng, Carlos Cepeda, Yao Wang, Shumin Duan, and Xiaoping Tong. Interactions of glial cells with neuronal synapses, from astrocytes to microglia and oligodendrocyte lineage cells. *Glia*, 71(6):1383–1401, 2023. ISSN 1098-1136. doi: 10.1002/glia.24343.

[11] Won-Suk Chung, Laura E. Clarke, Gordon X. Wang, Benjamin K. Stafford, Alexander Sher, Chandrani Chakraborty, Julia Joung, Lynette C. Foo, Andrew Thompson, Chinfei Chen, Stephen J. Smith, and Ben A. Barres. Astrocytes mediate synapse elimination through MEGF10 and MERTK pathways. *Nature*, 504(7480):394–400, December 2013. ISSN 1476-4687. doi: 10.1038/nature12776.

[12] Nicola J. Allen, Mariko L. Bennett, Lynette C. Foo, Gordon X. Wang, Chandrani Chakraborty, Stephen J. Smith, and Ben A. Barres. Astrocyte glypicans 4 and 6 promote formation of excitatory synapses via GluA1 AMPA receptors. *Nature*, 486(7403):410–414, May 2012. ISSN 1476-4687. doi: 10.1038/nature11059.

[13] Hakan Kucukdereli, Nicola J. Allen, Anthony T. Lee, Ava Feng, M. Ilcim Ozlu, Laura M. Conatser, Chandrani Chakraborty, Gail Workman, Matthew Weaver, E. Helene Sage, Ben A. Barres, and Cagla Eroglu. Control of excitatory CNS synaptogenesis by astrocyte-secreted proteins Hevin and SPARC. *Proceedings of the National Academy of Sciences of the United States of America*, 108 (32):E440–449, August 2011. ISSN 1091-6490. doi: 10.1073/pnas.1104977108.

[14] Baoyou Fan, Zhijian Wei, and Shiqing Feng. Progression in translational research on spinal cord injury based on microenvironment imbalance. *Bone Research*, 10(1):1–26, April 2022. ISSN 2095-6231. doi: 10.1038/s41413-022-00199-9.

[15] Nicola J. Allen and Ben A. Barres. Glia — more than just brain glue. *Nature*, 457(7230):675–677, February 2009. ISSN 1476-4687. doi: 10.1038/457675a.

[16] Khawaja Husnain Haider, editor. *Handbook of Stem Cell Therapy*. Springer Nature Singapore, Singapore, 2022. ISBN 978-981-19265-4-9 978-981-19265-5-6. doi: 10.1007/978-981-19-2655-6.

[17] Faith H. Brennan, Yang Li, Cankun Wang, Anjun Ma, Qi Guo, Yi Li, Nicole Pukos, Warren A. Campbell, Kristina G. Witcher, Zhen Guan, Kristina A. Kigerl, Jodie C. E. Hall, Jonathan P. Godbout, Andy J. Fischer, Dana M. McTigue, Zhigang He, Qin Ma, and Phillip G. Popovich. Microglia coordinate cellular interactions during spinal cord repair in mice. *Nature Communications*, 13 (1):4096, July 2022. ISSN 2041-1723. doi: 10.1038/s41467-022-31797-0.

[18] Axel Nimmerjahn, Frank Kirchhoff, and Fritjof Helmchen. Resting microglial cells are highly dynamic surveillants of brain parenchyma in vivo. *Science (New York, N.Y.)*, 308(5726):1314–1318, May 2005. ISSN 1095-9203. doi: 10.1126/science.1110647.

[19] Brad T. Casali and Erin G. Reed-Geaghan. Microglial Function and Regulation during Development, Homeostasis and Alzheimer's Disease. *Cells*, 10(4):957, April 2021. ISSN 2073-4409. doi: 10.3390/cells10040957.

[20] Nuno A. Silva, Nuno Sousa, Rui L. Reis, and António J. Salgado. From basics to clinical: A comprehensive review on spinal cord injury. *Progress in Neurobiology*, 114:25–57, March 2014. ISSN 1873-5118. doi: 10.1016/j.pneurobio.2013.11.002.

[21] Christopher S. Ahuja, Jefferson R. Wilson, Satoshi Nori, Mark R. N. Kotter, Claudia Druschel, Armin Curt, and Michael G. Fehlings. Traumatic spinal cord injury. *Nature Reviews Disease Primers*, 3 (1):1–21, April 2017. ISSN 2056-676X. doi: 10.1038/nrdp.2017.18.

[22] Michael G. Fehlings, Alexander R. Vaccaro, and Maxwell Boakye. *Essentials of Spinal Cord Injury: Basic Research to Clinical Practice*. Thieme, October 2012. ISBN 978-1-60406-727-9.

[23] Charles Watson, George Paxinos, and Gulgun Kayalioglu. *The Spinal Cord: A Christopher and Dana Reeve Foundation Text and Atlas*. Academic Press, November 2009. ISBN 978-0-08-092138-9.

[24] Inês M. Pereira, Ana Marote, António J. Salgado, and Nuno A. Silva. Filling the Gap: Neural Stem Cells as A Promising Therapy for Spinal Cord Injury. *Pharmaceuticals*, 12(2):65, June 2019. ISSN 1424-8247. doi: 10.3390/ph12020065.

[25] Brian A. Karamian, Nicholas Siegel, Blake Nourie, Mijail D. Serruya, Robert F. Heary, James S. Harrop, and Alexander R. Vaccaro. The role of electrical stimulation for rehabilitation and regeneration after spinal cord injury. *Journal of Orthopaedics and Traumatology*, 23(1):2, January 2022. ISSN 1590-9999. doi: 10.1186/s10195-021-00623-6.

[26] Grégoire Courtine and Michael V. Sofroniew. Spinal cord repair: Advances in biology and technology. *Nature Medicine*, 25(6):898–908, June 2019. ISSN 1546-170X. doi: 10.1038/s41591-019-0475-6.

[27] James W. Rowland, Gregory W. J. Hawryluk, Brian Kwon, and Michael G. Fehlings. Current status of acute spinal cord injury pathophysiology and emerging therapies: Promise on the horizon. *Neurosurgical Focus*, 25(5):E2, 2008. ISSN 1092-0684. doi: 10.3171/FOC.2008.25.11.E2.

[28] Rui Lima, Andreia Monteiro, António J. Salgado, Susana Monteiro, and Nuno A. Silva. Pathophysiology and Therapeutic Approaches for Spinal Cord Injury. *International Journal of*

Molecular Sciences, 23(22):13833, November 2022. ISSN 1422-0067. doi: 10.3390/ijms232213833.

[29] Arsalan Alizadeh, Scott Matthew Dyck, and Soheila Karimi-Abdolrezaee. Traumatic Spinal Cord Injury: An Overview of Pathophysiology, Models and Acute Injury Mechanisms. *Frontiers in Neurology*, 10, 2019. ISSN 1664-2295.

[30] Leonie Müller-Jensen, Christoph Johannes Ploner, Daniel Kroneberg, and Wolf Ulrich Schmidt. Clinical Presentation and Causes of Non-traumatic Spinal Cord Injury: An Observational Study in Emergency Patients. *Frontiers in Neurology*, 12, 2021. ISSN 1664-2295.

[31] Wen Guo, Xindan Zhang, Jiliang Zhai, and Jiajia Xue. The roles and applications of neural stem cells in spinal cord injury repair. *Frontiers in Bioengineering and Biotechnology*, 10, 2022. ISSN 2296-4185.

[32] Zahra Hassannejad, Shayan Abdollah Zadegan, Aida Shakouri-Motlagh, Mona Mokhatab, Motahareh Rezvan, Mahdi Sharif-Alhoseini, Farhad Shokraneh, Pouria Moshayedi, and Vafa Rahimi-Movaghar. The fate of neurons after traumatic spinal cord injury in rats: A systematic review. *Iranian Journal of Basic Medical Sciences*, 21(6):546–557, June 2018. ISSN 2008-3866. doi: 10.22038/IJBMS.2018.24239.6052.

[33] Syed A. Quadri, Mudassir Farooqui, Asad Ikram, Atif Zafar, Muhammad Adnan Khan, Sajid S. Suriya, Chad F. Claus, Brian Fiani, Mohammed Rahman, Anirudh Ramachandran, Ian I. T. Armstrong, Muhammad A. Taqi, and Martin M. Mortazavi. Recent update on basic mechanisms of spinal cord injury. *Neurosurgical Review*, 43(2):425–441, April 2020. ISSN 1437-2320. doi: 10.1007/s10143-018-1008-3.

[34] Ryan M. Dorrian, Carolyn F. Berryman, Antonio Lauto, and Anna V. Leonard. Electrical stimulation for the treatment of spinal cord injuries: A review of the cellular and molecular mechanisms that drive functional improvements. *Frontiers in Cellular Neuroscience*, 17:1095259, February 2023. ISSN 1662-5102. doi: 10.3389/fncel.2023.1095259.

[35] Michael D. Ehlers. Deconstructing the axon: Wallerian degeneration and the ubiquitin–proteasome system. *Trends in Neurosciences*, 27(1):3–6, January 2004. ISSN 0166-2236, 1878-108X. doi: 10.1016/j.tins.2003.10.015.

[36] Paul Lu, Ken Kadoya, and Mark H. Tuszynski. Axonal growth and connectivity from neural stem cell grafts in models of spinal cord injury. *Current Opinion in Neurobiology*, 27:103–109, August 2014. ISSN 1873-6882. doi: 10.1016/j.conb.2014.03.010.

[37] Weizhong Ding, Shian Hu, Pengju Wang, Honglei Kang, Renpeng Peng, Yimin Dong, and Feng Li. Spinal Cord Injury: The Global Incidence, Prevalence, and Disability From the Global Burden of Disease Study 2019. *Spine*, 47(21):1532–1540, November 2022. ISSN 1528-1159. doi: 10.1097/BRS.0000000000004417.

[38] F. Martins, F. Freitas, L. Martins, J. F. Dartigues, and M. Barat. Spinal cord injuries–epidemiology in Portugal's central region. *Spinal Cord*, 36(8):574–578, August 1998. ISSN 1362-4393. doi: 10.1038/sj.sc.3100657.

[39] Steven Kirshblum, Brittany Snider, Rüdiger Rupp, and Mary Schmidt Read. Updates of the International Standards for Neurologic Classification of Spinal Cord Injury: 2015 and 2019. *Physical Medicine and Rehabilitation Clinics of North America*, 31(3):319–330, August 2020. ISSN 1047-9651. doi: 10.1016/j.pmr.2020.03.005.

[40] Timothy T. Roberts, Garrett R. Leonard, and Daniel J. Cepela. Classifications In Brief: American Spinal Injury Association (ASIA) Impairment Scale. *Clinical Orthopaedics and Related Research*, 475(5):1499–1504, May 2017. ISSN 1528-1132. doi: 10.1007/s11999-016-5133-4.

[41] National Spinal Cord Injury Statistical Center. SCI Facts and Figures. *The Journal of Spinal Cord Medicine*, 40(1):126–127, January 2017. ISSN 2045-7723. doi: 10.1080/10790268.2017.1294349.

[42] Nuno A. Silva, Michael J. Cooke, Roger Y. Tam, Nuno Sousa, António J. Salgado, Rui L. Reis, and Molly S. Shoichet. The effects of peptide modified gellan gum and olfactory ensheathing glia cells on neural stem/progenitor cell fate. *Biomaterials*, 33(27):6345–6354, September 2012. ISSN 1878-5905. doi: 10.1016/j.biomaterials.2012.05.050.

[43] Hong Cheng, Yan Huang, Hangqi Yue, and Yubo Fan. Electrical Stimulation Promotes Stem Cell Neural Differentiation in Tissue Engineering. *Stem Cells International*, 2021:6697574, April 2021. ISSN 1687-966X. doi: 10.1155/2021/6697574.

[44] Andreia Pinho, Jorge Cibrão, Nuno Silva, Susana Monteiro, and Antonio Salgado. Cell Secretome:

Basic Insights and Therapeutic Opportunities for CNS Disorders. *Pharmaceuticals*, 13:31, February 2020. doi: 10.3390/ph13020031.

[45] Liumin He, Zhongqing Sun, Jianshuang Li, Rong Zhu, Ben Niu, Ka Long Tam, Qiao Xiao, Jun Li, Wenjun Wang, Chi Ying Tsui, Vincent Wing Hong Lee, Kwok-Fai So, Ying Xu, Seeram Ramakrishna, Qinghua Zhou, and Kin Chiu. Electrical stimulation at nanoscale topography boosts neural stem cell neurogenesis through the enhancement of autophagy signaling. *Biomaterials*, 268:120585, January 2021. ISSN 1878-5905. doi: 10.1016/j.biomaterials.2020.120585.

[46] Bin Lv, Xing Zhang, Jishan Yuan, Yongxin Chen, Hua Ding, Xinbing Cao, and Anquan Huang. Biomaterial-supported MSC transplantation enhances cell–cell communication for spinal cord injury. *Stem Cell Research & Therapy*, 12:36, January 2021. ISSN 1757-6512. doi: 10.1186/s13287-020-02090-y.

[47] Cristina Sobacchi, Eleonora Palagano, Anna Villa, and Ciro Menale. Soluble Factors on Stage to Direct Mesenchymal Stem Cells Fate. *Frontiers in Bioengineering and Biotechnology*, 5:32, May 2017. ISSN 2296-4185. doi: 10.3389/fbioe.2017.00032.

[48] Andreia Pinho, Jorge Cibrão, Rui Lima, Eduardo Gomes, Sofia Serra, José Lentilhas-Graça, C. Ribeiro, Senentxu Lanceros-Méndez, S. Teixeira, Susana Monteiro, Nuno Silva, and Antonio Salgado. Immunomodulatory and regenerative effects of the full and fractioned adipose tissue derived stem cells secretome in spinal cord injury. *Experimental Neurology*, 351:113989, January 2022. doi: 10.1016/j.expneurol.2022.113989.

[49] Rong Zhu, Zhongqing Sun, Chuping Li, Seeram Ramakrishna, Kin Chiu, and Liumin He. Electrical stimulation affects neural stem cell fate and function in vitro. *Experimental Neurology*, 319:112963, September 2019. ISSN 1090-2430. doi: 10.1016/j.expneurol.2019.112963.

[50] Liudmila Leppik, Karla Oliveira, Mit Bhavsar, and John Barker. Electrical stimulation in bone tissue engineering treatments. *European Journal of Trauma and Emergency Surgery*, 46, April 2020. doi: 10.1007/s00068-020-01324-1.

[51] Michelle O'Hara-Wright, Sahba Mobini, and Anai Gonzalez-Cordero. Bioelectric Potential in Next-Generation Organoids: Electrical Stimulation to Enhance 3D Structures of the Central Nervous System. *Frontiers in Cell and Developmental Biology*, 10, 2022. ISSN 2296-634X.

[52] Fernanda Martins de Almeida, Suelen Adriani Marques, Anne Caroline Rodrigues dos Santos, Caio Andrade Prins, Fellipe Soares dos Santos Cardoso, Luiza dos Santos Heringer, Henrique Rocha Mendonça, and Ana Maria Blanco Martinez. Molecular approaches for spinal cord injury treatment. *Neural Regeneration Research*, 18(1):23–30, April 2022. ISSN 1673-5374. doi: 10.4103/1673-5374.344830.

[53] Shuo Wang, George M Smith, Michael E. Selzer, and Shuxin Li. Emerging molecular therapeutic targets for spinal cord injury. *Expert opinion on therapeutic targets*, 23(9):787–803, September 2019. ISSN 1472-8222. doi: 10.1080/14728222.2019.1661381.

[54] Robert B. Shultz and Yinghui Zhong. Minocycline targets multiple secondary injury mechanisms in traumatic spinal cord injury. *Neural Regeneration Research*, 12(5):702–713, May 2017. ISSN 1673-5374. doi: 10.4103/1673-5374.206633.

[55] Sang M. Lee, Tae Y. Yune, Sun J. Kim, Do W. Park, Young K. Lee, Young C. Kim, Young J. Oh, George J. Markelonis, and Tae H. Oh. Minocycline reduces cell death and improves functional recovery after traumatic spinal cord injury in the rat. *Journal of Neurotrauma*, 20(10):1017–1027, October 2003. ISSN 0897-7151. doi: 10.1089/089771503770195867.

[56] Narihito Nagoshi, Hiroaki Nakashima, and Michael G. Fehlings. Riluzole as a neuroprotective drug for spinal cord injury: From bench to bedside. *Molecules (Basel, Switzerland)*, 20(5):7775–7789, April 2015. ISSN 1420-3049. doi: 10.3390/molecules20057775.

[57] Patrick H. Kitzman. Effectiveness of riluzole in suppressing spasticity in the spinal cord injured rat. *Neuroscience Letters*, 455(2):150–153, May 2009. ISSN 1872-7972. doi: 10.1016/j.neulet.2009.03.016.

[58] Xiaohong Chen, Lifang Feng, Hui Yao, Luhong Yang, and Yuan Qin. Efficacy and safety of diazoxide for treating hyperinsulinemic hypoglycemia: A systematic review and meta-analysis. *PloS One*, 16 (2):e0246463, 2021. ISSN 1932-6203. doi: 10.1371/journal.pone.0246463.

[59] Katsuhiro Yamanaka, Mohamed Eldeiry, Muhammad Aftab, Thomas J. Ryan, Gavriel Roda, Xianzhong Meng, Michael J. Weyant, Joseph C. Cleveland, David A. Fullerton, and T. Brett Reece. Pretreatment With Diazoxide Attenuates Spinal Cord Ischemia-Reperfusion Injury Through Signaling Transducer and Activator of Transcription 3 Pathway. *The Annals of Thoracic Surgery*, 107(3): 733–739, March 2019. ISSN 1552-6259. doi: 10.1016/j.athoracsur.2018.09.031.

[60] Christopher T. Tsui, Preet Lal, Katelyn V. R. Fox, Matthew A. Churchward, and Kathryn G. Todd. The effects of electrical stimulation on glial cell behaviour. *BMC Biomedical Engineering*, 4:7, September 2022. ISSN 2524-4426. doi: 10.1186/s42490-022-00064-0.

[61] Claudia Eder. Regulation of microglial behavior by ion channel activity. *Journal of Neuroscience Research*, 81(3):314–321, August 2005. ISSN 0360-4012. doi: 10.1002/jnr.20476.

[62] Pablo Izquierdo, David Attwell, and Christian Madry. Ion Channels and Receptors as Determinants of Microglial Function. *Trends in Neurosciences*, 42(4):278–292, April 2019. ISSN 1878-108X. doi: 10.1016/j.tins.2018.12.007.

[63] Michelle L. Olsen, Baljit S. Khakh, Serguei N. Skatchkov, Min Zhou, C. Justin Lee, and Nathalie Rouach. New Insights on Astrocyte Ion Channels: Critical for Homeostasis and Neuron-Glia Signaling. *The Journal of Neuroscience: The Official Journal of the Society for Neuroscience*, 35 (41):13827–13835, October 2015. ISSN 1529-2401. doi: 10.1523/JNEUROSCI.2603-15.2015.

[64] Jessica McNeill, Christopher Rudyk, Michael E. Hildebrand, and Natalina Salmaso. Ion Channels and Electrophysiological Properties of Astrocytes: Implications for Emergent Stimulation Technologies. *Frontiers in Cellular Neuroscience*, 15, 2021. ISSN 1662-5102.

[65] Sónia Guerra-Gomes, Nuno Sousa, Luísa Pinto, and João F. Oliveira. Functional Roles of Astrocyte Calcium Elevations: From Synapses to Behavior. *Frontiers in Cellular Neuroscience*, 11, 2018. ISSN 1662-5102.

[66] Tomoko Ishibashi, Kelly A. Dakin, Beth Stevens, Philip R. Lee, R. Douglas Fields, Serguei V. Kozlov, and Colin L. Stewart. Astrocytes Promote Myelination in Response to Electrical Impulses. *Neuron*, 49(6):823–832, March 2006. ISSN 0896-6273. doi: 10.1016/j.neuron.2006.02.006.

[67] Cen Chen, Xue Bai, Yahui Ding, and In-Seop Lee. Electrical stimulation as a novel tool for regulating cell behavior in tissue engineering. *Biomaterials Research*, 23(1):25, December 2019. ISSN 2055-7124. doi: 10.1186/s40824-019-0176-8.

[68] Fabien B. Wagner, Jean-Baptiste Mignardot, Camille G. Le Goff-Mignardot, Robin Demesmaeker, Salif Komi, Marco Capogrosso, Andreas Rowald, Ismael Seáñez, Miroslav Caban, Elvira Pirondini, Molywan Vat, Laura A. McCracken, Roman Heimgartner, Isabelle Fodor, Anne Watrin, Perrine Seguin, Edoardo Paoles, Katrien Van Den Keybus, Grégoire Eberle, Brigitte Schurch, Etienne Pralong, Fabio Becce, John Prior, Nicholas Buse, Rik Buschman, Esra Neufeld, Niels Kuster,

Stefano Carda, Joachim von Zitzewitz, Vincent Delattre, Tim Denison, Hendrik Lambert, Karen Minassian, Jocelyne Bloch, and Grégoire Courtine. Targeted neurotechnology restores walking in humans with spinal cord injury. *Nature*, 563(7729):65–71, November 2018. ISSN 1476-4687. doi: 10.1038/s41586-018-0649-2.

[69] Milan R. Dimitrijevic, Yuri Gerasimenko, and Michaela M. Pinter. Evidence for a Spinal Central Pattern Generator in Humansa. *Annals of the New York Academy of Sciences*, 860(1):360–376, 1998. ISSN 1749-6632. doi: 10.1111/j.1749-6632.1998.tb09062.x.

[70] Susan Harkema, Yury Gerasimenko, Jonathan Hodes, Joel Burdick, Claudia Angeli, Yangsheng Chen, Christie Ferreira, Andrea Willhite, Enrico Rejc, Robert G. Grossman, and V. Reggie Edgerton. Effect of epidural stimulation of the lumbosacral spinal cord on voluntary movement, standing, and assisted stepping after motor complete paraplegia: A case study. *The Lancet*, 377(9781): 1938–1947, June 2011. ISSN 0140-6736, 1474-547X. doi: 10.1016/S0140-6736(11)60547-3.

[71] Megan L. Gill, Peter J. Grahn, Jonathan S. Calvert, Margaux B. Linde, Igor A. Lavrov, Jeffrey A. Strommen, Lisa A. Beck, Dimitry G. Sayenko, Meegan G. Van Straaten, Dina I. Drubach, Daniel D. Veith, Andrew R. Thoreson, Cesar Lopez, Yury P. Gerasimenko, V. Reggie Edgerton, Kendall H. Lee, and Kristin D. Zhao. Neuromodulation of lumbosacral spinal networks enables independent stepping after complete paraplegia. *Nature Medicine*, 24(11):1677–1682, November 2018. ISSN 1546-170X. doi: 10.1038/s41591-018-0175-7.

[72] Johannie Audet and Charly G. Lecomte. Epidural electrical stimulation to facilitate locomotor recovery after spinal cord injury. *Journal of Neurophysiology*, 126(5):1751–1755, November 2021. ISSN 0022-3077. doi: 10.1152/jn.00261.2021.

[73] Prithvi K. Shah and Igor Lavrov. Spinal Epidural Stimulation Strategies: Clinical Implications of Locomotor Studies in Spinal Rats. *The Neuroscientist*, 23(6):664–680, December 2017. ISSN 1073-8584. doi: 10.1177/1073858417699554.

[74] Ian G. Malone, Rachel L. Nosacka, Marissa A. Nash, Kevin J. Otto, and Erica A. Dale. Electrical epidural stimulation of the cervical spinal cord: Implications for spinal respiratory neuroplasticity after spinal cord injury. *Journal of Neurophysiology*, 126(2):607–626, August 2021. ISSN 0022-3077. doi: 10.1152/jn.00625.2020.

[75] Jonathan S. Calvert, Peter J. Grahn, Jeffrey A. Strommen, Igor A. Lavrov, Lisa A. Beck, Megan L. Gill, Margaux B. Linde, Desmond A. Brown, Meegan G. Van Straaten, Daniel D. Veith, Cesar Lopez,

Dimitry G. Sayenko, Yury P. Gerasimenko, V. Reggie Edgerton, Kristin D. Zhao, and Kendall H. Lee. Electrophysiological Guidance of Epidural Electrode Array Implantation over the Human Lumbosacral Spinal Cord to Enable Motor Function after Chronic Paralysis. *Journal of Neurotrauma*, 36(9):1451–1460, May 2019. ISSN 0897-7151. doi: 10.1089/neu.2018.5921.

[76] J. R. Huie, S. M. Garraway, K. M. Baumbauer, K. C. Hoy, B. S. Beas, K. S. Montgomery, J. L. Bizon, and J. W. Grau. Brain-derived neurotrophic factor promotes adaptive plasticity within the spinal cord and mediates the beneficial effects of controllable stimulation. *Neuroscience*, 200: 74–90, January 2012. ISSN 0306-4522. doi: 10.1016/j.neuroscience.2011.10.028.

[77] Tanefumi Baba, Masahiro Kameda, Takao Yasuhara, Takamasa Morimoto, Akihiko Kondo, Tetsuro Shingo, Naoki Tajiri, Feifei Wang, Yasuyuki Miyoshi, Cesario V. Borlongan, Mitsunori Matsumae, and Isao Date. Electrical stimulation of the cerebral cortex exerts antiapoptotic, angiogenic, and anti-inflammatory effects in ischemic stroke rats through phosphoinositide 3-kinase/Akt signaling pathway. *Stroke*, 40(11):e598–605, November 2009. ISSN 1524-4628. doi: 10.1161/STROKEAHA.109.563627.

[78] Jonathan S. Calvert, Peter J. Grahn, Kristin D. Zhao, and Kendall H. Lee. Emergence of Epidural Electrical Stimulation to Facilitate Sensorimotor Network Functionality After Spinal Cord Injury. *Neuromodulation*, 22(3):244–252, April 2019. ISSN 1094-7159, 1525-1403. doi: 10.1111/ner.12938.

[79] Daniel R. Merrill, Marom Bikson, and John G. R. Jefferys. Electrical stimulation of excitable tissue: Design of efficacious and safe protocols. *Journal of Neuroscience Methods*, 141(2):171–198, February 2005. ISSN 0165-0270. doi: 10.1016/j.jneumeth.2004.10.020.

[80] Stuart F. Cogan. Neural stimulation and recording electrodes. *Annual Review of Biomedical Engineering*, 10:275–309, 2008. ISSN 1523-9829. doi: 10.1146/annurev.bioeng.10.061807.160518.

[81] Andreas Rowald, Salif Komi, Robin Demesmaeker, Edeny Baaklini, Sergio Daniel Hernandez-Charpak, Edoardo Paoles, Hazael Montanaro, Antonino Cassara, Fabio Becce, Bryn Lloyd, Taylor Newton, Jimmy Ravier, Nawal Kinany, Marina D'Ercole, Aurélie Paley, Nicolas Hankov, Camille Varescon, Laura McCracken, Molywan Vat, Miroslav Caban, Anne Watrin, Charlotte Jacquet, Léa Bole-Feysot, Cathal Harte, Henri Lorach, Andrea Galvez, Manon Tschopp, Natacha Herrmann, Moïra Wacker, Lionel Geernaert, Isabelle Fodor, Valentin Radevich, Katrien Van

Den Keybus, Grégoire Eberle, Etienne Pralong, Maxime Roulet, Jean-Baptiste Ledoux, Eleonora Fornari, Stefano Mandija, Loan Mattera, Roberto Martuzzi, Bruno Nazarian, Stefan Benkler, Simone Callegari, Nathan Greiner, Benjamin Fuhrer, Martijn Froeling, Nik Buse, Tim Denison, Rik Buschman, Christian Wende, Damien Ganty, Jurriaan Bakker, Vincent Delattre, Hendrik Lambert, Karen Minassian, Cornelis A. T. van den Berg, Anne Kavounoudias, Silvestro Micera, Dimitri Van De Ville, Quentin Barraud, Erkan Kurt, Niels Kuster, Esra Neufeld, Marco Capogrosso, Leonie Asboth, Fabien B. Wagner, Jocelyne Bloch, and Grégoire Courtine. Activity-dependent spinal cord neuromodulation rapidly restores trunk and leg motor functions after complete paralysis. *Nature Medicine*, 28(2):260–271, February 2022. ISSN 1546-170X. doi: 10.1038/s41591-021-01663-5.

[82] L. R. Stevens, K. J. Gilmore, G. G. Wallace, and M. in het Panhuis. Tissue engineering with gellan gum. *Biomaterials Science*, 4(9):1276–1290, August 2016. ISSN 2047-4849. doi: 10.1039/C6BM00322B.

[83] Lara Yildirimer, Qiang Zhang, Shifeng Kuang, Chung-Wai James Cheung, Kyle Alexander Chu, Yong He, Mo Yang, and Xin Zhao. Engineering three-dimensional microenvironments towards in vitro disease models of the central nervous system. *Biofabrication*, 11(3):032003, June 2019. ISSN 1758-5090. doi: 10.1088/1758-5090/ab17aa.

[84] Luís A. Rocha, Deolinda Silva, Sandra Barata-Antunes, Helena Cavaleiro, Eduardo D. Gomes, Nuno A. Silva, and António J. Salgado. Cell and Tissue Instructive Materials for Central Nervous System Repair. *Advanced Functional Materials*, 30(44):1909083, 2020. ISSN 1616-3028. doi: 10.1002/adfm.201909083.

[85] E. Oliveira, R. C. Assunção-Silva, O. Ziv-Polat, E. D. Gomes, F. G. Teixeira, N. A. Silva, A. Shahar, and A. J. Salgado. Influence of Different ECM-Like Hydrogels on Neurite Outgrowth Induced by Adipose Tissue-Derived Stem Cells. *Stem Cells International*, 2017:6319129, 2017. ISSN 1687-966X. doi: 10.1155/2017/6319129.

[86] Rossana Boni, Azam Ali, Amin Shavandi, and Andrew N. Clarkson. Current and novel polymeric biomaterials for neural tissue engineering. *Journal of Biomedical Science*, 25(1):90, December 2018. ISSN 1423-0127. doi: 10.1186/s12929-018-0491-8.

[87] Paul Lu, Yaozhi Wang, Lori Graham, Karla McHale, Mingyong Gao, Di Wu, John Brock, Armin Blesch, Ephron S. Rosenzweig, Leif A. Havton, Binhai Zheng, James M. Conner, Martin Marsala,

and Mark H. Tuszynski. Long-distance growth and connectivity of neural stem cells after severe spinal cord injury. *Cell*, 150(6):1264–1273, September 2012. ISSN 1097-4172. doi: 10.1016/j.cell.2012.08.020.

[88] Ana H. Bacelar, Joana Silva-Correia, Joaquim M. Oliveira, and Rui L. Reis. Recent progress in gellan gum hydrogels provided by functionalization strategies. *Journal of Materials Chemistry B*, 4 (37):6164–6174, September 2016. ISSN 2050-7518. doi: 10.1039/C6TB01488G.

[89] Rita C. Assunção-Silva, Eduardo D. Gomes, Nuno Sousa, Nuno A. Silva, and António J. Salgado. Hydrogels and Cell Based Therapies in Spinal Cord Injury Regeneration. *Stem Cells International*, 2015:e948040, June 2015. ISSN 1687-966X. doi: 10.1155/2015/948040.

[90] Tomasz Osmałek, Anna Froelich, and Sylwia Tasarek. Application of gellan gum in pharmacy and medicine. *International Journal of Pharmaceutics*, 466(1):328–340, May 2014. ISSN 0378-5173. doi: 10.1016/j.ijpharm.2014.03.038.

[91] Nuno A. Silva, Antonio J. Salgado, Rui A. Sousa, Joao T. Oliveira, Adriano J. Pedro, Hugo Leite-Almeida, Rui Cerqueira, Armando Almeida, Fabrizio Mastronardi, João F. Mano, Nuno M. Neves, Nuno Sousa, and Rui L. Reis. Development and characterization of a novel hybrid tissue engineering-based scaffold for spinal cord injury repair. *Tissue Engineering. Part A*, 16(1):45–54, January 2010. ISSN 1937-335X. doi: 10.1089/ten.TEA.2008.0559.

[92] Eduardo D. Gomes, Sofia S. Mendes, Hugo Leite-Almeida, Jeffrey M. Gimble, Roger Y. Tam, Molly S. Shoichet, Nuno Sousa, Nuno A. Silva, and António J. Salgado. Combination of a peptide-modified gellan gum hydrogel with cell therapy in a lumbar spinal cord injury animal model. *Biomaterials*, 105:38–51, October 2016. ISSN 0142-9612. doi: 10.1016/j.biomaterials.2016.07.019.

[93] Eduardo D. Gomes, Biswarup Ghosh, Rui Lima, Miguel Goulão, Tiago Moreira-Gomes, Joana Martins-Macedo, Mark W. Urban, Megan C. Wright, Jeffrey M. Gimble, Nuno Sousa, Nuno A. Silva, Angelo C. Lepore, and António J. Salgado. Combination of a Gellan Gum-Based Hydrogel With Cell Therapy for the Treatment of Cervical Spinal Cord Injury. *Frontiers in Bioengineering and Biotechnology*, 8, 2020. ISSN 2296-4185.

[94] Behnam A. Baghbaderani, Karim Mukhida, Arindom Sen, Michael S. Kallos, Murray Hong, Ivar Mendez, and Leo A. Behie. Bioreactor expansion of human neural precursor cells in serum-free media retains neurogenic potential. *Biotechnology and Bioengineering*, 105(4):823–833, 2010. ISSN 1097-0290. doi: 10.1002/bit.22590.

[95] STEMCELL Technologies. In Vitro Proliferation and Differentiation of Human Neural Stem and Progenitor Cells Using NeuroCult™ or NeuroCult™-XF, May 2020.

[96] Julius Zimmermann, Kai Budde, Nils Arbeiter, Francia Molina, Alexander Storch, Adelinde M. Uhrmacher, and Ursula van Rienen. Using a Digital Twin of an Electrical Stimulation Device to Monitor and Control the Electrical Stimulation of Cells in vitro. *Frontiers in Bioengineering and Biotechnology*, 9:765516, December 2021. ISSN 2296-4185. doi: 10.3389/fbioe.2021.765516.

[97] Hong Bae Kim, Saeyoung Ahn, Hee Jin Jang, Sung Bo Sim, and Ki Woo Kim. Evaluation of corrosion behaviors and surface profiles of platinum-coated electrodes by electrochemistry and complementary microscopy: Biomedical implications for anticancer therapy. *Micron*, 38(7): 747–753, October 2007. ISSN 0968-4328. doi: 10.1016/j.micron.2007.04.003.

[98] A. Pavesi, M. Soncini, A. Zamperone, S. Pietronave, E. Medico, A. Redaelli, M. Prat, and G. B. Fiore. Electrical conditioning of adipose-derived stem cells in a multi-chamber culture platform. *Biotechnology and Bioengineering*, 111(7):1452–1463, July 2014. ISSN 1097-0290. doi: 10.1002/bit.25201.

[99] Zhiqiang Zhao, Kan Zhu, Yan Li, Zijie Zhu, Linjie Pan, Tingrui Pan, Richard B. Borgens, and Min Zhao. Optimization of Electrical Stimulation for Safe and Effective Guidance of Human Cells. *Bioelectricity*, 2(4):372–381, December 2020. ISSN 2576-3105. doi: 10.1089/bioe.2020.0019.

[100] João Meneses, Sofia Fernandes, Nuno Alves, Paula Pascoal-Faria, and Pedro Cavaleiro Miranda. How to correctly estimate the electric field in capacitively coupled systems for tissue engineering: A comparative study. *Scientific Reports*, 12(1):11049, June 2022. ISSN 2045-2322. doi: 10.1038/s41598-022-14834-2.

[101] Jose Hurst, Sandra Kuehn, Adelina Jashari, Teresa Tsai, Karl Bartz-Schmidt, Sven Schnichels, and Stephanie Joachim. A Novel Porcine Ex Vivo Retina Culture Model for Oxidative Stress Induced by H2O2. *ATLA Alternatives to Laboratory Animals*, 45:11–25, March 2017. doi: 10.1177/026119291704500105.

[102] T. Ning, K. Zhang, B. C. Heng, and Z. Ge. Diverse effects of pulsed electrical stimulation on cells - with a focus on chondrocytes and cartilage regeneration. *European Cells & Materials*, 38:79–93, September 2019. ISSN 1473-2262. doi: 10.22203/eCM.v038a07.

[103] Susanne Staehlke, Meike Bielfeldt, Julius Zimmermann, Martina Gruening, Ingo Barke, Thomas Freitag, Sylvia Speller, Ursula Van Rienen, and Barbara Nebe. Pulsed Electrical Stimulation Affects Osteoblast Adhesion and Calcium Ion Signaling. *Cells*, 11(17):2650, January 2022. ISSN 2073-4409. doi: 10.3390/cells11172650.

[104] J. A. Spadaro and R. O. Becker. Function of implanted cathodes in electrode-induced bone growth. *Medical and Biological Engineering and Computing*, 17(6):769–775, November 1979. ISSN 1741-0444. doi: 10.1007/BF02441560.

[105] In Sook Kim, Jong Keun Song, Yu Lian Zhang, Tae Hyung Lee, Tae Hyung Cho, Yun Mi Song, Do Kyun Kim, Sung June Kim, and Soon Jung Hwang. Biphasic electric current stimulates proliferation and induces VEGF production in osteoblasts. *Biochimica Et Biophysica Acta*, 1763(9): 907–916, September 2006. ISSN 0006-3002. doi: 10.1016/j.bbamcr.2006.06.007.

[106] Robart Babona-Pilipos, Alex Pritchard-Oh, Milos R Popovic, and Cindi M Morshead. Biphasic monopolar electrical stimulation induces rapid and directed galvanotaxis in adult subependymal neural precursors. *Stem Cell Research & Therapy*, 6(1):67, April 2015. ISSN 1757-6512. doi: 10.1186/s13287-015-0049-6.

[107] Kasama Srirussamee, Ruikang Xue, Sahba Mobini, Nigel Cassidy, and Sarah Cartmell. Changes in the extracellular microenvironment and osteogenic responses of mesenchymal stem/stromal cells induced by in vitro direct electrical stimulation. *Journal of Tissue Engineering*, 12: 204173142097414, February 2021. doi: 10.1177/2041731420974147.

[108] Helmut Sies. Hydrogen peroxide as a central redox signaling molecule in physiological oxidative stress: Oxidative eustress. *Redox Biology*, 11:613–619, April 2017. ISSN 2213-2317. doi: 10.1016/j.redox.2016.12.035.

[109] Qian Liu, Vsevolod Telezhkin, Wenkai Jiang, Yu Gu, Yan Wang, Wei Hong, Weiming Tian, Polina Yarova, Gaofeng Zhang, Simon Ming-Yuen Lee, Peng Zhang, Min Zhao, Nicholas D. Allen, Emilio Hirsch, Josef Penninger, and Bing Song. Electric field stimulation boosts neuronal differentiation of neural stem cells for spinal cord injury treatment via PI3K/Akt/GSK-3β/β-catenin activation. *Cell & Bioscience*, 13(1):4, January 2023. ISSN 2045-3701. doi: 10.1186/s13578-023-00954-3.

[110] Colin D. McCaig, Ann M. Rajnicek, Bing Song, and Min Zhao. Controlling cell behavior electrically: Current views and future potential. *Physiological Reviews*, 85(3):943–978, July 2005. ISSN 0031-9333. doi: 10.1152/physrev.00020.2004.

[111] Elise Stewart, Nao R. Kobayashi, Michael J. Higgins, Anita F. Quigley, Sina Jamali, Simon E. Moulton, Robert M.I. Kapsa, Gordon G. Wallace, and Jeremy M. Crook. Electrical Stimulation Using Conductive Polymer Polypyrrole Promotes Differentiation of Human Neural Stem Cells: A Biocompatible Platform for Translational Neural Tissue Engineering. *Tissue Engineering Part C: Methods*, 21(4):385–393, April 2015. ISSN 1937-3384. doi: 10.1089/ten.tec.2014.0338.

[112] Jian Du, Gehua Zhen, Huanwen Chen, Shuming Zhang, Liming Qing, Xiuli Yang, Gabsang Lee, Hai-Quan Mao, and Xiaofeng Jia. Optimal electrical stimulation boosts stem cell therapy in nerve regeneration. *Biomaterials*, 181:347–359, October 2018. ISSN 1878-5905. doi: 10.1016/j.biomaterials.2018.07.015.

[113] L. Anglister, I. C. Farber, A. Shahar, and A. Grinvald. Localization of voltage-sensitive calcium channels along developing neurites: Their possible role in regulating neurite elongation. *Developmental Biology*, 94(2):351–365, December 1982. ISSN 0012-1606. doi: 10.1016/0012-1606(82)90353-0.

[114] A. Ghosh and M. E. Greenberg. Calcium signaling in neurons: Molecular mechanisms and cellular consequences. *Science (New York, N.Y.)*, 268(5208):239–247, April 1995. ISSN 0036-8075. doi: 10.1126/science.7716515.

[115] P. Thomas Vernier, Yinghua Sun, Laura Marcu, Sarah Salemi, Cheryl M Craft, and Martin A Gundersen. Calcium bursts induced by nanosecond electric pulses. *Biochemical and Biophysical Research Communications*, 310(2):286–295, October 2003. ISSN 0006-291X. doi: 10.1016/j.bbrc.2003.08.140.

[116] Liza J. Kobelt, Ashley E. Wilkinson, Aleesha M. McCormick, Rebecca Kuntz Willits, and Nic D. Leipzig. Short Duration Electrical Stimulation to Enhance Neurite Outgrowth and Maturation of Adult Neural Stem Progenitor Cells. *Annals of Biomedical Engineering*, 42(10):2164–2176, October 2014. ISSN 1573-9686. doi: 10.1007/s10439-014-1058-9.

[117] Eva Tomaskovic-Crook, Peikai Zhang, Annika Ahtiainen, Heidi Kaisvuo, Chong-Yong Lee, Stephen Beirne, Zaid Aqrawe, Darren Svirskis, Jari Hyttinen, Gordon G. Wallace, Jadranka Travas-Sejdic, and Jeremy M. Crook. Human Neural Tissues from Neural Stem Cells Using Conductive Biogel and Printed Polymer Microelectrode Arrays for 3D Electrical Stimulation. *Advanced Healthcare Materials*, 8(15):1900425, 2019. ISSN 2192-2659. doi: 10.1002/adhm.201900425.

[118] Gordon Minru Xiong, Anh Tuan Do, Jun Kit Wang, Chee Leong Yeoh, Kiat Seng Yeo, and Cleo Choong. Development of a miniaturized stimulation device for electrical stimulation of cells. *Journal of Biological Engineering*, 9(1):14, September 2015. ISSN 1754-1611. doi: 10.1186/s13036-015-0012-1.

[119] Menghang Wang, Ping Li, Meili Liu, Wei Song, Qian Wu, and Yubo Fan. Potential protective effect of biphasic electrical stimulation against growth factor-deprived apoptosis on olfactory bulb neural progenitor cells through the brain-derived neurotrophic factor-phosphatidylinositol 3'-kinase/Akt pathway. *Experimental Biology and Medicine (Maywood, N.J.)*, 238(8):951–959, August 2013. ISSN 1535-3699. doi: 10.1177/1535370213494635.

[120] Matthew Wood and Rebecca Kuntz Willits. Short-duration, DC electrical stimulation increases chick embryo DRG neurite outgrowth. *Bioelectromagnetics*, 27(4):328–331, May 2006. ISSN 0197-8462. doi: 10.1002/bem.20214.

[121] Jia Liu, Bangfu Zhu, Gaofeng Zhang, Jian Wang, Weiming Tian, Gong Ju, Xiaoqing Wei, and Bing Song. Electric signals regulate directional migration of ventral midbrain derived dopaminergic neural progenitor cells via Wnt/GSK3β signaling. *Experimental Neurology*, 263:113–121, January 2015. ISSN 1090-2430. doi: 10.1016/j.expneurol.2014.09.014.

[122] Carlos Atico Ariza, Asha T. Fleury, Christian J. Tormos, Vadim Petruk, Sagar Chawla, Jisun Oh, Donald S. Sakaguchi, and Surya K. Mallapragada. The influence of electric fields on hippocampal neural progenitor cells. *Stem Cell Reviews and Reports*, 6(4):585–600, December 2010. ISSN 2629-3277. doi: 10.1007/s12015-010-9171-0.

[123] Li Yao, Abhay Pandit, Sheng Yao, and Colin D. McCaig. Electric field-guided neuron migration: A novel approach in neurogenesis. *Tissue Engineering. Part B, Reviews*, 17(3):143–153, June 2011. ISSN 1937-3376. doi: 10.1089/ten.TEB.2010.0561.

[124] Wakako Tsuji, J Peter Rubin, and Kacey G Marra. Adipose-derived stem cells: Implications in tissue regeneration. *World Journal of Stem Cells*, 6(3):312–321, July 2014. ISSN 1948-0210. doi: 10.4252/wjsc.v6.i3.312.

[125] Nina Tandon, Brian Goh, Anna Marsano, Pen-Hsiu Grace Chao, Chrystina Montouri-Sorrentino, Jeffrey Gimble, and Gordana Vunjak-Novakovic. Alignment and Elongation of Human Adipose-Derived Stem Cells in Response to Direct-Current Electrical Stimulation. *Conference proceedings :*

... Annual International Conference of the IEEE Engineering in Medicine and Biology Society. IEEE Engineering in Medicine and Biology Society. Conference, 1:6517–6521, 2009. ISSN 1557-170X. doi: 10.1109/IEMBS.2009.5333142.

[126] Nora Hlavac, Deanna Bousalis, Raffae N. Ahmad, Emily Pallack, Angelique Vela, Yuan Li, Sahba Mobini, Erin Patrick, and Christine E. Schmidt. Effects of Varied Stimulation Parameters on Adipose-Derived Stem Cell Response to Low-Level Electrical Fields. *Annals of Biomedical Engineering*, 49 (12):3401–3411, December 2021. ISSN 1573-9686. doi: 10.1007/s10439-021-02875-z.

[127] Maria R. Love, Siripong Palee, Siriporn C. Chattipakorn, and Nipon Chattipakorn. Effects of electrical stimulation on cell proliferation and apoptosis. *Journal of Cellular Physiology*, 233(3):1860–1876, 2018. ISSN 1097-4652. doi: 10.1002/jcp.25975.

[128] Sahba Mobini, Liudmila Leppik, Vishnu Thottakkattumana Parameswaran, and John Howard Barker. In vitro effect of direct current electrical stimulation on rat mesenchymal stem cells. *PeerJ*, 5:e2821, January 2017. ISSN 2167-8359. doi: 10.7717/peerj.2821.

[129] Liudmila Leppik, Han Zhihua, Sahba Mobini, Vishnu Thottakkattumana Parameswaran, Maria Eischen-Loges, Andrei Slavici, Judith Helbing, Lukas Pindur, Karla M. C. Oliveira, Mit B. Bhavsar, Lukasz Hudak, Dirk Henrich, and John H. Barker. Combining electrical stimulation and tissue engineering to treat large bone defects in a rat model. *Scientific Reports*, 8(1):6307, April 2018. ISSN 2045-2322. doi: 10.1038/s41598-018-24892-0.

[130] Sahba Mobini, Liudmila Leppik, and John H. Barker. Direct current electrical stimulation chamber for treating cells in vitro. *BioTechniques*, 60(2):95–98, February 2016. ISSN 0736-6205. doi: 10.2144/000114382.

[131] Maria Eischen-Loges, Karla M. C. Oliveira, Mit B. Bhavsar, John H. Barker, and Liudmila Leppik. Pretreating mesenchymal stem cells with electrical stimulation causes sustained long-lasting pro-osteogenic effects. *PeerJ*, 6:e4959, 2018. ISSN 2167-8359. doi: 10.7717/peerj.4959.

[132] Greeshma Thrivikraman, Prafulla K. Mallik, and Bikramjit Basu. Substrate conductivity dependent modulation of cell proliferation and differentiation in vitro. *Biomaterials*, 34(29):7073–7085, September 2013. ISSN 0142-9612. doi: 10.1016/j.biomaterials.2013.05.076.

[133] Sami Curtze, Micah Dembo, Miguel Miron, and David B. Jones. Dynamic changes in traction forces

with DC electric field in osteoblast-like cells. *Journal of Cell Science*, 117(13):2721–2729, June 2004. ISSN 0021-9533. doi: 10.1242/jcs.01119.

[134] Gang Yang, Haiyan Long, Xiaomei Ren, Kunlong Ma, Zhenghua Xiao, Ying Wang, and Yingqiang Guo. Regulation of adipose-tissue-derived stromal cell orientation and motility in 2D- and 3D-cultures by direct-current electrical field. *Development, Growth & Differentiation*, 59(2):70–82, 2017. ISSN 1440-169X. doi: 10.1111/dgd.12340.

[135] Hanna Hanna, Franck M. Andre, and Lluis M. Mir. Electrical control of calcium oscillations in mesenchymal stem cells using microsecond pulsed electric fields. *Stem Cell Research & Therapy*, 8(1):91, April 2017. ISSN 1757-6512. doi: 10.1186/s13287-017-0536-z.

[136] Huai Bai, John V. Forrester, and Min Zhao. DC electric stimulation upregulates angiogenic factors in endothelial cells through activation of VEGF receptors. *Cytokine*, 55(1):110–115, July 2011. ISSN 1043-4666. doi: 10.1016/j.cyto.2011.03.003.

[137] Huai Bai, Colin D. McCaig, John V. Forrester, and Min Zhao. DC Electric Fields Induce Distinct Preangiogenic Responses in Microvascular and Macrovascular Cells. *Arteriosclerosis, Thrombosis, and Vascular Biology*, 24(7):1234–1239, July 2004. doi: 10.1161/01.ATV.0000131265.76828.8a.

[138] Jip Beugels, Daniel G. M. Molin, Daan R. M. G. Ophelders, Teun Rutten, Lilian Kessels, Nico Kloosterboer, Andrzej A. Piatkowski de Grzymala, Boris W. W. Kramer, René R. W. J. van der Hulst, and Tim G. A. M. Wolfs. Electrical stimulation promotes the angiogenic potential of adipose-derived stem cells. *Scientific Reports*, 9(1):12076, August 2019. ISSN 2045-2322. doi: 10.1038/s41598-019-48369-w.

[139] Iris Bertha Hovens, Csaba Nyakas, and Regien Geertruida Schoemaker. A novel method for evaluating microglial activation using ionized calcium-binding adaptor protein-1 staining: Cell body to cell size ratio. *Neuroimmunology and Neuroinflammation*, 1:82–88, August 2014. ISSN 2347-8659. doi: 10.4103/2347-8659.139719.

[140] Samuel C. Woodburn, Justin L. Bollinger, and Eric S. Wohleb. The semantics of microglia activation: Neuroinflammation, homeostasis, and stress. *Journal of Neuroinflammation*, 18:258, November 2021. ISSN 1742-2094. doi: 10.1186/s12974-021-02309-6.

[141] Nuno A. Silva, Joana Moreira, Silvina Ribeiro-Samy, Eduardo D. Gomes, Roger Y. Tam, Molly S. Shoichet, Rui L. Reis, Nuno Sousa, and António J. Salgado. Modulation of bone marrow mesenchymal stem cell secretome by ECM-like hydrogels. *Biochimie*, 95(12):2314–2319, December 2013. ISSN 1638-6183. doi: 10.1016/j.biochi.2013.08.016.

[142] Puneet Manocha, Gitanjali Chandwani, and Soumen Das. Characterization of Dielectrophoresis Based Relay Assisted Molecular Communication Using Analogue Transmission Line. *IEEE Access*, PP:1–1, February 2020. doi: 10.1109/ACCESS.2020.2974067.

[143] Yasuhiro Takashimizu and Maiko Iiyoshi. New parameter of roundness R: Circularity corrected by aspect ratio. *Progress in Earth and Planetary Science*, 3(1):2, January 2016. ISSN 2197-4284. doi: 10.1186/s40645-015-0078-x.

[144] Manuel Schöchlin, Stephanie E. Weissinger, Arnd R. Brandes, Markus Herrmann, Peter Möller, and Jochen K. Lennerz. A nuclear circularity-based classifier for diagnostic distinction of desmoplastic from spindle cell melanoma in digitized histological images. *Journal of Pathology Informatics*, 5: 40, October 2014. ISSN 2229-5089. doi: 10.4103/2153-3539.143335.

Appendices

A Culture Medium Electrical Resistance Calculation

According to Pouillet's law:

$$R = \rho \cdot \frac{l}{A}$$

where R is the electrical resistance of a uniform specimen of the material (measured in ohms, Ω); ρ is the electrical resistivity of a uniform specimen of the material (measured in ohms·meter, Ω·m); l is the depth of the piece of material (measured in metres, m); A is the cross-sectional area of the specimen (measured in square metres, m^2). In this case study (Figure 31a), the cross-section is a rectangle with the approximate length of the electrodes (b) and culture medium height (h): $A = b \cdot h$ (Figure 31b).

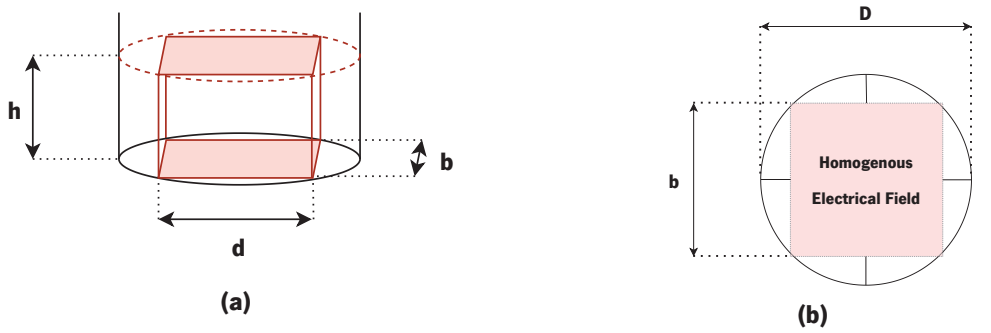

Figure 31. (a) Diagram used for the calculation of R as a function of h. (b) Top view of the well with an approximation of the area where the electrical field is homogenous.

Between the electrodes the electrical field can be considered uniform [142]. The depth (l) of the area where the electrical field is uniform is the distance between the electrodes (d). Therefore, the resistance of this rectangle is:

$$R = \rho \cdot \frac{d}{b \cdot h}$$

Knowing that the conductivity (σ) is the inverse of resistivity (ρ):

$$\sigma = \frac{1}{\rho}$$

Finally, the total resistance of the medium:

$$R = \frac{d}{b \cdot h \cdot \sigma}$$

B Circularity in ImageJ software

Circularity can be calculated as a shape parameter index in the ImageJ software. The definition of circularity (C) in the ImageJ software is as follows:

$$C = 4\pi \cdot \frac{A}{P^2}$$

where A and P are the area and perimeter measured using ImageJ, respectively. For example, when supplied with two different P values for digital photographs with the identical A values, the image with high circularity will have a shorter perimeter than the other image [143]. The shapes of cells based into four categories: Spindled (circularity values $\in [0, 0.35]$), elongated (circularity $\in]0.35, 0.6]$), oval (circularity $\in]0.6, 0.8]$), and round (circularity $\in]0.8, 1.0]$) (Table 9) [144].

Table 9. Shape of the cell based on its circularity value.

Shape	Spindle	Elongated	Oval	Round
Circularity	$[0, 0.35]$	$]0.35, 0.6]$	$]0.6, 0.8]$	$]0.8, 1.0]$
Example